

DISSERTATIONES MATHEMATICAE UNIVERSITATIS TARTUENSIS

DISSERTATIONES MATHEMATICAE UNIVERSITATIS TARTUENSIS

JULIA POLIKARPUS

Elastic plastic analysis and optimization of
axisymmetric plates

Institute of Mathematics and Statistics, Faculty of Science and Technology,
University of Tartu, Tartu, Estonia

Supervisor: Professor Jaan Lellep, D.Sci.
Institute of Mathematics,
University of Tartu, Estonia

Opponents: Professor Emeritus Niels Olhoff, Dr. Techn.
Department of Mechanical and Manufacturing Engineering
Aalborg University, Denmark

Professor Juha Paavola, D.Sc. (Tech.)
Department of Civil and Structural Engineering
Aalto University, Finland

Copyright by Julia Polikarpus, 2015

CONTENTS

Notation	7
Introduction	9
1 Basic equations and concepts	14
1.1 Equations of equilibrium	14
1.2 Hooke's law	15
1.3 Yield criteria	18
1.4 Associated flow rule	20
2 Bending of elastic plastic plates	22
2.1 Preliminaries and basic hypotheses	22
2.2 Integration of governing equations in elastic regions	24
2.3 Elastic stage of deformation	25
2.4 Optimization of stepped elastic circular plate	28
2.5 Solution of governing equations in plastic regions in the case of diamond yield criterion	29
2.6 Elastic plastic solution in the case of material obeying the diamond criterion	30
2.7 Elastic plastic bending of an annular plate	35
2.7.1 Elastic stage of deformation	36
2.7.2 Elastic plastic stage of deformation	37
2.8 Numerical results	41
2.9 Concluding remarks	45
3 Elastic plastic bending of stepped annular plates	47
3.1 The model of the plate	47
3.2 Basic equations and concepts	47
3.3 General solutions in elastic and plastic regions	50
3.4 The pure elastic stage of deformation (stage I)	51
3.5 Elastic plastic stage with the hinge circle (stage II)	53
3.6 The elastic plastic stage with a plastic region of finite length (stage III)	53
3.7 Several plastic regions	54
3.8 Numerical results	55
3.9 Concluding remarks	59

4 Optimization of elastic circular plates with additional supports	60
4.1 Optimality criteria	60
4.2 Boundary conditions	61
4.3 Necessary optimality conditions	62
4.4 Solution of governing equations	65
4.5 Solution of the adjoint system	67
4.6 Discussion of results	69
4.7 Concluding remarks	73
5 Anisotropic plate	74
5.1 The optimization problem	74
5.2 Equations of equilibrium and strain components	74
5.3 Constitutive equations	75
5.4 Solution of governing equations	77
5.5 Bending of a one-stepped plate	79
5.6 Optimal design of a stepped plate	81
5.7 Numerical results and discussion	82
5.8 Concluding remarks	84
Concluding remarks	85
Appendix	86
A.1 Elastic stage of deformation of the annular plate	86
A.2 Elastic plastic stage of deformation (Tresca criterion)	87
A.3 Elastic plastic stage of deformation (diamond yield condition)	88
References	89
Kokkuvõte (Summary in Estonian)	97
Acknowledgements	99
Curriculum vitae	100
Elulookirjeldus (Curriculum Vitae in Estonian)	102
List of publications	104

NOTATION

A_e	external work
a	inner radius of an annular plate, step location of a circular plate
a_1, \dots, a_n	locations of the steps
D, D_0, D_1	bending stiffnesses
E, E_1, E_2	Young's moduli
E_i	internal energy
H	thickness of a sandwich plate
h	thickness of a solid plate, thickness of a carrying layer
h_*	thickness of a reference plate
I_*, J_*	extended functions (functionals)
J	cost function (functional)
M_0	yield moment
M_1, M_2, M_{12}	principal bending moments
M_*	yield moment of a reference plate
N_1, N_2	membrane forces
P	transverse load intensity
p	dimensionless loading
Q	shear force
$[Q]$	reduced stiffness matrix
Q_{ij}	reduced stiffnesses
q	dimensionless shear force
R	radius of a circular plate, outer radius of an annular plate
r	polar coordinate (current radius)
u, v, w	displacements
V	volume of a plate
\bar{V}	dimensionless volume of a plate
W	transverse deflection
W_0	maximum transverse deflection
\bar{w}	dimensionless deflection
y	radius of a circle between the elastic and plastic regions
Z	auxiliary variable
z	distance between a current point and the middle surface of the plate

α	step coordinate
γ	ratio of thicknesses
$\gamma_{12}, \gamma_{23}, \gamma_{13}$	shear strains
ΔJ	total variaton of J
δJ	weak variation of J
$\varepsilon_1, \varepsilon_2, \varepsilon_3$	principal normal strains
η	dimensionless radius of a circle between the elastic and plastic regions
θ	polar angle
\varkappa_1, \varkappa_2	principal curvatures
λ	Lagrangian multiplier
ν, ν_{12}, ν_{21}	Poisson's ratios
σ_0	yield stress
$\sigma_1, \sigma_2, \sigma_3$	principal normal stresses
$\tau_{12}, \tau_{23}, \tau_{13}$	shear stresses
ψ_1, \dots, ψ_4	adjoint variables

INTRODUCTION

Reduction of the structural compliance of thin-walled beams, plates and shells is often the primary concern in the engineering mechanics. The need for reduction of the compliance and for an increase in the structural stiffness is related to the use of lightweight structures which are less material-consuming than the traditional structures.

It is well known that the material is used in a more efficient manner and the ratio of the strength to weight is larger if inelastic deformations are taken into account when designing the structure. Although the early results of the behaviour of elastic plastic circular and annular plates were obtained already long ago by Naghdi [72], Hodge [27], Tekinalp [93] and others, most of the attention was paid to plates of constant thickness only. Comprehensive reviews of these investigations can be found in the books by Chakrabarty [11], Cohn [15], Kaliszky [35], Save et al [86], Yu and Zhang [109]. Hodge [29] introduced an essential simplification of inelastic problems in the case of a Tresca's material, making use of the yield surface consisting of two hexagons in the planes of moments and membrane forces, respectively. It was used by many investigators for getting approximate solutions. Among others, Sherbourne and Srivastava [89] found an analytical solution to the elastic plastic bending problem in the range of large deflections.

The exact analysis of elastic plastic plates is quite complicated. This involves the need for physically reasonable simplifications. An effective simplification was introduced by Haythornthwaite [25] and Tekinalp [93, 94]. Haythornthwaite [25] suggested to ignore the changes of the stresses across the thickness of the plate. This assumption is fulfilled in the case of a sandwich plate consisting of two carrying layers and of a core material between the rims. Haythornthwaite [25] investigated the elastic plastic bending of an annular plate loaded by the central absolutely rigid boss. The plate is clamped to the boss at the inner edge and simply supported at the outer edge. An exact theoretical solution is derived for a plate made of a Tresca's material.

Tekinalp [93] studied the circular plate simply supported at the edge and subjected to the uniformly distributed transverse pressure. The solution for a plate clamped at the outer edge was obtained a little later by Tekinalp [94]. In both cases, the solutions consist of the initial elastic stage and several subsequent elastic plastic stages of deformation.

The complete elastic plastic analysis of centrally clamped annular plates carrying a uniformly distributed transverse load was undertaken by French [19] within the frameworks of the pure bending theory of thin plates. Exact stress profiles lying

partly inside and partly on the yield hexagon were developed for the elastic and elastic plastic stages of the deformation. It was assumed by French [19] that the plate is a sandwich construction and that the material of the carrying layers obeys the Tresca's yield criterion. The elastic plastic bending of circular and annular plates made of a Tresca's material was also studied by Hodge [27, 28].

Elastic plastic deformations of axisymmetric plates made of a von Mises material were investigated by Eason [18], Sokolovsky [90], Lackman [39], Popov et al [80], Turvey [96], Turvey and Lim [97], Turvey and Salehi [98], Ohashi, Murakami and Endo [74, 75].

The classical concept of an elastic plastic body admits the exact definitions of yielding and of the yield-point load. It was shown earlier by Tekinalp [93], Hodge [27] and others that in the case of the Tresca's material and a plate subjected to the uniformly distributed transverse pressure of intensity P , the onset of yielding corresponds to the values of the pressure $P = \frac{16M_0}{R^2(3 + \nu)}$ and $P = \frac{8M_0}{R^2}$ for simply supported and clamped plates, respectively. Here ν is the Poisson's ratio, R and M_0 stand for the radius of the plate and the yield moment, respectively. The concept of gradual yielding for one-dimensional structures, introduced by Richard and Abbott [84], was extended to circular and annular plates by Upadrasta et al [100], Khalili and Peddieson [36].

Elastic plastic bending of axisymmetric plates in the range of large deflections was investigated by Ohashi et al [75], Sherbourne and Srivastava [89], also Gorji and Akileh [23] and Turvey [95]. Stress and strain distributions in rotating disks made of Tresca's material were determined by Güven [24] and Gamer [20]. In the cited papers solid and sandwich plates and rotating disks are investigated assuming that the material is an ideal elastic plastic material without strain hardening. Plates made of hardening material were studied by Boyce [8], Hwang [31], Tanaka [92]. Wen [108], Kirs [37] considered work-hardening circular plates subjected to dynamic loading under different circumstances.

The use of the classical bending theory based on Kirchhoff hypotheses is justified in the case of thin plates and homogeneous materials. In more complicated cases the shear stresses must be taken into account as shown by Oblak [73], Nagai and Ito [71]. Sawczuk and Duszek [87] developed a similar concept for ideal plastic plates.

Wang et al [104, 105] established designs of rigid-plastic solid plates with a maximum thickness constraint.

Reddy and Wang [83] investigated relationships between the classical pure bending theory and the shear deformation theory applied to the bending of circular and annular plates. The full description of the shear deformation theory of plates and shells can be found in the book by Wang et al [103]. A variational approach to shear deformable plates within gradient elasticity was developed by Mousavi and Paavola

[67, 68].

One of the ways of increasing the ability of beams, plates and shells to carry external loads is to furnish these structural elements with additional supports. Evidently, it is reasonable to settle these supports at the optimal positions.

The problem of minimization of the compliance of elastic beams and determination of the optimal location of the additional support was first formulated by Mróz and Rozvany [70]. In paper Mróz and Rozvany [70], design of minimum compliance of beams is established in the case of quasistatic loading. Later, Szelag and Mróz [91], Åkesson and Olhoff [1], Chou et al [14] treated the problems of maximal eigenfrequency for a given stiffness with respect to the location of the additional support. Bojczuk and Mróz [6] developed a new method for simultaneous optimization of topology, configuration and cross-sectional dimensions of elastic beams and beam structures, extending earlier results by Garstecki and Mróz [21], Mróz and Lekszycki [69], also by Lepik [62]. In the subsequent papers by Bojczuk and Mróz [7] this concept was applied for the optimal design of active supports with force actuators. Olhoff and Åkesson [77] treated the stability of columns and Wang et al [106] studied the buckling of axisymmetric plates.

A lot of attention has been paid in the literature to the optimization of internal supports to beam, plate and shell structures in the case of inelastic materials. Probably the first paper in this area was written by Prager and Rozvany [81]. Systematic reviews of results obtained in earlier papers were presented by Rozvany [85], also by Lellep and Lepik [47]. Optimal design of circular cylindrical shells with additional supports was investigated by Lellep [42, 45] in the case of dynamic loading and an ideal plastic material. The behaviour of geometrically non-linear cylindrical shells with internal supports was studied in [43, 44, 45, 48].

Optimal design of axisymmetric plates and shells of various shape made of elastic and inelastic materials was investigated in [51, 56, 57, 58, 59]. Inelastic spherical and conical shells were studied in [56, 57, 58] whereas a stress strain analysis of an annular plate made of an elastic plastic material was presented in [50].

A design sensitivity analysis for the deflection of beam or plate structures was undertaken by Wang [107] in the case of simple supports located at given mesh nodes. Stiffened sector plates were studied in [98].

In the present work, an analytical method for determining the positions of rigid ring supports for circular plates has been developed. The analysis is confined to the axisymmetric response of elastic plates subjected to loads.

Plates and shells are widely used in various fields of technology and engineering. This is why it is very important to strive for the optimal shape of the plates, also for the optimal layout of supports and for the optimal distributions of stresses in the structures. This enables to save material of the structures. The behaviour of plates

and shells in the range of elastic deformations has been studied by many authors (see Reddy [82], Vinson [102], Ventsel and Krauthammer [101]).

The practical need for lightweight structures has increased the importance of investigations of composite materials, also sandwich plates and shells and of those manufactured from composites. The foundations of the analysis and design of sandwich structures were developed by Allen [2] and Plantema [79]. The stability problem of a three-layered plate with a soft core was solved by Pawlus [78]. The critical loads are obtained analytically and numerically. Elastic circular sandwich plates subjected to the ring load have been studied by Magnucki et al [65]. The comparison of the analytical, numerical and experimental results reveals small discrepancies between theoretical predictions and experimental data. These are probably due to the approximate determination of the mechanical properties of the core material. The influence of shear forces on the bending of circular plates was studied by Reddy and Wang [83].

A large number of books have been dedicated to the foundations of composite materials. It is worthwhile to mention, among others, the books by Herakovich [26], Jones [33], Daniel and Ishai [16], Gibson [22], Andreev and Nemirovskii [3], Tuttle [99].

Researchers and engineers often encounter the need for the optimization of structural elements in order to produce cheaper details and save materials. The problems of optimization of thin-walled plates and shells were investigated by Banichuk [4], Bendsøe [5], Kirsch [38], Cherkaev [13], Melerski [66], Olhoff [76, 12] in the case of elastic materials. The essential benchmark problems of this kind are presented in the books by Lellep [46], Brandt [9].

The optimization of structural elements made of inelastic materials was started by establishing the Drucker-Shield criterion in the form $\frac{D}{h} = \text{const}$ where D is the dissipation of the internal energy and h stands for the thickness of the plate (Drucker and Shield [17]). The Drucker-Shield criterion is based on the lower and upper bound theorems of limit analysis. In its original form it holds good in the case of ideal rigid plastic structures. This approach to the optimal design of structural elements is called “the optimality criteria-based design”.

Various other approaches based on the finite element method (FEM), variational methods, the principle of maximum and other methods were developed later.

Lepik [60, 61] is a pioneer in the application of the principle of maximum in the optimal design of rigid-plastic beams, plates and shells. In [60, 61] optimal design of inelastic circular plates was undertaken for the collapse load assuming that the thickness of the plate is constrained by the given upper and lower bounds. Lepik and Mróz [63, 64] developed new approaches to the optimal design of beams, plates and shells subjected to dynamic loading. Both the impulsive loading and the rectangular

pressure loading of beams with piecewise constant thickness were investigated and the optimal projects corresponding to different optimality criteria were developed.

Resorting to the principle of maximum, optimal design of circular plates subjected to the concentrated load was developed by Lellep [40].

An approach to the optimal design of geometrically non-linear inelastic beams and cylindrical shells was developed by Lellep [41, 44, 45] making use of variational methods of the theory of optimal control. This method appeared to be very effective in the determination of optimal locations for additional supports to beams and cylindrical shells [42, 43].

The current thesis is devoted to the analysis and optimization of circular and annular plates made of elastic plastic materials. It is assumed that the material obeys a piecewise linear yield condition and the associated gradientality law. The dissertation consists of five chapters.

In the first chapter of the thesis the governing equations for the analysis of axisymmetric plates are presented, provided the material is an ideal elastic plastic material.

In the second chapter the bending analysis of elastic plastic circular and annular plates is undertaken in the cases of the Tresca's yield criterion and the diamond criterion, respectively. The results of Chapter 2 are published in [49, 53, 55].

The elastic plastic response of an annular plate to the transverse pressure is studied in the third chapter. It is assumed that the plate is clamped at the inner edge and absolutely free at the outer edge. The results of Chapter 3 are published in [50].

In the fourth chapter an optimization procedure is developed for circular plates with additional ring supports. The results of Chapter 4 are published in [51, 52].

The fifth chapter of the thesis is devoted to the analysis and optimization of stepped plates made of an anisotropic composite material. The results of Chapter 5 are published in [54].

New results are presented in sections 2.4 – 2.8 of Chapter 2 and in Chapters 3–5.

CHAPTER 1

BASIC EQUATIONS AND CONCEPTS

In this chapter the governing equations for thin plates are presented. This system of equations consists of the equations of equilibrium and of the physical and geometrical relations of elastic and plastic regions of the thin-walled circular and annular plates. For the sake of simplicity, a thin-walled plate with constant thickness is considered in this chapter.

1.1 Equations of equilibrium

We consider axisymmetric deformations of a circular plate subjected to the axisymmetric transverse loading of intensity $P = P(r)$. Here r is the current radius e. g. the distance from the centre of the plate. As we are studying the axisymmetric response of the plate, all points lying at a circle with radius r have common displacements $W(r)$ in the transverse direction, as well as common deformations and curvatures κ_1 , κ_2 in the radial and circumferential directions, respectively. Note that the radial displacement will be neglected in the present study since the classical equations of the bending theory of thin plates will be used.

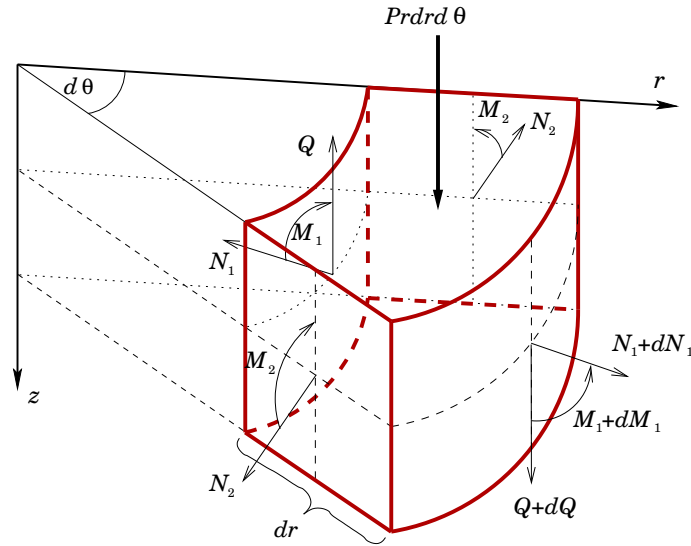


Figure 1.1: An element of the circular plate.

In the present study, we shall employ the linear theory of thin plates (see Reddy [82], Vinson [102]). According to this approach, one can treat the equilibrium of internal and external forces and couples on the basis of an undeformed element of the plate. Let M_1 , M_2 be the generalized couples called bending moments in the radial and circumferential directions, respectively. Bending moments M_1 , M_2 are the only generalized stress components contributing to the internal energy. Note that the membrane forces are assumed to be small so that one can neglect the membrane action of internal forces. Although the shear force Q may be finite, it does not contribute to the internal energy in the classical plate theory. The reason is that the corresponding strain component vanishes.

In the frameworks of the classical plate theory where axial symmetry is retained, the couples M_1 , M_2 with the forces Q and P form a system of moments and forces which keep the element of the plate in equilibrium. The equilibrium conditions of the plate element presented in Fig. 1.1 can be written as

$$\begin{aligned}\frac{d}{dr}(rN_1) - N_2 &= 0, \\ \frac{d}{dr}(rM_1) - M_2 - rQ &= 0, \\ \frac{d}{dr}(rQ) + P(r)r &= 0.\end{aligned}\tag{1.1}$$

Note that in the following, the influence of membrane forces N_1 , N_2 will be neglected.

1.2 Hooke's law

If the material of the plate is an ideal elastic material, the Hooke's law holds good. In the case of an isotropic elastic material the Hooke's law reads

$$\begin{aligned}\varepsilon_1 &= \frac{1}{E}[\sigma_1 - \nu(\sigma_2 + \sigma_3)]; & \gamma_{12} &= \frac{\tau_{12}}{G}; \\ \varepsilon_2 &= \frac{1}{E}[\sigma_2 - \nu(\sigma_1 + \sigma_3)]; & \gamma_{13} &= \frac{\tau_{13}}{G}; \\ \varepsilon_3 &= \frac{1}{E}[\sigma_3 - \nu(\sigma_1 + \sigma_2)]; & \gamma_{23} &= \frac{\tau_{23}}{G}.\end{aligned}\tag{1.2}$$

Here ε_j , γ_{ij} ($i = 1, 2, 3$, $j = 1, 2, 3$) stand for the strain components whereas σ_j , τ_{ij} ($i = 1, 2, 3$, $j = 1, 2, 3$) are the stress components; E is the Young's modulus, ν is the Poisson's ratio and $G = \frac{E}{2(1 + \nu)}$. In the case of plane stress state when

$\tau_{13} = \tau_{23} = \sigma_3 = 0$ one has

$$\begin{aligned}\varepsilon_1 &= \frac{1}{E}(\sigma_1 - \nu\sigma_2), \\ \varepsilon_2 &= \frac{1}{E}(\sigma_2 - \nu\sigma_1), \\ \gamma_{12} &= \frac{\tau_{12}}{G}\end{aligned}\tag{1.3}$$

or in the inverted form as

$$\begin{aligned}\sigma_1 &= \frac{E}{1-\nu^2}(\varepsilon_1 + \nu\varepsilon_2), \\ \sigma_2 &= \frac{E}{1-\nu^2}(\varepsilon_2 + \nu\varepsilon_1), \\ \tau_{12} &= G\gamma_{12}.\end{aligned}\tag{1.4}$$

The strain components can be expressed via the displacements u , v , w in the direction of coordinate axes, respectively. Making use of polar coordinates (now u is directed in the radial direction and v in the circumferential direction) one has

$$\begin{aligned}\varepsilon_1 &= \frac{\partial u}{\partial r}, \\ \varepsilon_2 &= \frac{u}{r} + \frac{1}{r} \frac{\partial v}{\partial \Theta}, \\ \gamma_{12} &= \frac{\partial v}{\partial r} - \frac{v}{r} + \frac{1}{r} \frac{\partial u}{\partial \Theta}.\end{aligned}\tag{1.5}$$

In the case of axisymmetric loading it is expected that the stress strain state is also axisymmetric, provided the boundary conditions at the edges of the plate are axisymmetric. Now the displacements do not depend on the polar angle Θ and one has

$$\begin{aligned}\varepsilon_1 &= \frac{du}{dr}, \\ \varepsilon_2 &= \frac{u}{r}, \\ \gamma_{12} &= \frac{dv}{dr} - \frac{v}{r}.\end{aligned}\tag{1.6}$$

According to Kirchhoff hypotheses one has (see Reddy [82], Vinson [102])

$$\begin{aligned}\varepsilon_1 &= \mathcal{K}_1, \\ \varepsilon_2 &= \mathcal{K}_2\end{aligned}\tag{1.7}$$

where z is the distance between a current point and the middle surface of the plate. Principal curvatures \varkappa_1, \varkappa_2 can be expressed as

$$\begin{aligned}\varkappa_1 &= -\frac{d^2 W}{dr^2}, \\ \varkappa_2 &= -\frac{1}{r} \frac{dW}{dr}\end{aligned}\tag{1.8}$$

where W is the transverse deflection or displacement in the z -axis of points lying on the middle surface.

Let us introduce the generalized stresses (bending moments)

$$\begin{aligned}M_1 &= \int_{-\frac{h}{2}}^{\frac{h}{2}} \sigma_1 z dz, \\ M_2 &= \int_{-\frac{h}{2}}^{\frac{h}{2}} \sigma_2 z dz, \\ M_{12} &= \int_{-\frac{h}{2}}^{\frac{h}{2}} \tau_{12} z dz\end{aligned}\tag{1.9}$$

and the shear force

$$Q = \int_{-\frac{h}{2}}^{\frac{h}{2}} \tau_{13} dz.\tag{1.10}$$

Substituting equations (1.4) with (1.7), (1.8) in (1.9) after integration one has

$$\begin{aligned}M_1 &= D(\varkappa_1 + \nu \varkappa_2), \\ M_2 &= D(\varkappa_2 + \nu \varkappa_1)\end{aligned}\tag{1.11}$$

where

$$D = \frac{Eh^3}{12(1 - \nu^2)}\tag{1.12}$$

in the case of a solid plate h denotes the total thickness. In the case of a sandwich plate

$$D = \frac{EhH^2}{2(1 - \nu^2)}.\tag{1.13}$$

In (1.13) H stands for the total thickness and h is the thickness of a carrying layer.

The stress strain state is determined according to equations (1.1). Substituting equations (1.11), (1.8) in formula (1.1) leads to a fourth order equation with respect

to the deflection W known from the theory of elastic plates (see Reddy [82], Vinson [102], Ventsel and Krauthammer [101])

$$\frac{1}{r} \frac{d}{dr} \left\{ r \frac{d}{dr} \left[\frac{1}{r} \frac{d}{dr} \left(r \frac{dW}{dr} \right) \right] \right\} = \frac{P(r)}{D}. \quad (1.14)$$

The general solution of this equation can be presented in the case $P = \text{const}$ as

$$W = \frac{Pr^4}{64D} + A_1 r^2 \ln r + A_2 r^2 + A_3 \ln r + A_4 \quad (1.15)$$

where $A_1 - A_4$ are the integration constants.

1.3 Yield criteria

The theories of plasticity are based on experimental observations regarding the behaviour of inelastic materials. The experiments show that in a simple tension test a rod remains elastic as far as the absolute value of the stress is less than a limit value, called the yield stress σ_0 . In this thesis it is assumed that the stress strain curve can be approximated by two straight lines shown in Fig. 1.2. Thus, according to this model, a one-dimensional body (a rod under tension) remains elastic if $|\sigma| < \sigma_0$.

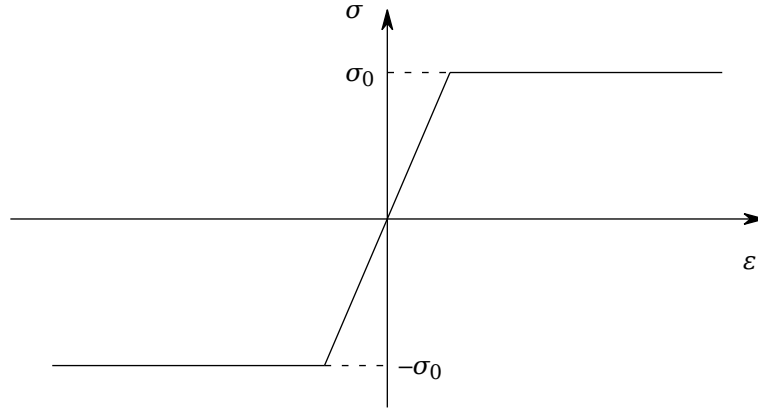


Figure 1.2: The stress strain curve.

However, in the general case the stress state of a material element can be represented by a point in a nine-dimensional stress space with coordinates σ_{ij} ($i = 1, 2, 3$,

$j = 1, 2, 3$). Theoretical considerations and experimental investigations show that around the origin of the stress space there exists a closed convex surface

$$\Phi_0(\sigma_{11}, \sigma_{12}, \dots, \sigma_{33}) = 0 \quad (1.16)$$

surrounding the region where elastic deformations take place. The points lying on this surface correspond to the points of the body where plastic deformations occur.

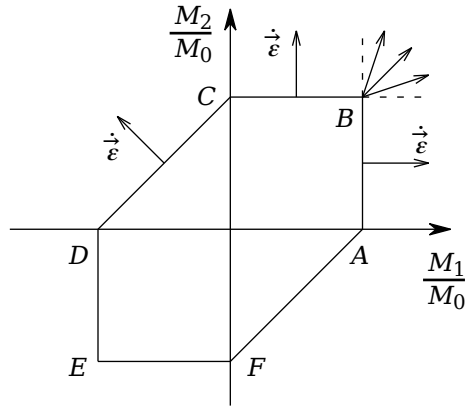


Figure 1.3: Tresca's yield hexagon.

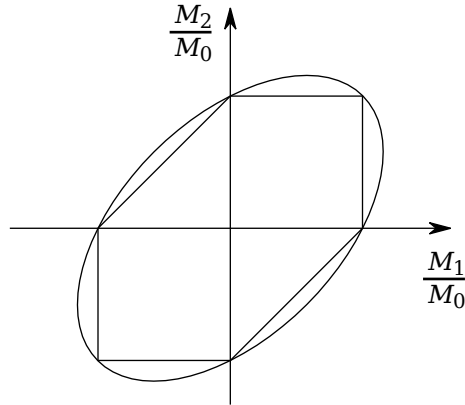


Figure 1.4: Von Mises yield ellipse.

In the case of axisymmetric thin-walled plates, the yield surface (1.16) can be expressed via bending moments as

$$\Phi(M_1, M_2, M_0) = 0 \quad (1.17)$$

where M_0 stands for the yield moment. Evidently

$$M_0 = \frac{\sigma_0 h^2}{4} \quad (1.18)$$

for solid plates and

$$M_0 = \sigma_0 hH \quad (1.19)$$

for sandwich plates.

The most often used yield criteria are the Tresca's (Fig. 1.3) and von Mises (Fig. 1.4) conditions.

1.4 Associated flow rule

In the general case the yield criterion $\Phi \leq 0$ holds good. In an elastic region one has $\Phi < 0$ and in a plastic region $\Phi = 0$. In the theory of plasticity it is shown that in a plastic region of a body where $\Phi = 0$ the strain rate vector $\dot{\epsilon}$ is directed outwards the yield surface (see Chakrabarty [11], Kaliszky [35], Sawczuk and Sokół-Supel [88]). Thus

$$\dot{\epsilon}_{ij} = \frac{\lambda \partial \Phi}{\partial \sigma_{ij}} \quad (1.20)$$

for $i = 1, 2, 3, j = 1, 2, 3$. In equation (1.20) λ stands for a non-negative scalar multiplier and the dot denotes the derivative with respect to time or the loading parameter. Using the generalized stresses and the yield surface in the form (1.17) one has

$$\begin{aligned} \kappa_1 &= \frac{\lambda \partial \Phi}{\partial M_1}, \\ \kappa_2 &= \frac{\lambda \partial \Phi}{\partial M_2} \end{aligned} \quad (1.21)$$

where κ_1, κ_2 stand for the curvatures.

At the non-regular points of the yield surface the strain rate vector is formed as a linear combination with unknown coefficients of outward normals to the adjacent portions of the yield surface.

Note that in the "deformation theory" of plasticity, the strain components themselves are used instead of strain rates.

Let us consider the case where the behaviour of the material in the plastic stage corresponds to the Tresca's yield criterion (Fig. 1.3) and to the associated gradientality law in more detail. The latter means that if the stress point is lying at the edge of the Tresca's hexagon then the vector of curvatures with components (1.8) is directed parallel to the external normal to the hexagon. It will be shown that in the case of a circular plate subjected to unidirectional transverse loading, the yield regime $M_2 = M_0$ takes place, where M_0 stands for the yield moment.

If the stress state of the plate corresponds to an internal point of the side BC (Fig. 1.3) of the yield hexagon, then according to the gradientality law $\kappa_1 = 0, \kappa_2 \geq 0$. Thus

$$\frac{d^2 \dot{W}}{dr^2} = 0 \quad (1.22)$$

in this case. Making use of the deformation theory, the general solution of the equation (1.22) can be presented as

$$W = Ar + B \quad (1.23)$$

where A and B are the constants of integration.

If the stress strain state of the plate in a certain region corresponds to a non-regular point of the yield curve (for instance, the corner point B in Fig. 1.3), then the strain rate vector lies inside the angle formed by external normals to crossing sides.

At the point B of the Tresca's hexagon (Fig. 1.3) $M_1 = M_2 = M_0$ and the associated yield law states that $\kappa_1 \geq 0, \kappa_2 \geq 0$. Thus the exact expressions of strain rates remain unknown here. Similar conclusions can be drawn in the case of the diamond and the square yield criteria.

Note that if the stress strain state corresponds to an interior point of the yield hexagon (Fig. 1.3) then the plate material remains elastic in this region and Hooke's law holds good.

CHAPTER 2

BENDING OF ELASTIC PLASTIC PLATES

2.1 Preliminaries and basic hypotheses

Let us consider the quasistatic behaviour of an elastic plastic circular plate of radius R under the lateral pressure of intensity P . It is assumed that the plate is of sandwich type consisting of the carrying layers of thickness h and a core material between the rims. The thickness of the layer of the core material is H . We assume that

$$h = h_j, \quad (2.1)$$

for $r \in (a_j, a_{j+1})$; $j = 0, \dots, n$. The quantities a_j, h_j are treated as preliminarily known parameters. For the sake of convenience we take $a_0 = 0$; $a_{n+1} = R$ (see Fig. 2.1). The response of the plate to the external loading will be prescribed by the classical plate theory. The generalized stress components contributing to the strain energy are the bending moments M_1, M_2 in the radial and hoop direction defined by (1.9). The curvatures κ_1, κ_2 which can be determined via the transverse deflection $W = W(r)$ are the corresponding strain components. It is assumed that the radial

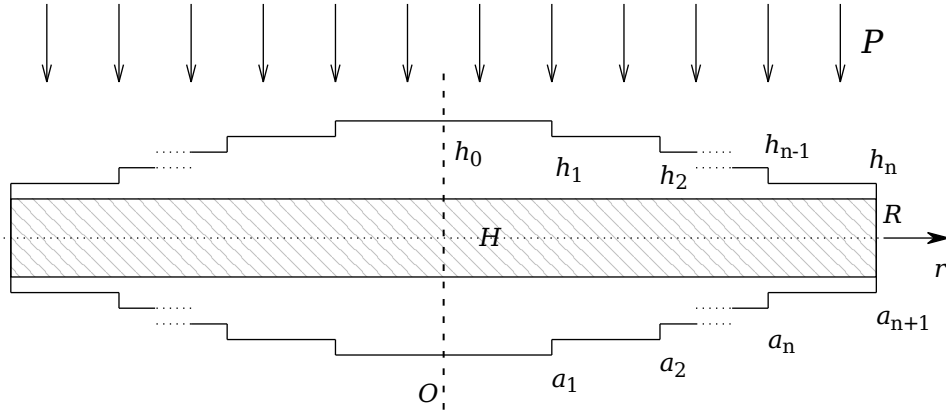


Figure 2.1: Cross section of the stepped circular plate.

bending moment M_1 as well as the shear force Q , deflection W are continuous for each $r \in (0, R)$. However, the deflection slope dW/dr may have discontinuities at sections where $M_1 = \pm M_0$ (see Chakrabarty [11], Kachanov [34], Yu and Zhang

[109]). It means that

$$[W(a_j)] = 0, \quad (2.2)$$

$$[M_1(a_j)] = 0$$

and

$$(|M_1(a_j)| - M_0) \left[\frac{dW(a_j)}{dr} \right] = 0. \quad (2.3)$$

In (2.2) and henceforth the square brackets denote finite jumps of discontinuous functions at the given point. According to this notation

$$[z(a)] = z(a + 0) - z(a - 0) \quad (2.4)$$

where $z(a \pm 0)$ stand for the right-hand and left-hand limits of the function z , respectively.

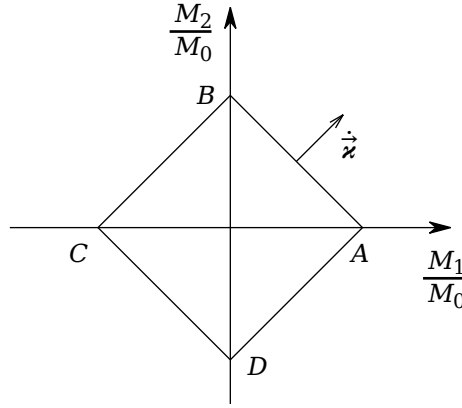


Figure 2.2: Diamond yield criterion.

The aim of this chapter is to determine the stress strain state of the plate for the initial elastic and subsequent elastic plastic stages of loading.

If the load intensity is high enough, plastic deformations occur in certain regions. Now the plate is divided into elastic and plastic regions. Let us denote these regions S_e and S_p , respectively. In a plastic region the stress state corresponds to a point lying on the yield surface (or a yield curve). It is assumed that the yield condition can be presented by the diamond $ABCD$ shown in Fig. 2.2. Here M_{0j} denotes the yield moment. In the case of a sandwich plate with the rim thickness h_j

$$M_{0j} = \sigma_0 h_j H, \quad (2.5)$$

σ_0 being the yield stress of the material. Since $M_1 \geq 0$, $M_2 \geq 0$, in most cases one can assume that in the plastic region

$$M_1 + M_2 = M_{0j} \quad (2.6)$$

for $r \in (a_j, a_{j+1})$. Note that the diamond yield criterion was suggested by Jones [32] for an approximate solution of dynamic problems of plastic plates.

According to the associated flow rule on the side AB of the diamond, one has $\dot{\kappa}_1 = \dot{\kappa}_2$ where dots denote the differentiation with time or a time-like parameter. Making use of (1.8) and the deformation-type theory of plasticity, the gradientality law results in the equation

$$\frac{d^2 W}{dr^2} - \frac{1}{r} \frac{dW}{dr} = 0. \quad (2.7)$$

2.2 Integration of governing equations in elastic regions

Assume that the portion of the plate for $r \in (a_j, a_{j+1})$ is in the pure elastic stress strain state. For the determination of stresses, strains and displacements one has the equations (1.1)–(1.11). Substituting (1.11) with the help of (1.8) in the equilibrium equations (1.1) results in

$$\frac{1}{r} \frac{d}{dr} \left\{ r \frac{d}{dr} \left[\frac{1}{r} \frac{d}{dr} \left(r \frac{dW}{dr} \right) \right] \right\} = \frac{P(r)}{D_j} \quad (2.8)$$

for $r \in (a_j, a_{j+1})$ where

$$D_j = \frac{Eh_j H^2}{2(1 - \nu^2)}. \quad (2.9)$$

This is true under the condition that this interval belongs to the set S_e .

One can easily recheck that the general solution of the equation (2.8) is

$$W = A_{1j} r^2 \ln r + A_{2j} r^2 + A_{3j} \ln r + A_{4j} + \frac{Pr^4}{64D_j} \quad (2.10)$$

where $A_{1j} - A_{4j}$ are arbitrary constants.

Calculating the bending moments according to (1.11) and making use of (1.8), (2.10)

one eventually obtains

$$\begin{aligned}
M_1 &= -D_j \left\{ \frac{Pr^2(3+\nu)}{16D_j} + A_{1j}[2\ln r + 3 + \nu(2\ln r + 1)] \right. \\
&\quad \left. + 2A_{2j}(1+\nu) + \frac{A_{3j}(\nu-1)}{r^2} \right\}, \\
M_2 &= -D_j \left\{ \frac{Pr^2(1+3\nu)}{16D_j} + A_{1j}[2\ln r + 1 + \nu(2\ln r + 3)] \right. \\
&\quad \left. + 2A_{2j}(1+\nu) + \frac{A_{3j}(1-\nu)}{r^2} \right\}.
\end{aligned} \tag{2.11}$$

2.3 Elastic stage of deformation

In the case of smaller values of the intensity of the transverse pressure the plate remains elastic. In the elastic stage the stress strain state of the plate is defined by (2.10) and (2.11). Let us consider now a particular case of the problem posed above when $n = 1$ and the thickness distribution is

$$h = \begin{cases} h_0, & r \in [0, a] \\ h_1, & r \in [a, R]. \end{cases} \tag{2.12}$$

Let the applied loading be of constant intensity. For the sake of concreteness let us assume that the plate is simply supported at the edge. Thus at the boundary of the plate

$$M_1(R) = 0, \tag{2.13}$$

$$W(R) = 0.$$

According to (2.1) and (2.10) – (2.12) one has to take $j = 0$, if $r \in [0, a]$ and $j = 1$, if $r \in [a, R]$.

Calculating the shear force for the elastic plate one reaches the relation

$$Q = \frac{1}{r} \left(\frac{d}{dr}(rM_1) - M_2 \right). \tag{2.14}$$

Substituting M_1 , M_2 from (2.11) in (2.14) one can see that the shear force is continuous all over the plate if constants $A_{1j} = 0$.

Evidently, $M_1(0)$ must be finite. Thus it follows from (2.10) that $A_{30} = 0$. For the determination of the rest of unknown constants A_{20} , A_{40} , A_{21} , A_{31} , A_{41} , one can use

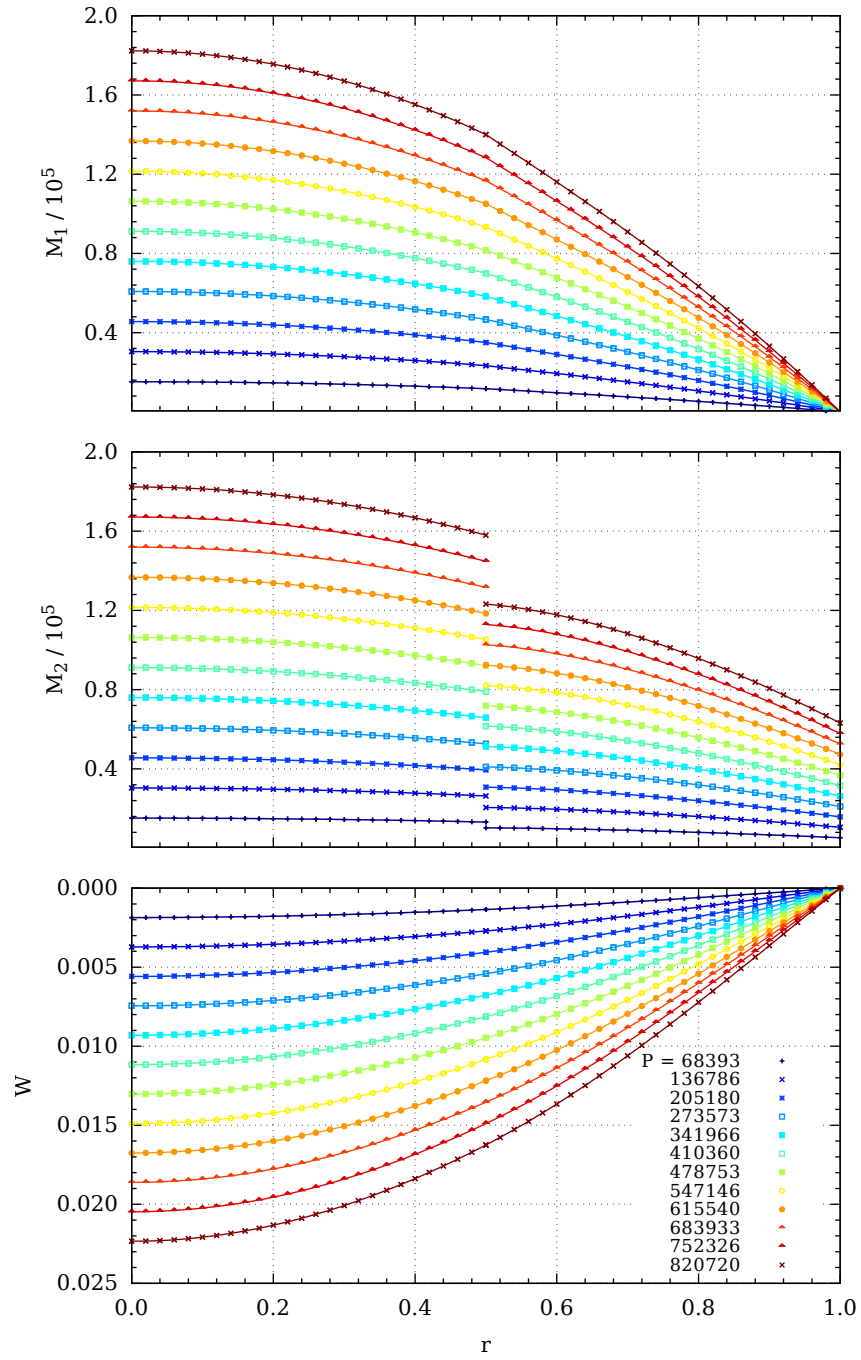


Figure 2.3: Bending moments and deflections of the stepped elastic plate.

the boundary conditions (2.13) and the continuity requirements (2.2), (2.3). Since during the elastic stage $M_1 \neq M_0$ one has

$$\begin{aligned} [W(a)] &= 0, \\ [M_1(a)] &= 0, \\ \left[\frac{dW(a)}{dr} \right] &= 0. \end{aligned} \quad (2.15)$$

From the first equation in (2.13) one can express the constant

$$A_{21} = \frac{-PR^2(3 + \nu)}{32D_1(1 + \nu)} + \frac{A_{31}(1 - \nu)}{2R^2(1 + \nu)}. \quad (2.16)$$

Substituting the constant A_{21} from equation (2.16) in the second equation in (2.13) one can determine

$$A_{41} = \frac{PR^4(5 + \nu)}{64D_1(1 + \nu)} - \frac{A_{31}[1 - \nu + 2(1 + \nu) \ln R]}{2(1 + \nu)}. \quad (2.17)$$

Making use of the continuity of the bending moment M_1 at $r = a$ in (2.15) and equation (2.16) one can express

$$A_{20} = \frac{-PR^2(3 + \nu)}{32D_0(1 + \nu)} + \frac{A_{31}D_1(1 - \nu)(a^2 - R^2)}{2D_0(1 + \nu)R^2a^2}. \quad (2.18)$$

Substituting the constants A_{20} , A_{21} and A_{41} in the first equation in (2.15) one can obtain

$$\begin{aligned} A_{40} = & \frac{P[a^4(1 + \nu)(D_0 - D_1) + R^4D_0(5 + \nu) + 2R^2a^2(3 + \nu)(D_1 - D_0)]}{64D_0D_1(1 + \nu)} \\ & + \frac{A_{31}\{(1 - \nu)[(R^2 - a^2)D_1 + a^2D_0] + D_0R^2[2(1 + \nu)(\ln a - \ln R) - 1 + \nu]\}}{2D_0(1 + \nu)R^2}. \end{aligned} \quad (2.19)$$

Finally, making use of equations (2.18), (2.16) and the third equation in (2.15) one can express

$$A_{31} = \frac{Pa^2R^2(D_1 - D_0)[a^2(1 + \nu) - R^2(3 + \nu)]}{16D_1\{D_0[a^2(1 - \nu) + R^2(1 + \nu)] + D_1(\nu - 1)(a^2 - R^2)\}}. \quad (2.20)$$

Substituting (2.16) – (2.20) in (2.10) and (2.11) one can express the distributions of deflections and bending moments for the elastic stage of deformation. These distributions are shown in Fig. 2.3 for different values of the transverse pressure. It can

be seen from Fig. 2.3 that M_1 and W are continuous for $r \in [0, R]$ whereas the hoop moment M_2 is discontinuous at $r = a$ (Fig. 2.3 corresponds to the case $a = 0.5R$; $R = 1$ m; $\nu = 0.3$; $E = 2 \cdot 10^{11}$ Pa; $\sigma_0 = 4 \cdot 10^8$ Pa; $h_0 = 0.01$ m; $h_1 = 0.007$ m; $H = 0.05$ m).

2.4 Optimization of stepped elastic circular plate

Let us consider the problem of the minimization of the maximal deflection $W_0 = W(0)$ under the condition that the material volume V of the plate is constrained.

The deflection $W(0)$ is a function of design parameters; $W_0 = W_0(a_1, \dots, a_n, h_0, \dots, h_n)$. The constrained minimum of W_0 can be defined employing the extended function

$$J_* = W_0(a_1, \dots, a_n, h_0, \dots, h_n) + \lambda(V - \bar{V}\pi R^2 h_0) \quad (2.21)$$

where λ is an unknown Lagrangian multiplier.

The necessary optimality conditions of (2.21) can be written as

$$\begin{aligned} \frac{\partial J_*}{\partial a_i} &= 0; & i &= 1, \dots, n \\ \frac{\partial J_*}{\partial h_j} &= 0; & j &= 0, \dots, n \\ \frac{\partial J_*}{\partial \lambda} &= 0. \end{aligned} \quad (2.22)$$

The system (2.22) consists of $2n + 2$ algebraic equations. These allow determining $2n + 2$ unknown parameters a_i ($i = 1, \dots, n$), h_j ($j = 0, \dots, n$) and λ for each given volume \bar{V} of the plate.

The efficiency of the design established above (see Table 2.1) is assessed by the ratio

$$e = \frac{W_0}{W_*}, \quad (2.23)$$

W_* being the maximum deflection of the reference plate of constant thickness $h_* = \frac{V}{\pi R^2}$. The values of the coefficient e are accommodated in Table 2.1 together with optimal values $\alpha = \frac{a}{R}$ and $\gamma = \frac{h_1}{h_0}$. In the first column of Table 2.1 the values of the relative volume of the plate $\bar{V} = \frac{V}{\pi R^2 h_0}$ are presented. It reveals from Table 2.1 that for smaller values of \bar{V} the deflection of the reference plate of constant thickness W_* is larger, as might be expected. If \bar{V} increases then the optimal value of α also increases. The maximal deflection of the optimized plate decreases if the quantity \bar{V} increases.

Table 2.1: Optimal values of parameters.

$\frac{\bar{V}}{\pi}$	α	γ	$W_0 \cdot 10^6$	$W_* \cdot 10^6$	e
0.45	0.490363	0.275881	4.38282	5.15278	0.85057
0.50	0.549226	0.284027	3.86136	4.6375	0.83264
0.55	0.605052	0.290123	3.46249	4.21591	0.82129
0.60	0.658147	0.294337	3.15763	3.86458	0.81707
0.65	0.708775	0.296677	2.92554	3.56731	0.82010
0.70	0.757151	0.296968	2.74998	3.3125	0.83018
0.75	0.803436	0.294764	2.61823	3.09167	0.84687
0.80	0.847728	0.289161	2.5201	2.89844	0.86947
0.85	0.890033	0.278294	2.44735	2.72794	0.89714
0.90	0.930189	0.257875	2.39317	2.57639	0.92888
0.95	0.967623	0.21513	2.35191	2.44079	0.96358
0.99	0.99431	0.118785	2.32495	2.34217	0.99265

One can see from Table 2.1 that for $\frac{\bar{V}}{\pi} = 0.45$ the optimal values of parameters α and γ are approximately $\alpha = 0.4904$, $\gamma = 0.2759$, $h_0 = 0.01$ m, $H = 0.05$ m. In this case the maximal deflection of the stepped plate is 15% less than that of the reference plate of constant thickness.

2.5 Solution of governing equations in plastic regions in the case of diamond yield criterion

In a plastic region one has to satisfy the equations (2.6), (2.7) and the equilibrium equations (1.1). Integrating (2.7) one easily obtains

$$W = Ar^2 + B, \quad (2.24)$$

A and B being arbitrary constants. For determination of stress components one can use equations (1.1) and (2.6). The third equation in the system (1.1) gives after integration

$$Q = -\frac{1}{r} \int P(r) r dr + C_1. \quad (2.25)$$

It is worthwhile to mention that the shear force must be continuous for $r \in [0, R]$. However, the function $P = P(r)$ can be discontinuous. In the particular case when $P(r) = \text{const}$ instead of (2.25) one has for $r \in [0, R]$

$$Q = -\frac{Pr}{2} \quad (2.26)$$

where the symmetry condition $Q(0) = 0$ has been taken into account.

Substitution of equations (2.6) and (2.25) in the second equation in the system (1.1) leads to the linear differential equation

$$\frac{dM_1}{dr} + \frac{2M_1}{r} = \frac{M_{0j}}{r} - \frac{1}{r} \int Prdr + C_1 \quad (2.27)$$

for $r \in (0, a)$. In order to find the general solution for equation (2.27) let us first consider the corresponding homogeneous equation. Evidently, the general solution of it has the form

$$M_h = \frac{C}{r^2}. \quad (2.28)$$

The method of variation of the constant in equations (2.27), (2.28) yields

$$C(r) = \frac{M_{00}r^2}{2} - \int \left(r \cdot \frac{Pr^2}{2} \right) dr + \frac{C_1r^3}{3} + C_2. \quad (2.29)$$

Thus the radial bending moment in a plastic region $(0, y)$ is defined as

$$M_1 = \frac{M_{00}}{2} - \frac{1}{r^2} \int \frac{Pr^3}{2} dr + \frac{C_1r}{3} + \frac{C_2}{r^2}. \quad (2.30)$$

Integration constants C_1, C_2 in equation (2.30) can be determined using the continuity requirements of M_1 at the boundary of the plastic zone. If, for instance, the plastic region is located near the centre of the plate for $r \in [0, \eta R]$ where $\eta < 1$ then evidently $C_2 = 0$ because otherwise the moment M_1 is not limited. The constant C_1 also vanishes because the shear force $Q(0) = 0$ in the case of the plate of the constant thickness. Thus in this case

$$M_1 = \frac{M_{00}}{2} - \frac{Pr^2}{8}. \quad (2.31)$$

Here M_{00} denotes the limit moment for the portion of the plate with thickness h_0 . The circumferential moment can be found according to equations (2.6), (2.31) as

$$M_2 = \frac{M_{00}}{2} + \frac{Pr^2}{8}. \quad (2.32)$$

2.6 Elastic plastic solution in the case of material obeying the diamond criterion

During the subsequent increasing of the load intensity, the middle surface of the plate is divided into elastic and plastic regions. Plastic deformations occur in the

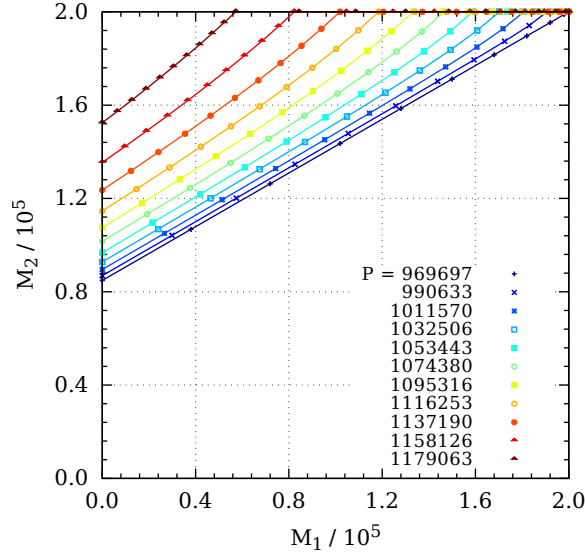


Figure 2.4: Stress profile (Tresca's criterion).

central part of the plate with radius y . However, the outward part of the plate remains elastic. The deflection in elastic region is defined by equation (2.10) and moments by equations (2.11). Here one has to take $j = 0$, if $r \in [y, R]$.

In the central plastic region the stress profile lies on the yield curve. Principal moments are defined by equations (2.31), (2.32).

For determination of the unknown constants A , B , A_{20} , A_{30} , A_{40} and y , one can use the boundary conditions (2.13) and the continuity conditions at $r = y$

$$\begin{aligned}
 [W(y)] &= 0, \\
 [M_1(y)] &= 0, \\
 \left[\frac{dW(y)}{dr} \right] &= 0, \\
 [M_2(y)] &= 0.
 \end{aligned} \tag{2.33}$$

Making use of the second and the fourth continuity condition in the system (2.33) one can determine the constants

$$A_{20} = -\frac{Py^2(\nu + 1) + 4M_0}{16D_0(1 + \nu)} \tag{2.34}$$

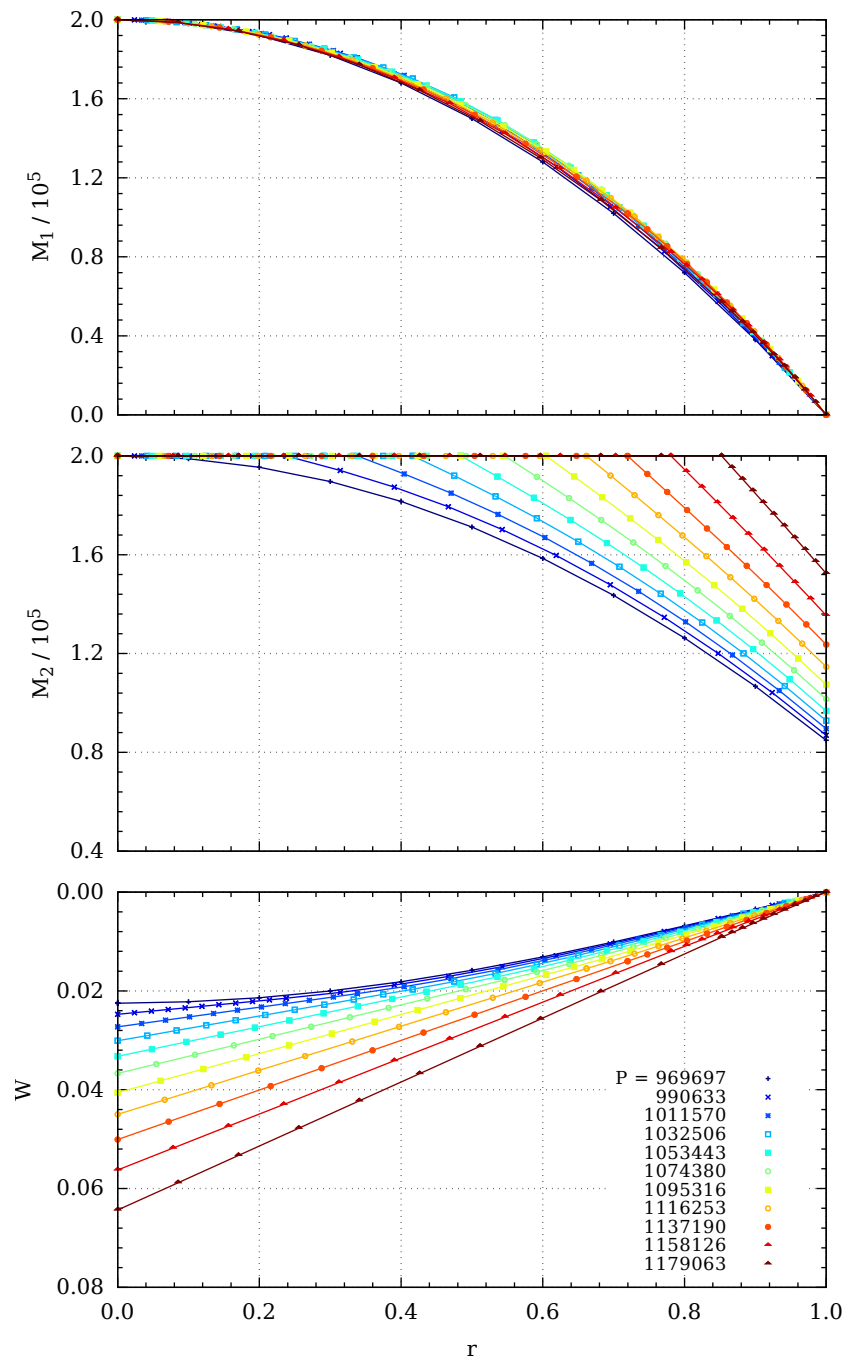


Figure 2.5: Bending moments and deflections (Tresca's criterion).

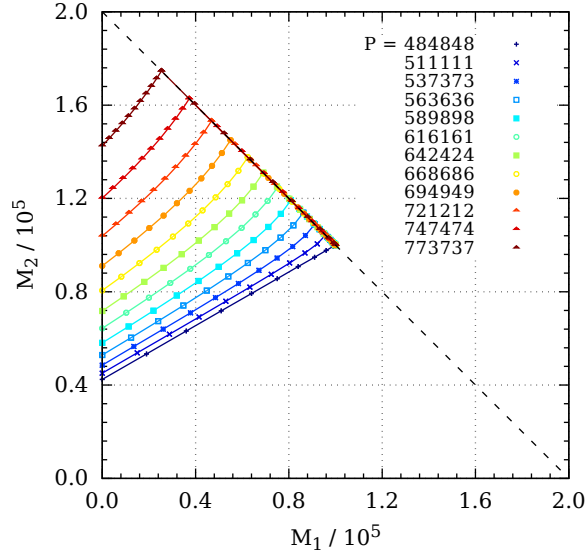


Figure 2.6: Stress profile (diamond criterion).

and

$$A_{30} = \frac{Py^4(\nu + 1)}{16D_0(\nu - 1)}. \quad (2.35)$$

From the third continuity condition in the system (2.33) one can express the constant

$$A = \frac{Py^2(\nu + 1) - 4M_0(\nu - 1)}{16D_0(\nu^2 - 1)}. \quad (2.36)$$

For determining the constant one can use the second boundary condition in equations (2.13). This results in

$$A_{40} = \frac{1}{64D_0(\nu^2 - 1)} \left\{ 4R^2(\nu - 1)[Py^2(\nu + 1) + 4M_0] - 4(\nu + 1)^2y^4P \ln R - PR^4(\nu^2 - 1) \right\} \quad (2.37)$$

Making use of the first continuity condition in the system (2.33) one can find the constant

$$B = \frac{Py^4[(\nu + 1) \ln y - \nu]}{16D_0(\nu - 1)} + \frac{1}{64D_0(\nu^2 - 1)} \left\{ 4R^2(\nu - 1) \cdot [Py^2(\nu + 1) + 4M_0] - 4(\nu + 1)^2y^4P \ln R + P(\nu^2 - 1)(y^4 - R^4) \right\}. \quad (2.38)$$

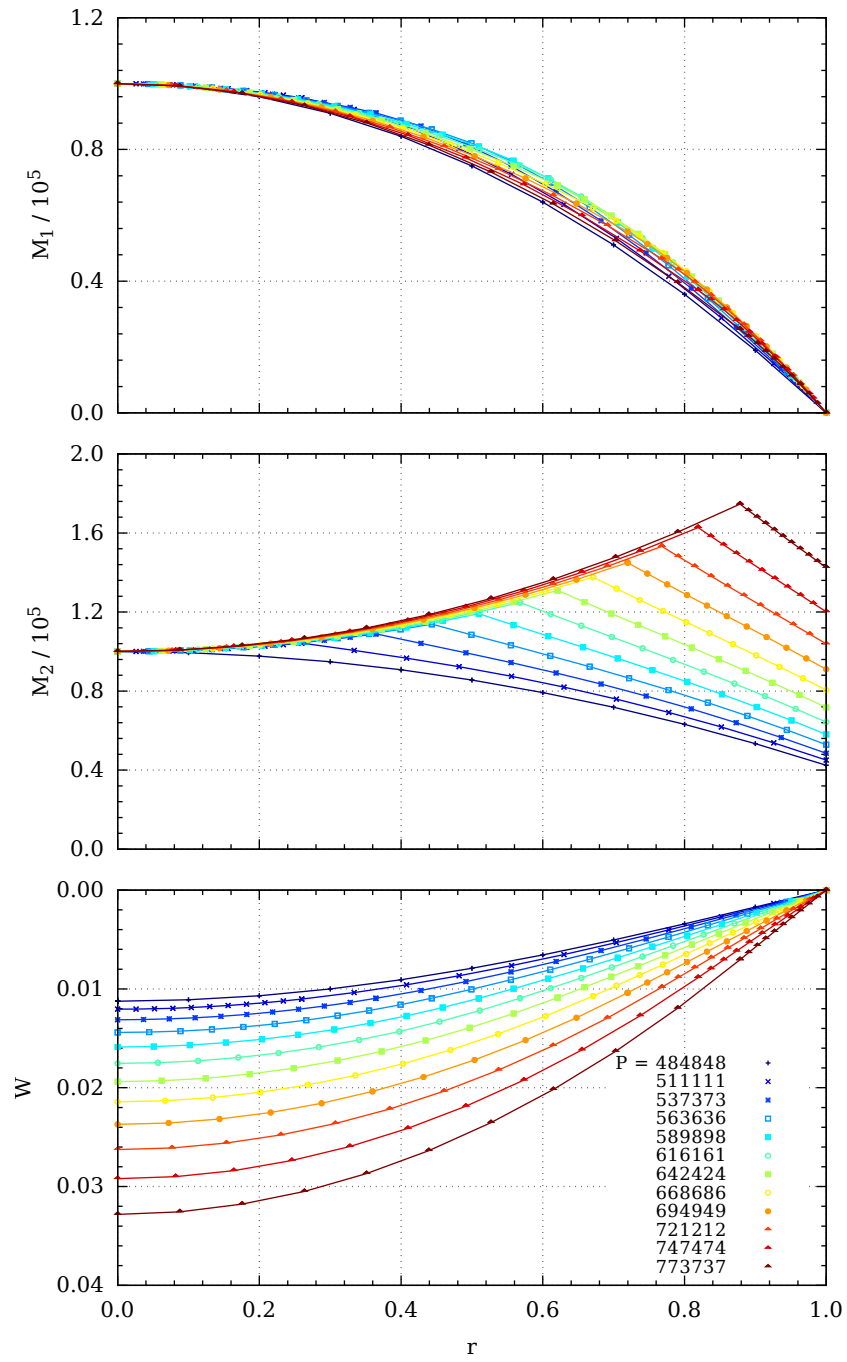


Figure 2.7: Bending moments and deflections (diamond criterion).

Finally, for expressing the constant y one can substitute (2.34) and (2.35) in the first boundary condition in equations (2.13). This leads to the equation

$$P(\nu + 1)y^4 - 2(\nu + 1)PR^2y^2 - 8M_0R^2 + PR^4(3 + \nu) = 0. \quad (2.39)$$

It is easy to solve the biquadratic equation (2.39) and get the constant

$$y = \sqrt{R^2 \pm \sqrt{\frac{-2R^2(PR^2 - 4M_0)}{P(\nu + 1)}}}. \quad (2.40)$$

Evidently, only the choice of the sign “minus” in (2.40) leads to a realistic solution.

The results of calculations are presented in Fig. 2.6 and Fig. 2.7 for different values of the transverse pressure. Fig. 2.4 – Fig. 2.8 correspond to the case $R = 1$ m; $\nu = 0.3$; $E = 2 \cdot 10^{11}$ Pa; $\sigma_0 = 4 \cdot 10^8$ Pa; $h_0 = 0.01$ m; $H = 0.05$ m. Comparing the results presented in Fig. 2.5 and Fig. 2.7 one can see that the plate made of a Tresca’s material is stronger than the plate corresponding to the diamond yield criterion. One can make the same conclusion observing Fig. 2.8. Although the hoop moment distributions are quite different in these cases the shapes of radial moments are similar. However, the moments are of different size in these cases.

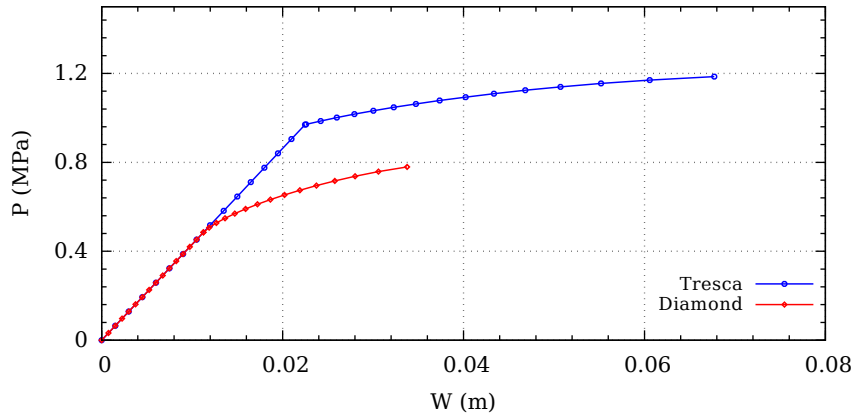


Figure 2.8: Load-deflection relations of circular plates.

2.7 Elastic plastic bending of an annular plate

Elastic plastic deformations of an annular plate with the radii a and R will be studied (see Fig. 2.9). The plate is subjected to the distributed transverse loading of intensity

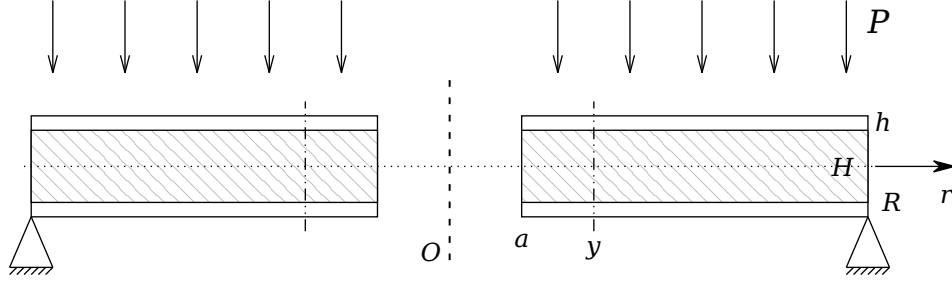


Figure 2.9: Cross section of the annular plate.

$P = P(r)$. Assume that the outer edge is simply supported whereas the inner edge of the plate is completely free. Therefore, at the outer edge the transverse deflection W and the radial bending moment M_1 must vanish. The radial bending moment is zero at the inner edge as well. Thus, the boundary conditions are at the outer edge

$$\begin{aligned} W(R) &= 0, \\ M_1(R) &= 0 \end{aligned} \quad (2.41)$$

and at the inner edge

$$\begin{aligned} M_1(a) &= 0, \\ Q(a) &= 0 \end{aligned} \quad (2.42)$$

where Q is the shear force. Note that the hoop moment M_2 can take arbitrary values at the edges. For the sake of simplicity it is assumed that the plate is of the sandwich type. The aim of this section is to determine the distributions of bending moments M_1 , M_2 and the transverse deflection W for the different magnitudes of the transverse load. It is expected that in the range of low loadings the plate is fully elastic and with the subsequent increase in the load level elastic plastic deformations occur.

2.7.1 Elastic stage of deformation

In the case of low stress level the plate remains elastic and the Hooke's law holds good. The stresses are coupled with external loads by the equilibrium equations (1.1). In the case $N_1 = N_2 = 0$ equations (1.1) can be presented as

$$\frac{d}{dr}(rM_1) - M_2 - rQ = 0 \quad (2.43)$$

and

$$\frac{d}{dr}(rQ) = -P(r)r. \quad (2.44)$$

In the present case it is assumed that $P(r) = \text{const.}$ This allows integrating the last equation. The solution of 2.44 satisfying the boundary condition (2.42) can be presented as

$$Q = -\frac{P(r^2 - a^2)}{2r}. \quad (2.45)$$

It can be rechecked that the solution of (1.14) satisfying (2.41) is

$$W = \frac{P(r^4 - R^4)}{64D} + A_1(r^2 \ln r - R^2 \ln R) + A_2(r^2 - R^2) + A_3 \ln \frac{r}{R}, \quad (2.46)$$

$A_1 - A_3$ being arbitrary constants. However, calculating the shear force Q from (2.43) making use of (1.11), (1.8), (2.46) and comparing with (2.45) one can see that

$$A_1 = -\frac{Pa^2}{8D}. \quad (2.47)$$

Substituting (2.46) in (1.11) one can determine the bending moments

$$M_1 = -\frac{Pr^2(3 + \nu)}{16} + \frac{Pa^2[2(1 + \nu) \ln r + 3 + \nu]}{8} - D \left[2A_2(1 + \nu) + \frac{A_3(\nu - 1)}{r^2} \right] \quad (2.48)$$

and

$$M_2 = -\frac{Pr^2(1 + 3\nu)}{16} + \frac{Pa^2[2(1 + \nu) \ln r + 1 + 3\nu]}{8} - D \left[2A_2(1 + \nu) + \frac{A_3(1 - \nu)}{r^2} \right]. \quad (2.49)$$

Applying the boundary conditions (2.41), (2.42) to (2.48) one can define

$$A_2 = \frac{P}{32D(1 + \nu)(R^2 - a^2)} \cdot \left\{ (3 + \nu)(a^4 - R^4) + 2a^2[(R^2 - a^2)[2(1 + \nu) \ln a + 3 + \nu] - 2R^2(1 + \nu)(\ln a - \ln R)] \right\}, \quad (2.50)$$

$$A_3 = \frac{Pa^2R^2[(3 + \nu)(R^2 - a^2) + 4a^2(1 + \nu)(\ln a - \ln R)]}{16D(\nu - 1)(R^2 - a^2)}. \quad (2.51)$$

2.7.2 Elastic plastic stage of deformation

The plate remains pure elastic while the stress profile lies entirely inside the Tresca's yield hexagon (Fig. 1.3). During the elastic stage the inequalities

$$|M_1| \leq M_0, \quad |M_2| \leq M_0, \quad |M_1 - M_2| \leq M_0 \quad (2.52)$$

are satisfied as strict inequalities. The elastic plastic stage begins at the load level $P = P_1$ when the stress profile in the plane of the bending moments reaches the yield locus. The analysis shows that the stress profile reaches the side BC of the yield hexagon where $M_2 = M_0$. The maximum of the hoop moment is achieved at the inner edge of the plate and thus, the quantity P_1 can be calculated from the equation $M_2(a) = M_0$. Therefore,

$$P_1 = \frac{8M_0(R^2 - a^2)}{R^4(3 + \nu) + 4a^2R^2[(1 + \nu)(\ln a - \ln R) - 1] + a^4(1 - \nu)}. \quad (2.53)$$

During the elastic plastic stage the plate is divided into two parts. In the inner part (a, y) plastic deformations take place, whereas the region (y, R) remains elastic. Let us consider the regions separately.

Plastic region, $r \in (a, y)$

For $r \in (a, y)$ the stress profile lies on the side $M_2 = M_0$ of the yield hexagon (Fig. 1.3). Substituting $M_2 = M_0$ in (2.43) and taking (2.45) into account one obtains for $r \in (a, y)$

$$rM_1 - rM_0 + \frac{P}{2} \left(\frac{r^3}{3} - a^2r \right) = C, \quad (2.54)$$

C being an arbitrary constant. Due to the boundary condition (2.42)

$$C = -aM_0 - \frac{Pa^3}{3}. \quad (2.55)$$

Thus (2.54) can be put into the form

$$M_1 = \frac{r - a}{r} \left[M_0 - \frac{P(r^2 + ar - 2a^2)}{6} \right]. \quad (2.56)$$

It is worthwhile to emphasize that (2.56) holds good for $r \in (a, y)$. The deflection W is expressed by the formula (1.23).

Elastic region, $r \in (y, R)$

In the elastic region of the plate the relations (2.46) – (2.49) hold good. However, (2.50) and (2.51) are not valid. For the determination of unknown constants A_2 , A_3 and A , B one can use the boundary conditions at $r = R$, also the continuity requirements of quantities W , $\frac{dW}{dr}$, M_1 , M_2 at $r = y$. The requirements $M_1(R) = 0$ and $M_2(y) = M_0$ give with the help of (2.48), (2.49)

$$\begin{aligned} & -\frac{PR^2(3 + \nu)}{16} + \frac{Pa^2[2(1 + \nu)\ln R + 3 + \nu]}{8} \\ & -D \left[2A_2(1 + \nu) + \frac{A_3(\nu - 1)}{R^2} \right] = 0 \end{aligned} \quad (2.57)$$

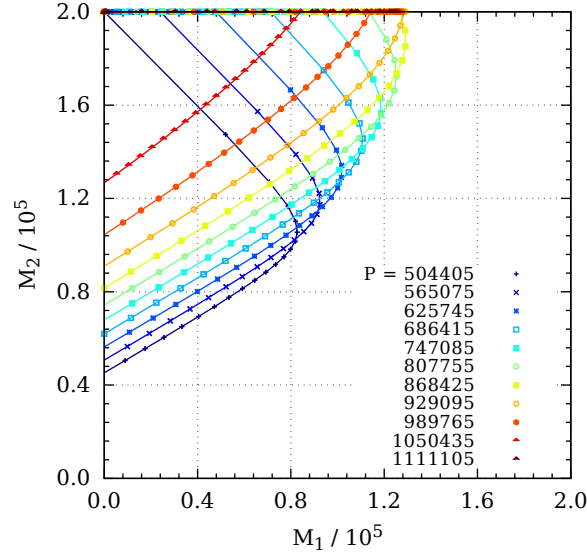


Figure 2.10: Stress profile ($a = 0.1R$).

and

$$-\frac{Py^2(1+3\nu)}{16} + \frac{Pa^2[2(1+\nu)\ln y + 1 + 3\nu]}{8} - D \left[2A_2(1+\nu) + \frac{A_3(1-\nu)}{y^2} \right] = M_0. \quad (2.58)$$

The continuity of the radial bending moment at $r = y$ with (2.48) and (2.56) furnishes the relation

$$\begin{aligned} & \frac{Pa^2[2(1+\nu)\ln y + 3 + \nu]}{8} - D \left[2A_2(1+\nu) + \frac{A_3(\nu-1)}{y^2} \right] \\ & - \frac{Py^2(3+\nu)}{16} - \frac{y-a}{y} \left[M_0 - \frac{P(y^2 + ay - 2a^2)}{6} \right] = 0. \end{aligned} \quad (2.59)$$

Due to the continuity of the deflection and its slope one has

$$A = \frac{Py^3}{16D} - \frac{Pa^2y(2\ln y + 1)}{8D} + 2A_2y + \frac{A_3}{y} \quad (2.60)$$

and

$$\begin{aligned} & \frac{P(y^4 - R^4)}{64D} - \frac{Pa^2(y^2 \ln y - R^2 \ln R)}{8D} + A_2(y^2 - R^2) \\ & + A_3 \ln \frac{y}{R} - Ay - B = 0. \end{aligned} \quad (2.61)$$

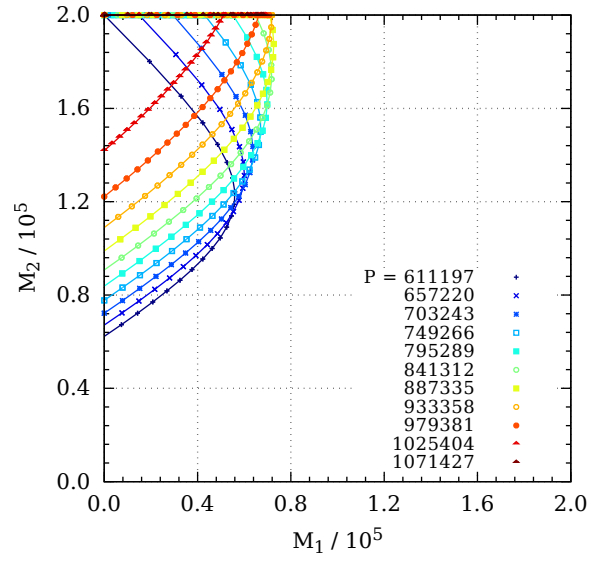


Figure 2.11: Stress profile ($a = 0.3R$).

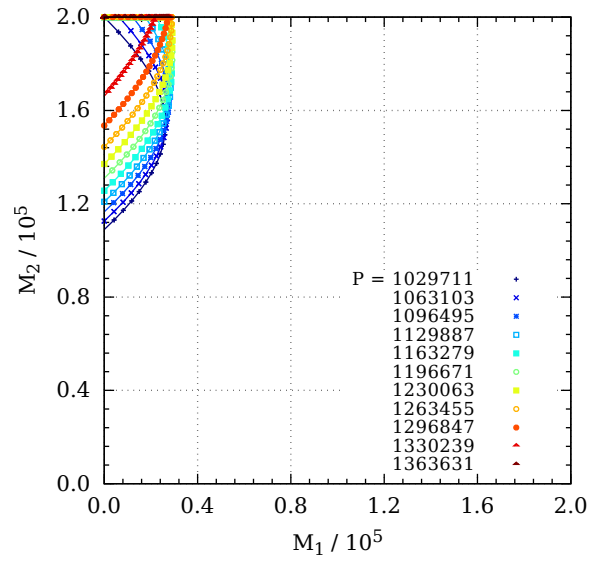


Figure 2.12: Stress profile ($a = 0.6R$).

From (2.58), (2.59) one can easily define

$$A_2 = \frac{1}{48D(1+\nu)y} \cdot \{-Py^3(1+3\nu) + 6Pa^2y[(\nu+1)\ln y + \nu] + 12M_0(a-2y) + 4Pa^3\} \quad (2.62)$$

and

$$A_3 = \frac{y[Py^3(1+3\nu) - 6Pa^2y(1+\nu) + 8a(3M_0 + Pa^2)]}{48D(\nu-1)}. \quad (2.63)$$

The equation (2.61) allows defining

$$B = \frac{P[-3y^4 + 8a^2y^2(\ln y + 1) - R^2(R^2 - 8a^2 \ln R)]}{64D} - (y^2 + R^2)A_2 + \left(\ln \frac{y}{R} - 1\right)A_3. \quad (2.64)$$

Substituting A_2, A_3 from (2.62), (2.63) in (2.57) one obtains the equation

$$\begin{aligned} & \frac{PR^2(3+\nu)}{16D} - \frac{Pa^2[2(1+\nu)\ln R + 3+\nu]}{8D} + \frac{1}{24Dy} \\ & \cdot \{-Py^3(1+3\nu) + 6Pa^2y[(\nu+1)\ln y + \nu] + 12M_0(a-2y) + 4Pa^3\} \\ & + \frac{y[Py^3(1+3\nu) - 6Pa^2y(1+\nu) + 8a(3M_0 + Pa^2)]}{48DR^2} = 0. \end{aligned} \quad (2.65)$$

The equation (2.65) serves for the determination of the quantity y for fixed load intensity P .

2.8 Numerical results

The equation (2.65) is solved numerically making use of the computer code *Mathematica*. The results of calculations are presented in Table 2.2 and Fig. 2.10 – Fig. 2.15 for the plate with the radius $R = 1$ m, $h_0 = 0.01$ m, $H = 0.05$ m, $\nu = 0.3$; $E = 2 \cdot 10^{11}$ Pa, $\sigma_0 = 4 \cdot 10^8$ Pa. Calculations carried out showed that the plastic region expands with the growth of the load intensity (Table 2.2). Table 2.2 corresponds to the case the inner radius $a = 0.3R$. The plate reaches the fully plastic stage when $P = 1071428,57$ Pa.

The distributions of bending moments of the plate are depicted in Fig. 2.10 – Fig. 2.12 for different values of the load intensity. It can be seen from Fig. 2.10 – Fig. 2.12 that the distributions of bending moments are statically admissible since at each $r \in [a, R]$ the corresponding values of M_1, M_2 , are such that the point either lies on the side of the yield hexagon or is located inside the hexagon. The elastic

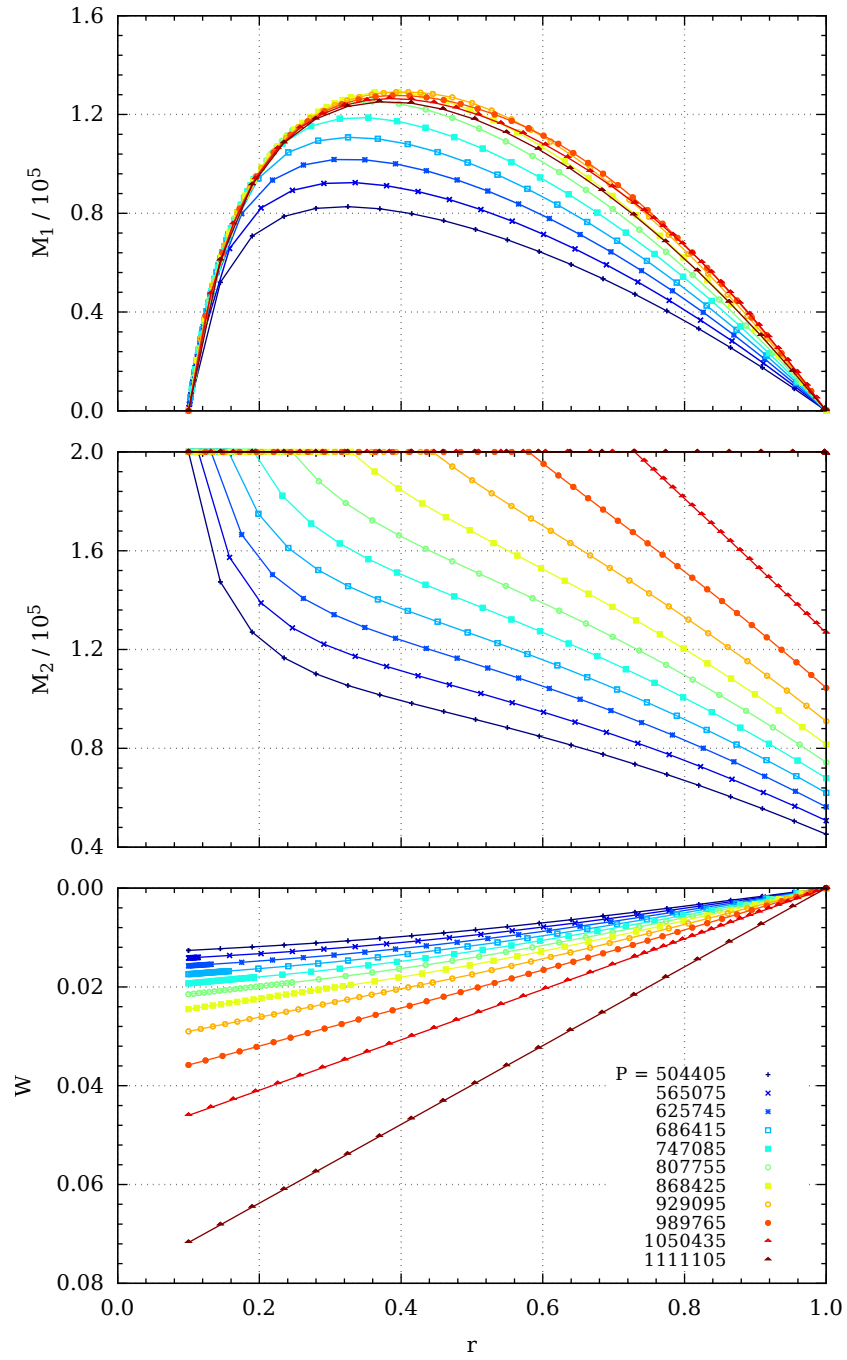


Figure 2.13: Bending moments and deflections ($a = 0.1R$).

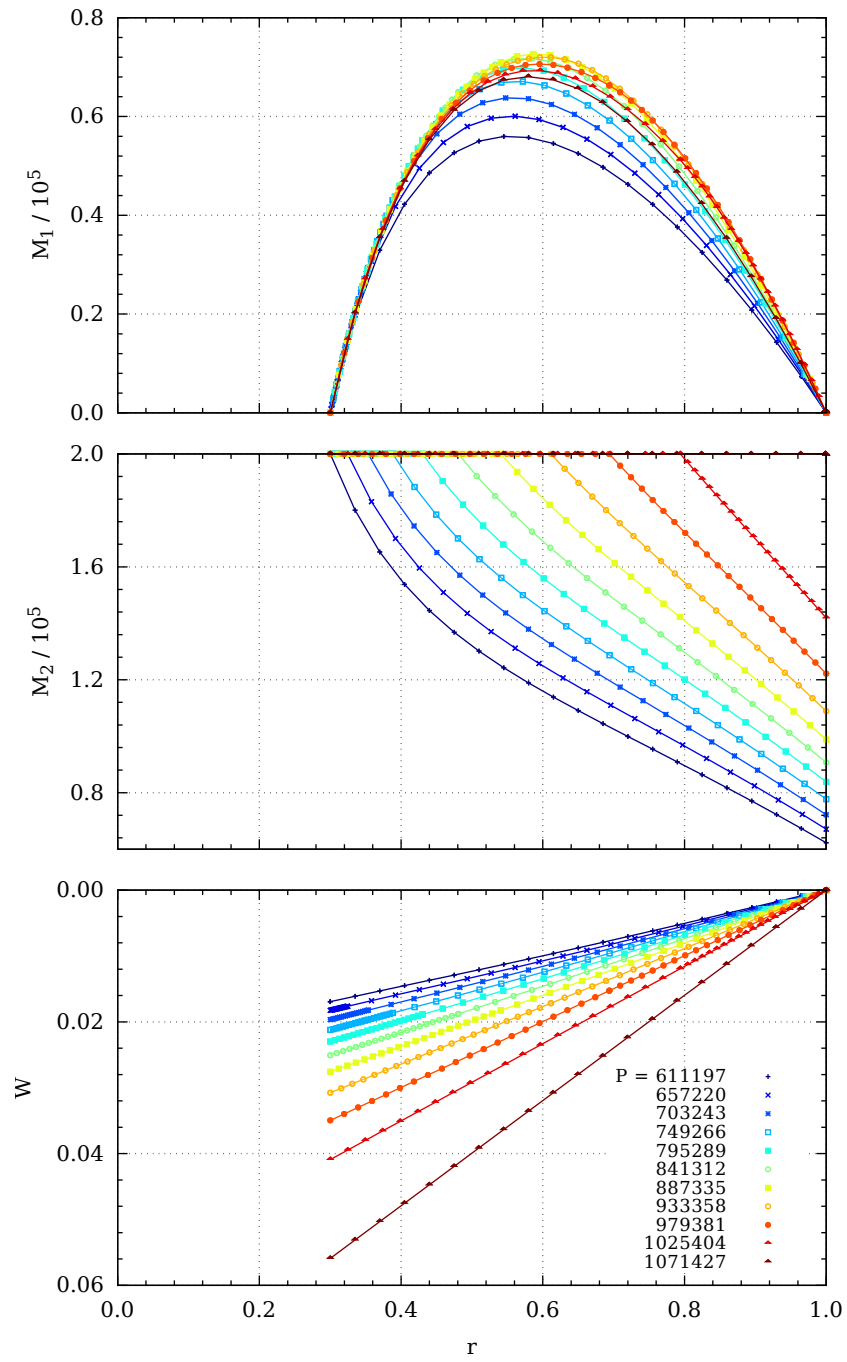


Figure 2.14: Bending moments and deflections ($a = 0.3R$).

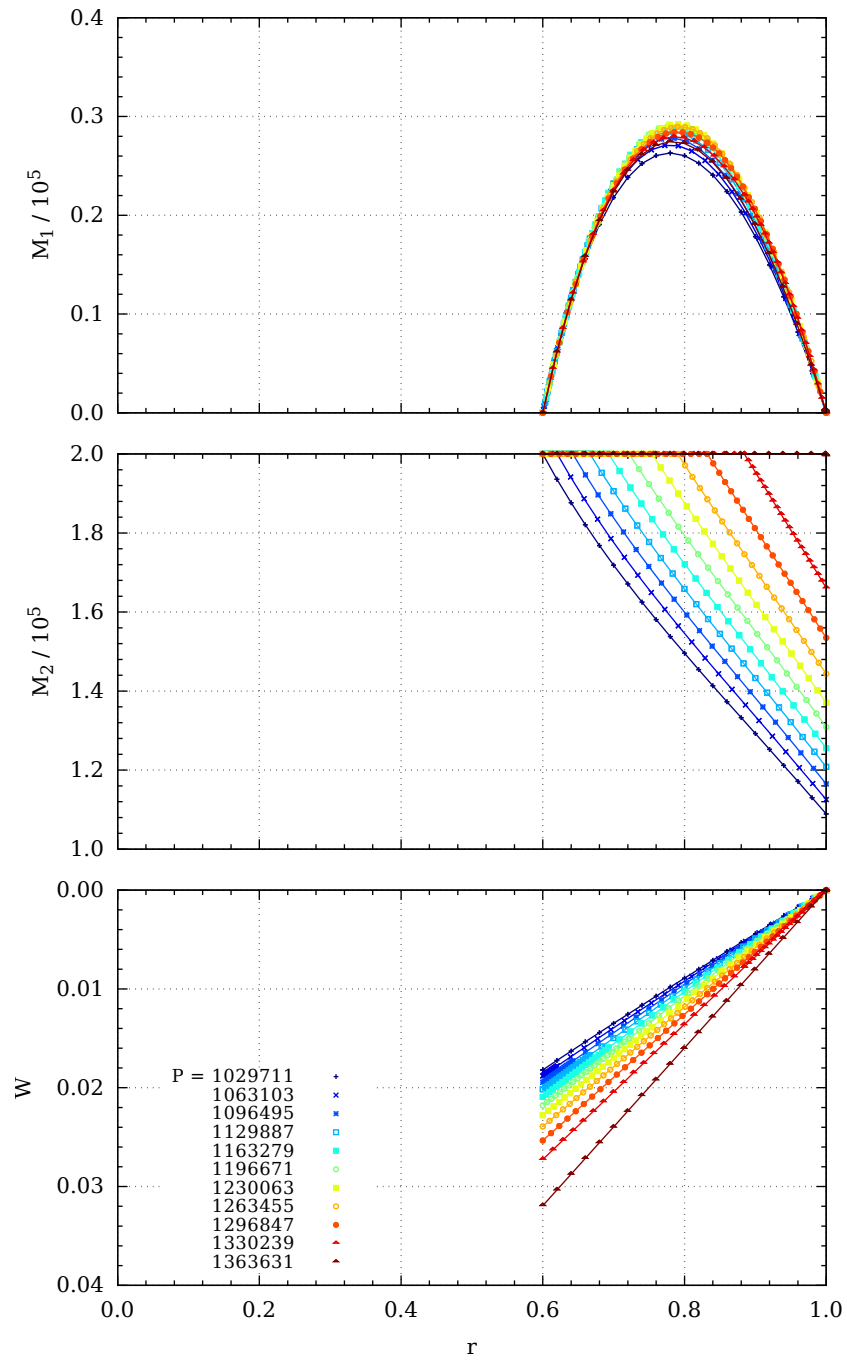


Figure 2.15: Bending moments and deflections ($a = 0.6R$).

Table 2.2: Radius of the plastic zone.

P	611197	657220	703243	749266	795289	841312
y	0.3	0.3245	0.3536	0.3884	0.4304	0.4808
P	887335	933358	979381	1025404	1071427	
y	0.5409	0.6115	0.6939	0.7941	0.9989	

plastic stage of deformation is completed at the loading level where the whole plate is plastic. This situation corresponds to

$$P = P_2 = \frac{6M_0(R - a)}{R^3 + 2a^3 - 3a^2R} \quad (2.66)$$

and $y = R$.

It is worthwhile to mention that the stress profiles (see Fig. 2.10 – Fig. 2.12, also Fig. 2.4, Fig. 2.6) do not present the bending moments as functions of the current radius. However, these figures allow to prove the statical admissibility of the current solution.

The transverse deflections and the bending moments are depicted in Fig. 2.13 – Fig. 2.15 for the plate of constant thickness with different inner radii. It can be seen from Fig. 2.13 – Fig. 2.15 that the distributions of radial moments depend slightly on the load intensity. However, the hoop moment distribution is completely different in the elastic and elastic plastic stages of deformation. As it was shown above $M_2 = M_0$ in the plastic region. If the load intensity P tends to the value P_2 then the hoop moment distribution tends to the value $M_2 \equiv M_0$ for $r \in [a, R]$. The load-deflection relations of plates made of different materials are presented in [97]. The results of [97] are compared with the current solution in Fig. 2.16. (Fig. 2.16 corresponds to the case $R = 0.125$ m; $\nu = 0.28$; $E = 2.0085 \cdot 10^{11}$ Pa; $\sigma_0 = 3.3834 \cdot 10^8$ Pa; $h_0 = \frac{H}{6}$ m; $H = 0.01$ m). It can be seen from Fig. 2.16 that the curve corresponding to the material obeying the diamond yield criterion is below those corresponding to the Mises yield criterion and its non-linear approximations. This matter coincides with our expectation because the diamond in the plane of principal moments can be considered as an inscribed polygon with respect to the Mises ellipse.

2.9 Concluding remarks

The bending problem for the elastic plastic circular plate, simply supported at the outer edge, was solved by finding the deflections, the radial and circumferential bend-

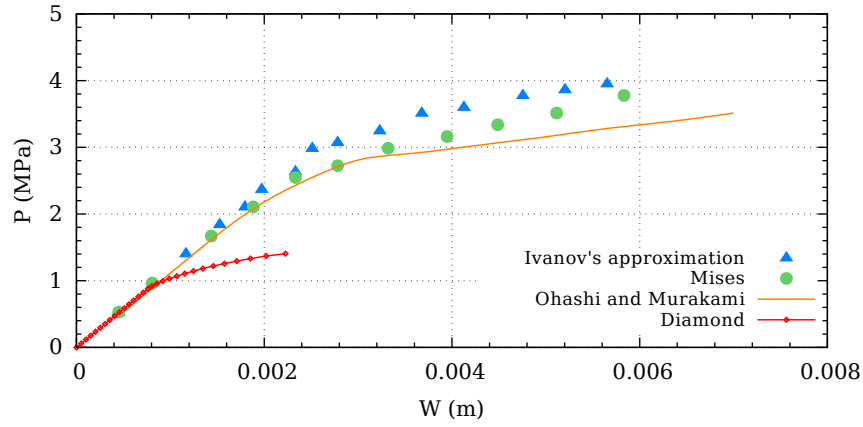


Figure 2.16: Load-deflection relations of circular plates.

ing moments for different loadings. It was assumed that the behaviour of the material in the plastic stage corresponds to the Tresca's or diamond yield criteria.

The optimization problem regarding to the stepped circular plate made of homogeneous sandwich material was solved numerically. For the fixed plate volume, the optimal values for the heights of the carrying layers and the location for the step were calculated while requiring minimal deflection at the centre of the plate.

The problem of determining the stress strain state of annular plates was solved in the case of a Tresca's material. For the sake of simplicity the model of a sandwich plate was employed. The plate under consideration was simply supported at the outer edge and absolutely free at the inner edge. Statically and kinematically admissible stress fields and distributions of displacements were constructed for the initial elastic and the subsequent elastic plastic stage of deformation. It was shown that with increasing the intensity of external loading the plate reaches a fully plastic state.

Comparison of the load-deflection relations of plates made of different materials showed that the curve corresponding to the diamond yield criterion is below those corresponding to the Tresca's and Mises yield criteria, as might be expected.

CHAPTER 3

ELASTIC PLASTIC BENDING OF STEPPED ANNULAR PLATES

3.1 The model of the plate

Let us consider the axisymmetric bending of an annular plate subjected to the transverse pressure of intensity P . Assume that the internal edge of the plate of radius a is clamped whereas the external edge of radius R is absolutely free. The plate under consideration has a sandwich cross section (see Fig. 3.1).

The behaviour of the plate will be prescribed with the first order bending theory of thin plates corresponding to small deformations and small displacements (see Reddy [82], Vinson [102]). The stress state is defined by the bending moments M_1 , M_2 and the shear force Q . The bending moments M_1 , M_2 are coupled with the principal stresses σ_1 , σ_2 by (1.9). Due to the axisymmetry, the moment $M_{12} = 0$. Note that the membrane forces will be neglected according to current approach. The third generalized stress component to be taken into account is the shear force Q but this component does not contribute to the strain energy when the bending theory is used. Moreover, the shear force, although appearing in the equilibrium conditions, can be eliminated from the equilibrium equations and thus is not involved in the set of governing equations.

It is assumed that the stress strain state induced by the axisymmetric transverse pressure is axisymmetric at each stage of the pressure. Thus the stress and strain components are defined at each point of the plate by the current radius and the given pressure level.

Material of the plate is assumed to be ideal elastic plastic obeying the square yield criterion in the plastic (inelastic) stage of deformation.

The aim of the chapter is to determine the transverse deflection as well as the bending moment distributions in the elastic and subsequent inelastic stages of deformation for given transverse pressure levels.

3.2 Basic equations and concepts

It is well known that in the case of lower values of the pressure loading the plate is pure elastic. The elastic behaviour of the material can be prescribed with Hooke's law. The latter is to be presented in the generalized form as

$$\begin{aligned} M_1 &= D_j(\kappa_1 + \nu\kappa_2), \\ M_2 &= D_j(\kappa_2 + \nu\kappa_1) \end{aligned} \tag{3.1}$$

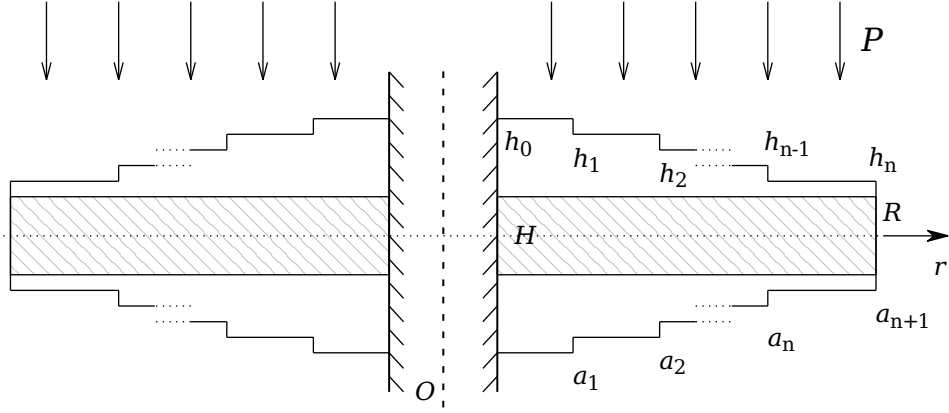


Figure 3.1: Cross section of the plate.

where $j = 0, \dots, n$. In the case of a sandwich plate, D_j is presented by the formula (2.9).

During the subsequent quasistatic increasing the external loading constitutive equations (3.1) hold good until the elastic limit is exhausted at an unknown point of the plate. In the case of a plate of constant thickness the yield limit is first reached at the internal edge of the plate. After that the plate is subdivided into elastic and plastic regions, respectively. Let these regions be S_e and S_p , respectively. Since we are studying the sandwich plate and the carrying layers are thin, no elastic plastic state of deformations occurs.

Assume that the material of the plate obeys the square yield criterion and the associated flow rule (Fig. 3.2). Thus for $r \in S_p$ the stress state of the point is such that the point $(M_1(r), M_2(r))$ lies on a side of the square (Fig. 3.2). It means that one of the inequalities

$$|M_1| \leq M_{0j}, \quad |M_2| \leq M_{0j} \quad (3.2)$$

is transformed into the equality in the plastic region for $r \in (a_j, a_{j+1})$, $j = 0, \dots, n$. Quantity M_{0j} stands for the yield moment corresponding to the thickness h_j . It is presented by (2.5).

Evidently, at the boundary of the plate requirements

$$\begin{aligned} M_1(R) &= 0, \\ Q(R) &= 0 \end{aligned} \quad (3.3)$$

and

$$W(a) = 0 \quad (3.4)$$

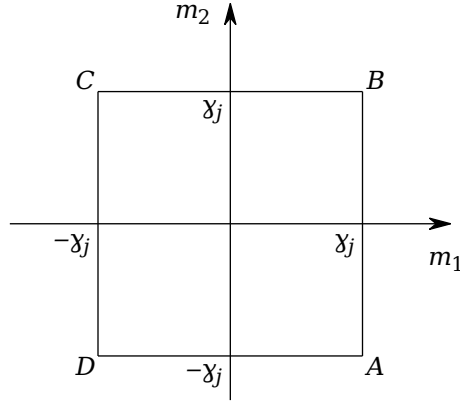


Figure 3.2: Square yield criterion.

must be satisfied at each loading level.

Let us consider the governing equations separately in elastic and plastic regions, respectively. In elastic regions the stress strain state is determined according to (1.1) and (3.1). The substitution of (3.1) and (1.8) in (1.1) easily leads to the equation (2.8).

In the following it is reasonable to use dimensionless quantities

$$\begin{aligned} \rho &= \frac{r}{R}, & m_1 &= \frac{M_1}{M_*}, & m_2 &= \frac{M_2}{M_*}, & q &= \frac{RQ}{M_*}, \\ \alpha &= \frac{a}{R}, & \alpha_j &= \frac{a_j}{R}, & p &= \frac{PR^2}{M_*}, & \bar{w} &= \frac{W}{H}, \\ \gamma_j &= \frac{h_j}{h_*}, & d_j &= \frac{EH^2h_j}{2(1-\nu^2)\sigma_0R^2h_*} \end{aligned} \quad (3.5)$$

where $M_* = \sigma_0 h_* H$ is the yield moment of a reference plate of constant thickness h_* .

Making use of variables (3.5) one can present the equilibrium equations (1.1) as

$$((\rho m_1)' - m_2)' + p\rho = 0 \quad (3.6)$$

where primes denote the differentiation with respect to the dimensionless radius ρ .

3.3 General solutions in elastic and plastic regions

Let us denote an elastic region (a_j, a_{j+1}) , $j = 0, \dots, n$ where the thickness of carrying layer is h_j by S_{ej} .

Making use of (2.8) and (3.5) it is easy to recheck that the general solution of (2.8) can be presented as

$$\bar{w} = A_{1j}\rho^2 \ln \rho + A_{2j}\rho^2 + A_{3j} \ln \rho + A_{4j} + \frac{p\rho^4}{64d_j} \quad (3.7)$$

where $\rho \in S_{ej}$ and $d_j = \frac{D_j H}{M_* R^2}$. Arbitrary constants $A_{1j} - A_{4j}$ will be determined from the boundary requirements and continuity conditions for \bar{w} , \bar{w}' , m_1 at the boundaries between the elastic and plastic regions.

Dimensionless bending moments can be determined according to (3.1) and (3.5) as

$$\begin{aligned} m_1 &= -d_j \left(\bar{w}'' + \frac{\nu}{\rho} \bar{w}' \right), \\ m_2 &= -d_j \left(\frac{\bar{w}'}{\rho} + \nu \bar{w}'' \right) \end{aligned} \quad (3.8)$$

for $\rho \in S_{ej}$. The terms with derivatives \bar{w}' , \bar{w}'' in (3.8) can be expressed as

$$\bar{w}' = A_{1j}(2\rho \ln \rho + \rho) + 2A_{2j}\rho + \frac{A_{3j}}{\rho} + \frac{p\rho^3}{16d_j} \quad (3.9)$$

and

$$\bar{w}'' = A_{1j}(2 \ln \rho + 3) + 2A_{2j} - \frac{A_{3j}}{\rho^2} + \frac{3p\rho^2}{16d_j} \quad (3.10)$$

for $\rho \in S_{ej}$.

The third general stress resultant besides the bending moments is the shear force. It is reasonable to calculate it from the equilibrium equations (1.1) or (3.6). From (3.6), (1.1) one easily obtains the equation

$$(\rho q)' = -p\rho \quad (3.11)$$

which holds good over the entire plate. The solution of this equation which satisfies the boundary condition $q(1) = 0$ is

$$q = -\frac{p}{2} \left(\rho - \frac{1}{\rho} \right) \quad (3.12)$$

for $\rho \in (\alpha, 1)$.

The solution of basic equations in the plastic region S_p depends on the particular yield regime. It appears that in the present case the stress strain state in the plastic region of the plate corresponds to the sides AD or DC of the square yield criterion (Fig. 3.2). Let us consider these yield regimes in more detail.

In the case of the yield profile CD one has $m_1 = -\gamma_j$ for $\rho \in S_{pj} \subset (a_j, a_{j+1})$. However, it can be rechecked (see [11, 86]) that this regime can not take place in any region of finite length.

If the stress profile lies on the side AD of the square (Fig. 3.2) then $m_2 = -\gamma_j$ and after integration of (3.6) with (3.12) one has

$$m_1 = -\gamma_j - \frac{p}{2} \left(\frac{\rho^2}{3} - 1 \right) + \frac{C_j}{\rho} \quad (3.13)$$

for $\rho \in S_{pj}$ and C_j is an arbitrary constant.

In the case of the yield regime AD (Fig. 3.2) according to the associated gradientality law one has $\kappa_1 = 0$ and thus

$$\bar{w} = A_j \rho + B_j \quad (3.14)$$

for $\rho \in S_{pj}$, where A_j, B_j are arbitrary constants. However, on the side CD of the square (Fig. 3.2) $\kappa_2 = 0$ and thus $\bar{w} = \text{const}$. This is one but not the only reason why the regime CD does not take place in a region of finite length.

3.4 The pure elastic stage of deformation (stage I)

As the intensity of the pressure loading is increased from zero, the entire plate is elastic until the stress profile reaches a side of the yield square. However, during the elastic stage the stress profile lies inside the square $ABCD$ (Fig. 3.2) for each $j = 0, \dots, n$.

During this stage of loading the deflection is defined by (3.7), bending moments and the shear force by (3.8) and (3.12), respectively. For the determination of unknown constants one can use the boundary conditions $\bar{w}'(a) = \bar{w}(a) = 0$, $m_1(1) = 0$ and the continuity requirements

$$\begin{aligned} [\bar{w}(\alpha_j)] &= 0, \\ [\bar{w}'(\alpha_j)] &= 0, \\ [m_1(\alpha_j)] &= 0 \end{aligned} \quad (3.15)$$

for $j = 1, \dots, n$.

It appears that the general solution in the form (3.7) may involve inadmissible solutions for particular cases. In order to avoid this, one has to check whether the shear force in the form (3.12) concides with that following from the third equation of the system (1.1).

Let us denote

$$\rho \bar{q} = (\rho m_1)' - m_2. \quad (3.16)$$

Evidently, $\bar{q} = q$. Thus, one has to check whether the constraints

$$\bar{q}(\rho) = q(\rho) \quad (3.17)$$

for $\rho \in S_{ej}$ ($j = 1, \dots, n$) with the boundary condition $\bar{q}(1) = 0$ are satisfied. Making use of (3.7) - (3.10) and (3.12) with (3.16) it is easy to show that the equality (3.17) takes place if

$$A_{1j} = -\frac{p}{8d_j} \quad (3.18)$$

for $j = 0, \dots, n$.

Thus, for the determination of $3n + 3$ unknown constants A_{2j}, A_{3j}, A_{4j} ($j = 0, \dots, n$) one has three boundary conditions and $3n$ continuity conditions (3.15).

Making use of (3.8), (3.9), (3.10) and taking (3.18) into account it is easy to determine the bending moments

$$\begin{aligned} m_1 = & \frac{-p\rho^2(3 + \nu)}{16} - \frac{p}{8}[2(1 + \nu)\ln\rho + 3 + \nu] \\ & - 2(1 + \nu)A_{2j}d_j + \frac{A_{3j}d_j(1 - \nu)}{\rho^2} \end{aligned} \quad (3.19)$$

and

$$\begin{aligned} m_2 = & \frac{-p\rho^2(1 + 3\nu)}{16} - \frac{p}{8}[2(1 + \nu)\ln\rho + 1 + 3\nu] \\ & - 2(1 + \nu)A_{2j}d_j + \frac{A_{3j}d_j(1 - \nu)}{\rho^2} \end{aligned} \quad (3.20)$$

for $\rho \in (a_j, a_{j+1})$, $j = 0, \dots, n$.

It is interesting to remark that the distribution of the shear force does not depend on the distribution of thickness, as it can be seen from (3.12). At the same time, other stress components (bending moments) do depend on the thickness.

The elastic loading stage is completed at the load level where the stress profile reaches the side CD of the yield square. In the case of a plate of constant thickness the plastic yielding first happens at the internal edge of the plate for $\rho = \alpha$. At the limit stage between the fully elastic stage and inelastic stage for $p = p_0$

$$m_1(\alpha) = -\gamma_0. \quad (3.21)$$

Note that, in principle, the plastic yielding may start elsewhere as well. If, for instance, the inner annulus is very narrow and the thickness h_0 is large whereas the next annulus has a very small thickness then the yield can start from the next annulus. However, these cases will be not studied in the present work.

3.5 Elastic plastic stage with the hinge circle (stage II)

Assume that during this stage of deformation the plastic hinge circle is located at the internal edge of the plate for $\rho = \alpha$. However, due to the hinge the boundary condition $\bar{w}'(\alpha) = 0$ is no more valid. For the determination of unknown constants A_{2j} , A_{3j} , A_{4j} one can use relations (3.15) with boundary conditions $\bar{w}(\alpha) = 0$, $m_1(1) = 0$ and (3.21). Note that (3.18) remains valid as well. The latter allows presenting the deflection for $\rho \in [\alpha_j, \alpha_{j+1}]$ as

$$\bar{w} = \frac{p\rho^2(\rho^2 - 8 \ln \rho)}{64d_j} + A_{2j}\rho^2 + A_{3j} \ln \rho + A_{4j}. \quad (3.22)$$

Making use of (3.22), (3.19) and satisfying the boundary conditions $\bar{w}(\alpha) = 0$, $m_1(\alpha) = -\gamma_0$ results in

$$\begin{aligned} A_{20}\alpha^2 + A_{30} \ln \alpha &= -A_{40} - \frac{p\alpha^2(\alpha^2 - 8 \ln \alpha)}{64d_0}, \\ -2A_{20}(1 + \nu)d_0 + \frac{d_0(1 - \nu)A_{30}}{\alpha^2} & \\ &= -\gamma_0 + \frac{p\alpha^2(3 + \nu)}{16} + \frac{p[2(1 + \nu) \ln \alpha + 3 + \nu]}{8} \end{aligned} \quad (3.23)$$

Finally, employing the continuity conditions (3.15) with the boundary conditions (3.23) and $m_1(1) = 0$ allows determining unknown constants A_{2j} , A_{3j} , A_{4j} for each $j = 0, \dots, n$.

This stage of deformation will be completed when the stress profile at $\rho = \alpha$ reaches the point D (Fig. 3.2) so that $m_2(\alpha) = -\gamma_0$. Let the corresponding value of the external load intensity be p_1 .

3.6 The elastic plastic stage with a plastic region of finite length (stage III)

It is reasonable to assume that during the subsequent increasing of the transverse pressure plastic deformations take place for $\rho \in S_{p0}$, $\rho \in [\alpha, \eta]$ where η is an unknown

constant. The plastic region corresponds to the yield regime DA (Fig. 3.2). Thus, for $\rho \in (\alpha, \eta)$

$$m_2 = -\gamma_0. \quad (3.24)$$

The distribution of the radial bending moment m_1 can be calculated by (3.13) taking $j = 0$. As at $\rho = \alpha$, $m_1 = -\gamma_0$ the arbitrary constant C_0 is to be

$$C_0 = \frac{\alpha p}{2} \left(\frac{\alpha^2}{3} - 1 \right). \quad (3.25)$$

Thus the bending moment is defined as

$$m_1 = -\gamma_0 - \frac{p}{2} \left(\frac{\rho^2}{3} - 1 \right) + \frac{\alpha p}{2\rho} \left(\frac{\alpha^2}{3} - 1 \right) \quad (3.26)$$

for $\rho \in [\alpha, \eta]$.

The transverse deflection has the form (3.14) in the plastic region S_{p0} . According to the boundary condition $\bar{w}(\alpha) = 0$ one obtains $B_0 = -A_0\alpha$. Thus

$$\bar{w} = A_0(\rho - \alpha) \quad (3.27)$$

for $\rho \in [\alpha, \eta]$.

Since we can now define $\bar{w}(\eta)$, $\bar{w}'(\eta)$, $m_1(\eta)$, the subsequent solution procedure is similar to that accomplished in the previous section. Note that for $\rho > \eta$ the plate is elastic. For the determination of the parameter η one has to use the continuity of the moment m_2 taking $m_2(\eta) = -\gamma_0$.

3.7 Several plastic regions

The previous stage of loading terminates at the moment when plastic yielding takes place in the section S_{p1} or in another section. Let us assume for the sake of concreteness that the stress profile reaches the corresponding yield level at $\rho = \alpha_1$ when $p = p_2$. Thus for $p \geq p_2$ the plastic deformations take place in the region (α_1, η_1) as well as in (α, η) which continues the extension. It means that $m_2 = -\gamma_1$ for $\rho \in (\alpha_1, \eta_1)$.

The bending moment distribution for $\rho \in S_{p1}$ can be defined according to (3.13) with the unknown constant C_1 . Similarly, the deflection \bar{w} is given by (3.14) with unknown constants A_1 , B_1 .

The procedure of the determination of constants of integration is similar to that accomplished in the previous case. Now we have to take into account that the region (η, α_1) between plastic regions remain elastic. Here we have unknown constants A_{21} ,

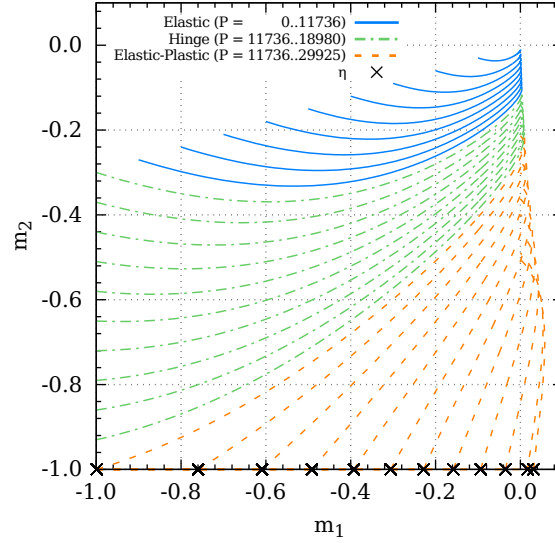


Figure 3.3: Stress profile.

A_{31} , A_{41} . The number of unknowns in each region is, thus, three. For the determination of these constants the continuity requirements for m_1 , \bar{w} , \bar{w}' are applicable. Finally, the parameters η , η_1 are to be determined from equations $m_2(\eta) = -\gamma_0$ and $m_2(\eta_1) = -\gamma_1$ where m_2 is calculated for an elastic region according to (3.20) with previously defined constants A_{2j} , A_{3j} .

3.8 Numerical results

Results of calculations in the case of plates with a single step are presented in Fig. 3.3 – 3.6. The results apply to the plate with inner radius $a = 0.2R$; $a_1 = 0.6$ m; $R = 1$ m; $\nu = 0.3$; $E = 2 \cdot 10^{11}$ Pa; $\sigma_0 = 2 \cdot 10^8$ Pa; $h_0 = 0.002$ m; $h_1 = 0.001$ m; $H = 0.02$ m.

The stress profiles in the plane of moments m_1 , m_2 are shown in Fig. 3.3 for different values of the load intensity. It can be seen from Fig. 3.3 that the profiles corresponding to smaller values of the load p lie wholly inside the square $|m_1| \leq 1$, $|m_2| \leq 1$. When the load intensity increases until $p = p_1$, the end of the profile reaches the side $m_1 = -1$ and for $p = p_2$ the corner point where $m_1 = m_2 = -1$. During the subsequent growth of the load intensity the end of the stress profile lies on the side $m_2 = -1$ as it was expected theoretically.

Distributions of bending moments m_1 and m_2 are presented in Fig. 3.4 and

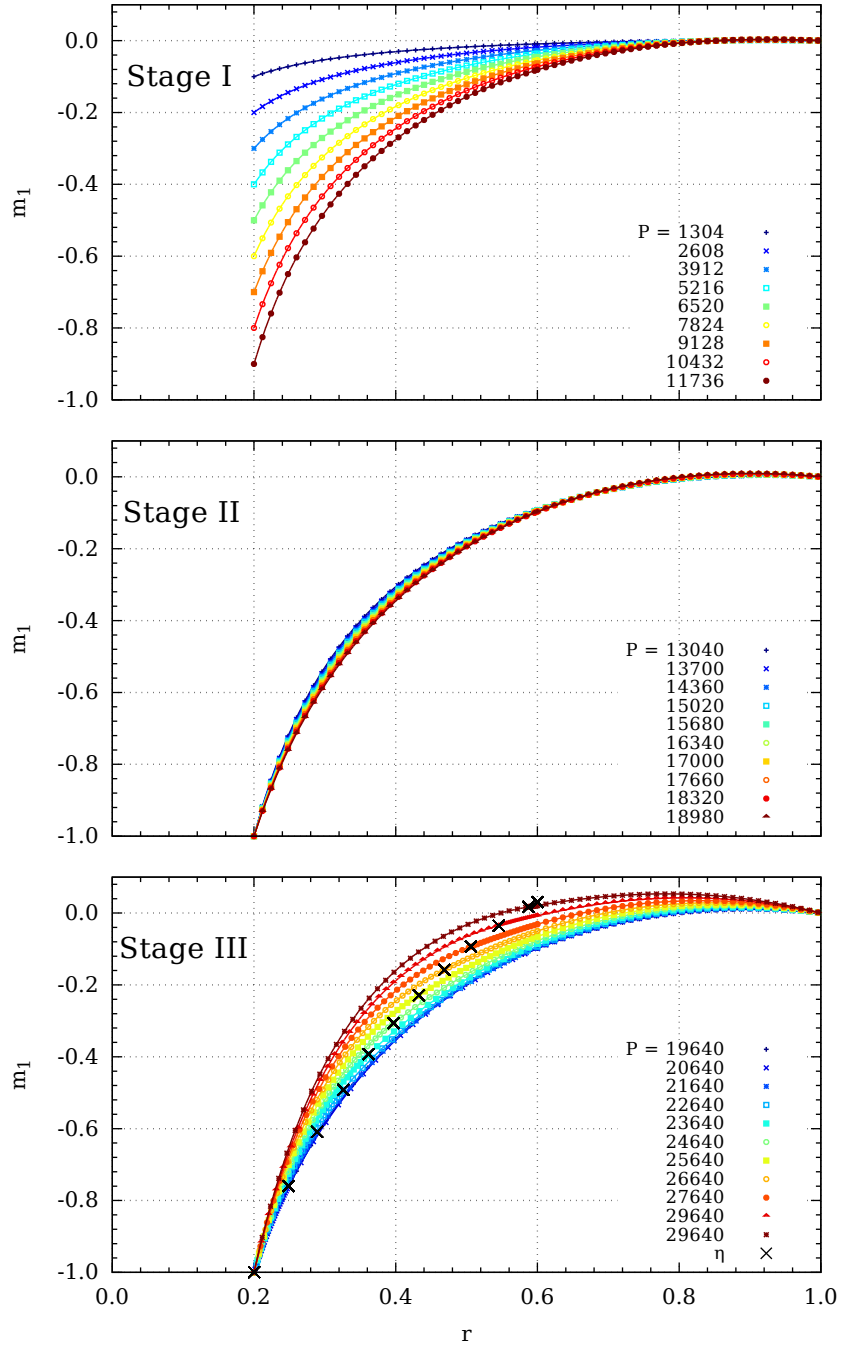


Figure 3.4: Radial bending moments m_1 .

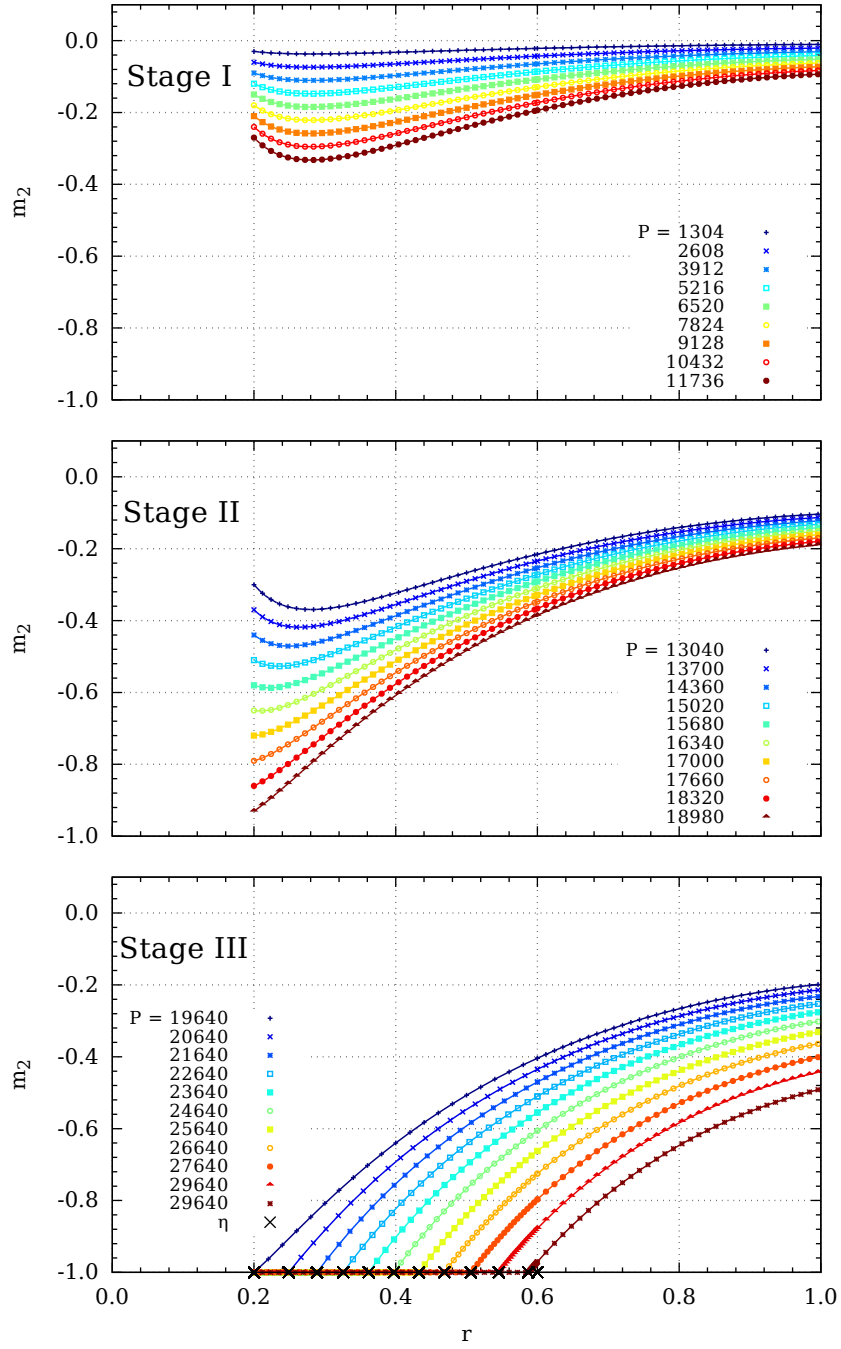


Figure 3.5: Circumferential moments m_2 .

Fig. 3.5, respectively. The locations of boundaries between elastic and plastic regions in Fig. 3.4 – 3.6 are shown by asterisks. It can be seen from Fig. 3.5 that when the load increases, the stress state tends to the pure plastic state. In the case of a plate of constant thickness in the pure plastic state $m_2 \equiv -1$. In the case of a stepped plate it can be such that $m_2 = -\gamma_j$ for $\rho \in (\alpha_j, \alpha_{j+1})$, $j = 0, \dots, n$. However, the question which is the stress state at the plastic collapse can be answered by the limit analysis of the plate of a particular shape.

3.9 Concluding remarks

A method for theoretical investigation of axisymmetric plates subjected to the distributed transverse pressure was developed. The material of plates was assumed to be an ideal elastic plastic material obeying the square yield criterion and the associated flow law in the range of inelastic deformations. In order to get maximal simplicity of the posed problem, hardening of the material as well as the geometrical non-linearity of the plate behaviour were neglected.

It was assumed that the plates under consideration had piecewise constant thickness with an arbitrary number of steps. Exact solutions were developed for the case when the plate is clamped at the inner edge whereas the outer edge is absolutely free. As a result of the solution procedure, a succession of stress states which are in equilibrium with the external loading were constructed that led from the wholly elastic to the elastic plastic state and finally to the plastic collapse state.

CHAPTER 4

OPTIMIZATION OF ELASTIC CIRCULAR PLATES WITH ADDITIONAL SUPPORTS

4.1 Optimality criteria

The plate under consideration is a circular (without the central hole) plate subjected to the transverse pressure simply supported at the edge and it is resting on an absolutely rigid ring support of unknown radius $r = s$. From practical considerations it is evident that the desirable position of the additional support is such that the maximal deflection of the plate is as small as possible. Thus the optimal location of the internal support should minimize the functional

$$J_1 = \max_{r \in [0, R]} W(r, P, s) \quad (4.1)$$

for the given loading $P = P(r)$ and thickness $h = h(r)$. However, the cost function presented in the form (4.1) has several drawbacks. First of all, it is a non-differentiable and non-additive functional. The use of non-differentiable functionals in the solution of optimization problems is quite complicated. On the other hand, the functional (4.1) ignores the expenditures necessary for manufacturing the additional support.

It can be shown that an approximation of the functional (4.1) can be presented as [4, 47]

$$J_2 = \left(\int_0^R W^k r dr \right)^{\frac{1}{k}} \quad (4.2)$$

where k is an integer. If $k \rightarrow \infty$ then $J_2 \rightarrow \|W\|$.

Due to the circumstances mentioned above in the present chapter the cost function

$$J = \int_0^R W^k r dr + 2\mu_0 \pi s \quad (4.3)$$

will be employed. In (4.3) μ_0 stands for the specific cost (cost per unique length) of the additional support. We assume herein that the material cost of the additional support is proportional to its length.

The aim of the chapter is to determine the design of the plate with an additional support (see Fig. 4.1) which minimizes the cost function (4.3) so that at each value of P the governing equations of the theory of thin axisymmetric plates with appropriate boundary conditions are satisfied.

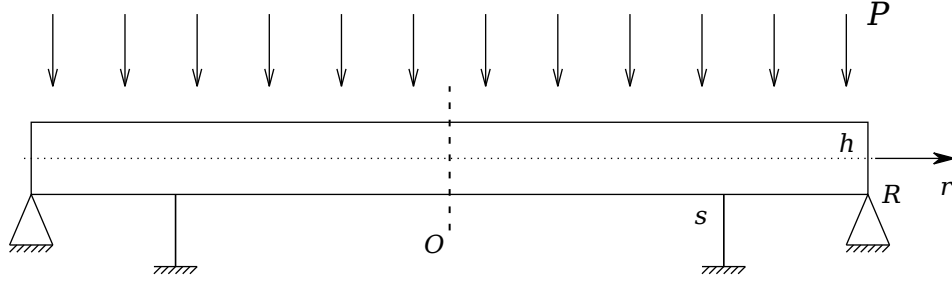


Figure 4.1: Circular plate with an additional support.

4.2 Boundary conditions

Taking a look at the equilibrium and constitutive equations with geometrical relations (1.1), (1.4), (1.7) – (1.9), (1.11) it appears that variables σ_1 , ε_1 , σ_2 , ε_2 , κ_1 , κ_2 and also M_2 can be eliminated from the set of basic equations. Introducing another new variable Z one can present the system of governing equations as

$$\begin{aligned} \frac{dW}{dr} &= Z, \\ \frac{dZ}{dr} &= -\frac{M_1}{D} - \frac{\nu Z}{r}, \\ \frac{dM_1}{dr} &= \frac{D(\nu^2 - 1)Z}{r^2} - \frac{M_1(1 - \nu)}{r} + Q, \\ \frac{dQ}{dr} &= -\frac{Q}{r} - P(r), \end{aligned} \tag{4.4}$$

where the flexural stiffness D is presented by formula (1.12).

Variables W , Z , M_1 , Q will be treated as state variables which satisfy the state equations (4.4) with the appropriate boundary and intermediate conditions. At the outer edge of the plate, e. g. at $r = R$, the bending moment M_1 and the deflection W must vanish. Thus

$$M_1(R) = 0, \quad W(R) = 0. \tag{4.5}$$

Due to the symmetry at the centre of the plate

$$\frac{dW}{dr}(0) = 0, \quad Q(0) = 0. \tag{4.6}$$

At $r = s$ where the rigid ring support is located must be

$$W(s) = 0. \tag{4.7}$$

Note that the state variables W, Z, M_1 are continuous whereas Q can be discontinuous at $r = s$.

4.3 Necessary optimality conditions

In order to establish the requirements to be satisfied by the optimal solution let us introduce the augmented functional (see Bryson [10], Hull [30], Lellep and Polikarpus [49])

$$J_* = \mu s + \int_0^s F_* dr + \int_s^R F_* dr \quad (4.8)$$

where according to (4.3), (4.4)

$$\begin{aligned} F_* = & W^k + \psi_1 \left(\frac{dW}{dr} - Z \right) + \psi_2 \left(\frac{dZ}{dr} + \frac{M_1}{D} + \frac{\nu Z}{r} \right) \\ & + \psi_3 \left(\frac{dM_1}{dr} - \frac{D(\nu^2 - 1)Z}{r^2} + \frac{M_1(1 - \nu)}{r} - Q \right) \\ & + \psi_4 \left(\frac{dQ}{dr} + \frac{Q}{r} + P(r) \right) \end{aligned} \quad (4.9)$$

and $\mu = 2\pi\mu_0$, the quantities $\psi_1 - \psi_4$ being adjoint variables.

Evidently, the problem posed above belongs to the class of optimal control problems with moving boundaries. Therefore, one has to employ total variations when deriving necessary conditions of minimum of the functional (4.8). The total variation of a state variable y at $r = s + 0$ or at $r = s - 0$ must be calculated by the following sample:

$$\Delta y(s \pm 0) = \delta y(s \pm 0) + \frac{dy(s \pm 0)}{dr} \cdot \Delta s \quad (4.10)$$

where Δy is the total variation and δy stands for the ordinary variation of the variable y . If the state variable is continuous at $r = s$ then $\Delta y(s - 0) = \Delta y(s + 0) = \Delta y(s)$. However, in the case of discontinuous variables one has to distinguish the quantities $\Delta y(s - 0)$ and $\Delta y(s + 0)$. Note that even in the case of continuous variables the quantities $\delta y(s - 0)$ and $\delta y(s + 0)$ must not be equal to each other.

The total variation of a Lagrangian functional is calculated by the rule (see Bryson [10], Lellep [46]),

$$\Delta \int_0^s F dr = \delta \int_0^s F dr + F|_s \cdot \Delta s \quad (4.11)$$

where Δs stands for an arbitrary increment of s . According to (4.11) one can write

$$\Delta J_* = \mu \Delta s + \delta \int_0^s F_* dr + \delta \int_s^R F_* dr + F_*|_{s-} \Delta s - F_*|_{s+} \Delta s. \quad (4.12)$$

Taking (4.9) into account one can easily determine the following weak variation

$$\begin{aligned}
\delta \int_a^b F_* dr = \int_a^b & \left\{ kW^{k-1} r \delta W - \frac{d\psi_1}{dr} \delta W - \psi_1 \delta Z - \frac{d\psi_2}{dr} \delta Z \right. \\
& + \frac{\psi_2}{D} \delta M_1 + \frac{\nu \psi_2}{r} \delta Z - \frac{d\psi_3}{dr} \delta M_1 - \frac{D(\nu^2 - 1)\psi_3}{r^2} \delta Z \\
& + \frac{\psi_3(1 - \nu)}{r} \delta M_1 - \psi_3 \delta Q - \frac{d\psi_4}{dr} \delta Q + \frac{\psi_4}{r} \delta Q \Big\} dr \\
& + (\psi_1 \delta W + \psi_2 \delta Z + \psi_3 \delta M_1 + \psi_4 \delta Q) \Big|_a^b
\end{aligned} \tag{4.13}$$

where a and b are the arbitrary boundaries of integration.

Substituting both integrals in (4.12) by (4.13) with the appropriate choice of boundaries a and b leads to the relation

$$\begin{aligned}
\Delta J_* = \mu \Delta s + \int_0^R & \left\{ kW^{k-1} r \delta W - \frac{d\psi_1}{dr} \delta W - \psi_1 \delta Z - \frac{d\psi_2}{dr} \delta Z \right. \\
& + \frac{\psi_2}{D} \delta M_1 + \frac{\nu \psi_2}{r} \delta Z - \frac{d\psi_3}{dr} \delta M_1 - \frac{D(\nu^2 - 1)\psi_3}{r^2} \delta Z \\
& + \frac{\psi_3(1 - \nu)}{r} \delta M_1 - \psi_3 \delta Q - \frac{d\psi_4}{dr} \delta Q + \frac{\psi_4}{r} \delta Q \Big\} dr \\
& + (\psi_1 \delta W + \psi_2 \delta Z + \psi_3 \delta M_1 + \psi_4 \delta Q) \Big|_0^s \\
& + (\psi_1 \delta W + \psi_2 \delta Z + \psi_3 \delta M_1 + \psi_4 \delta Q) \Big|_s^R
\end{aligned} \tag{4.14}$$

where the matter that $F_*(s) = 0$ has been taken into account.

Making use of (4.14) one easily obtains from the equation $\Delta J_* = 0$ the system of adjoint equations

$$\begin{aligned}
\frac{d\psi_1}{dr} &= rkW^{k-1}, \\
\frac{d\psi_2}{dr} &= -\psi_1 + \frac{\nu \psi_2}{r} - \frac{D(\nu^2 - 1)\psi_3}{r^2}, \\
\frac{d\psi_3}{dr} &= \frac{\psi_2}{D} + \frac{\psi_3(1 - \nu)}{r}, \\
\frac{d\psi_4}{dr} &= -\psi_3 + \frac{\psi_4}{r}.
\end{aligned} \tag{4.15}$$

Note that although the adjoint set (4.15) holds good for each $r \in [0, R]$ it must be integrated separately in regions $(0, s)$ and (s, R) , respectively. The reason is that some of adjoint variables can be discontinuous at $r = s$.

Boundary conditions (4.5), (4.6) allow presenting the transversality conditions as

$$\psi_1(0) = 0, \quad \psi_3(0) = 0 \quad (4.16)$$

and

$$\psi_2(R) = 0, \quad \psi_4(R) = 0. \quad (4.17)$$

Substituting (4.15) – (4.17) in (4.14) permits rewriting the equation $\Delta J_* = 0$ as

$$\mu \Delta s - (\psi_1 \delta W + \psi_2 \delta Z + \psi_3 \delta M_1 + \psi_4 \delta Q)|_{s-0}^{s+0} = 0. \quad (4.18)$$

From the physical considerations it is evident that W , Z and M_1 are continuous at $r = s$. Thus following (4.10) one can write

$$\begin{aligned} \delta W(s \pm 0) &= \Delta W(s) - \frac{dW}{dr}(s) \cdot \Delta s, \\ \delta Z(s \pm 0) &= \Delta Z(s) - \frac{dZ}{dr}(s) \cdot \Delta s, \\ \delta M_1(s \pm 0) &= \Delta M_1(s) - \frac{dM_1(s \pm 0)}{dr} \cdot \Delta s, \\ \delta Q(s \pm 0) &= \Delta Q(s \pm 0) - \frac{dQ(s \pm 0)}{dr} \cdot \Delta s. \end{aligned} \quad (4.19)$$

Substituting the weak variations of state variables from (4.19) in (4.18) and taking into account that $\Delta W(s) = 0$ and $\Delta Z(s)$, $\Delta M_1(s)$, $\Delta Q(s \pm 0)$ are independent leads to the requirements

$$\psi_2(s - 0) - \psi_2(s + 0) = 0, \quad (4.20)$$

$$\psi_3(s - 0) - \psi_3(s + 0) = 0$$

and

$$\psi_4(s - 0) = \psi_4(s + 0) = 0. \quad (4.21)$$

It was assumed above that Z and M_1 are continuous everywhere; thus in particular at $r = s$. Bearing in mind the continuity of M_1 it infers from (1.8) and (1.11) that $\kappa_1 = -\frac{dZ}{dr}$ is also continuous at $r = s$.

Substituting (4.19) – (4.21) in (4.18) and taking into account the continuity of Z , κ_1 , κ_2 and ψ_2 , ψ_3 , also the arbitrariness of the increment Δs , one can present (4.18) as

$$\mu + [\psi_1(s)] \frac{dW(s)}{dr} + \psi_3(s) \left[\frac{dM_1(s)}{dr} \right] = 0. \quad (4.22)$$

In (4.22) the square brackets denote the finite jumps of corresponding functions at $r = s$ (see the comment to (2.3)).

4.4 Solution of governing equations

Consider the solution of state equations (4.4) in more detail in the case when the plate thickness h is constant.

Integrating the last equation of the system (4.4) one obtains

$$Q = -\frac{1}{r} \left(\int P(r) dr + C_{\pm} \right) \quad (4.23)$$

where C_+ and C_- stand for the constants of integration in the regions $[0, s]$ and $[s, R]$, respectively. According to formula (1.15) the general solution can be presented as

$$W = \frac{Pr^4}{64D} + A_{1j}r^2 \ln r + A_{2j}r^2 + A_{3j} \ln r + A_{4j} \quad (4.24)$$

for $r \in [r_j, r_{j+1}]$ and $j = 0, 1$. Here the following notation is used: $r_0 = 0$, $r_1 = s$ and $r_2 = R$. Evidently,

$$Z = \frac{Pr^3}{16D} + A_{1j}r(2 \ln r + 1) + 2A_{2j}r + \frac{A_{3j}}{r} \quad (4.25)$$

and

$$\begin{aligned} M_1 &= -\frac{Pr^2(3 + \nu)}{16} - A_{1j}D[3 + \nu + 2(1 + \nu) \ln r] \\ &\quad - 2DA_{2j}(1 + \nu) - \frac{D(\nu - 1)}{r^2}A_{3j}, \\ M_2 &= -\frac{Pr^2(1 + 3\nu)}{16} - A_{1j}D[1 + 3\nu + 2(1 + \nu) \ln r] \\ &\quad - 2DA_{2j}(1 + \nu) + \frac{D(\nu - 1)}{r^2}A_{3j}. \end{aligned} \quad (4.26)$$

The integration constants $A_{1j} - A_{4j}$ will be determined from the boundary and continuity conditions. Let us consider first the solution in the internal region for $r \in [0, s]$. Here $j = 0$ in (4.24) – (4.26). Since at the centre of the plate the quantities $W(0)$, $M_1(0)$, $M_2(0)$ must be finite whereas according to (4.6) $Z(0) = 0$, one has

$$A_{10} = 0, \quad A_{30} = 0. \quad (4.27)$$

Boundary conditions (4.5) with (4.7) and the continuity requirements for Z and M_1

result in

$$\begin{aligned}
A_{20}s^2 + A_{40} + \frac{Ps^4}{64D} &= 0, \\
A_{11}s^2 \ln s + A_{21}s^2 + A_{31} \ln s + A_{41} + \frac{Ps^4}{64D} &= 0, \\
-2sA_{20} + A_{11}s(1 + 2 \ln s) + 2A_{21}s - \frac{A_{31}}{s} &= 0, \\
-2A_{20} + A_{11}(3 + 2 \ln s) + 2A_{21} - \frac{A_{31}}{s^2} &= 0, \\
A_{11}R^2 \ln R + A_{21}R^2 + A_{31} \ln R + A_{41} + \frac{PR^4}{64D} &= 0, \\
A_{11}[2(1 + \nu) \ln R + 3 + \nu] + 2(1 + \nu)A_{21} \\
- \frac{A_{31}(1 - \nu)}{R^2} + \frac{PR^2(3 + \nu)}{16D} &= 0.
\end{aligned} \tag{4.28}$$

The system (4.28) can be easily solved with respect to unknowns A_{20} , A_{40} , A_{11} , A_{21} , A_{31} , A_{41} and presented as

$$\begin{aligned}
A_{20} &= \frac{P}{K} \cdot [R^6[2(\nu + 5)(\ln s - \ln R) + 3\nu + 13] \\
&+ s^2R^4[4(\nu + 3)(\ln s - \ln R) - 3\nu - 13] \\
&+ s^4R^2[2(\nu + 1)(\ln s - \ln R) + \nu - 1] + s^6(1 - \nu)], \\
A_{40} &= \frac{-ps^2R^2}{K} \cdot [R^4[2(\nu + 5)(\ln s - \ln R) + 3\nu + 13] \\
&+ 4s^2R^2[(\nu + 3)(\ln s - \ln R) - \nu - 4] \\
&+ s^4[-2(\nu + 1)(\ln s - \ln R) + \nu + 3]], \\
A_{11} &= \frac{2pR^2}{K} \cdot [(\nu + 5)R^4 - 2(\nu + 3)s^2R^2 + (\nu + 1)s^4], \\
A_{21} &= \frac{-P}{K} [R^6[2(\nu + 5) \ln R - \nu - 3] \\
&+ s^2R^4[4(\nu + 3)(\ln R - 2 \ln s) - \nu + 1] \\
&+ s^4R^2[2(\nu + 1) \ln R + \nu + 3] + s^6(\nu - 1)], \\
A_{31} &= s^2 \cdot A_{11},
\end{aligned} \tag{4.29}$$

and

$$A_{41} = \frac{-ps^2R^2}{K} \left[R^4[2(\nu+5)(2\ln s - \ln R) + \nu+3] - 4s^2R^2[(\nu+3)\ln R + 1] + s^4[2(\nu+1)\ln R - \nu+1] \right], \quad (4.30)$$

where $K = 64D[(\nu-1)s^4 - (\nu+3)R^4 + 4s^2R^2[(\nu+1)(\ln R - \ln s) + 1]]$.

4.5 Solution of the adjoint system

The adjoint system (4.15) can be integrated after the substitution of (4.24) in (4.15). For the sake of simplicity let us consider the case where $k = 1$ in more detail.

It is easy to recheck that the general solution of (4.15) corresponding to the case $k = 1$ can be presented as

$$\begin{aligned} \psi_1 &= \frac{r^2}{2} + C_{1j}, \\ \psi_2 &= C_{2j}r + \frac{C_{3j}}{r} - \frac{(3+\nu)r^3}{16} - \frac{C_{1j}(1+\nu)r \ln r}{2}, \\ \psi_3 &= \frac{C_{2j}r^2}{D(\nu+1)} + \frac{C_{3j}}{D(\nu-1)} - \frac{r^4}{16D} \\ &\quad - \frac{C_{1j}r^2}{D(\nu^2-1)} + \frac{C_{1j}r^2[(1-\nu)\ln r + 1]}{2D(\nu-1)}, \\ \psi_4 &= -\frac{C_{2j}r^3}{2D(\nu+1)} - \frac{C_{3j}r \ln r}{D(\nu-1)} + C_{4j}r \\ &\quad + \frac{r^5}{64D} + \frac{C_{1j}r^3 \ln r}{4D} + \frac{C_{1j}(3-2\nu-\nu^2)r^3}{8D(\nu^2-1)} \end{aligned} \quad (4.31)$$

for $r \in [r_j, r_{j+1}]$ where $j = 0, 1$.

For the determination of 8 unknown constants $C_{1j}, C_{2j}, C_{3j}, C_{4j}$ where $j = 0, 1$, one has 8 boundary and intermediate conditions presented by (4.16), (4.17), (4.20) and (4.21).

It immediately follows from the boundary conditions (4.16) that

$$C_{10} = 0, \quad C_{30} = 0. \quad (4.32)$$

The boundary and intermediate conditions (4.17), (4.20), (4.21) lead to the linear

algebraic system

$$\begin{aligned}
& C_{21}R + \frac{C_{31}}{R} - \frac{C_{11}(1-\nu)R \ln R}{2} - \frac{(3-\nu)R^3}{16} = 0, \\
& -\frac{C_{21}R^3(\nu-1)}{2} - C_{31}(\nu+1)R \ln R + C_{41}(\nu^2-1)RD \\
& + \frac{R^5(\nu^2-1)}{64} + \frac{C_{11}(\nu^2-1)R^3 \ln R}{4} + \frac{C_{11}(3-2\nu-\nu^2)R^3}{8} = 0, \\
& -\frac{C_{21}s^3(\nu-1)}{2} - C_{31}(\nu+1)s \ln s + C_{41}(\nu^2-1)sD \\
& + \frac{s^5(\nu^2-1)}{64} + \frac{C_{11}(\nu^2-1)s^3 \ln s}{4} + \frac{C_{11}(3-2\nu-\nu^2)s^3}{8} = 0, \\
& -\frac{C_{20}s^3(\nu-1)}{2} + C_{40}s(\nu^2-1)D + \frac{s^5(\nu^2-1)}{64} = 0, \\
& (C_{21} - C_{20})s + \frac{C_{31}}{s} - \frac{C_{11}(1+\nu)s \ln s}{2} = 0, \\
& (C_{21} - C_{20})(\nu-1)s^2 + C_{31}(\nu+1) - C_{11}s^2 \\
& + \frac{C_{11}s^2(\nu+1)[(1-\nu) \ln s + 1]}{2} = 0.
\end{aligned} \tag{4.33}$$

From (4.33) one can easily determine the unknown constants C_{20} , C_{40} , C_{11} , C_{21} , C_{31} , C_{41} and present as

$$\begin{aligned}
C_{20} &= C_{21} + \frac{C_{31}}{s^2} - \frac{C_{11}(1+\nu) \ln s}{2}, \\
C_{40} &= \frac{C_{20}s^2}{2D(\nu+1)} - \frac{s^4}{64D}, \\
C_{11} &= \frac{R^2(R^2 - s^2)[2R^2(3+\nu) - (\nu+1)(R^2 + s^2)]}{8L}, \\
C_{21} &= \frac{C_{11}s^2(\nu-1)}{4R^2} + \frac{(3+\nu)R^2}{16} + \frac{C_{11}(1+\nu) \ln R}{2}, \\
C_{31} &= \frac{-C_{11}s^2(\nu-1)}{4}, \\
C_{41} &= \frac{C_{21}s^2}{2D(\nu+1)} + \frac{C_{31} \ln s}{D(\nu-1)} + \frac{s^4 - 16C_{11}s^2 \ln s}{64D} \\
& - \frac{C_{11}(-\nu^2 - 2\nu + 3)s^2}{8D(\nu^2 - 1)},
\end{aligned} \tag{4.34}$$

where

$$L = s^2(\nu - 1)(s^2 - R^2) + 2R^2(\nu + 1)(s^2 - R^2) \ln R - 2R^2 s^2(\nu + 1) (\ln s - \ln R) + 2R^2(\nu + 1)(R^2 \ln R - s^2 \ln s) - R^2(\nu + 3)(R^2 - s^2).$$

4.6 Discussion of results

Results of calculations are presented in Fig. 4.2 – Fig. 4.4. The calculations are implemented for $k = 1$ and $\mu = 0$.

In Fig. 4.2 the distributions of deflections of the plate are presented for various values of the transverse load intensity. The top panel and the bottom panels in Fig. 4.2 – Fig. 4.4 correspond to the positions of the support at $s = 0.2R$ and $s = 0.7R$, respectively, whereas the second one is associated with the optimal location of the intermediate support. The optimal solution corresponds to $s = 0.526R$. It can be seen from Fig. 4.2 that in the case of $s = 0.2R$, deflections at the central part of the plate for $r < 0.2R$ are directed upward despite the downward directed pressure. Similarly, in the case where $s = 0.7R$ one can see negative deflections in the outward region for $r > 0.7R$. However, in the case of the optimal position of the additional support the deflections are non-negative everywhere. It is somewhat surprising that the maximal deflections in the central and outward regions of the plate, respectively, are quite different in the optimal case. However, one has to take into account that the cost function (4.3) with $\mu_0 = 0$, $k = 1$ corresponds to the volume of the axisymmetric body.

In Fig. 4.3, the radial bending moment M_1 is presented for the cases where $s = 0.2R$, $s = 0.526R$ (optimal case) and $s = 0.7R$. It can be seen from Fig. 4.3 that the slope of the radial bending moment has finite jumps at the support position, as might be expected. It is somewhat surprising that the radial bending moment vanishes at an internal point for any values of the transverse pressure loading. It reveals from Fig. 4.3 that in the case of smaller values of the radius of the internal support the radial bending moment remains negative in the central part of the plate. It is negative in the vicinity of the support in the optimal case as well.

Distributions of the circumferential bending moment M_2 are presented in Fig. 4.4 for different values of the pressure loading. It reveals from Fig. 4.4 that the bending moment M_2 is unexpectedly continuous at $r = s$.

The efficiency of the design established can be assessed by the ratios

$$e_{1,2} = \frac{J_0}{J_{1,2}}$$

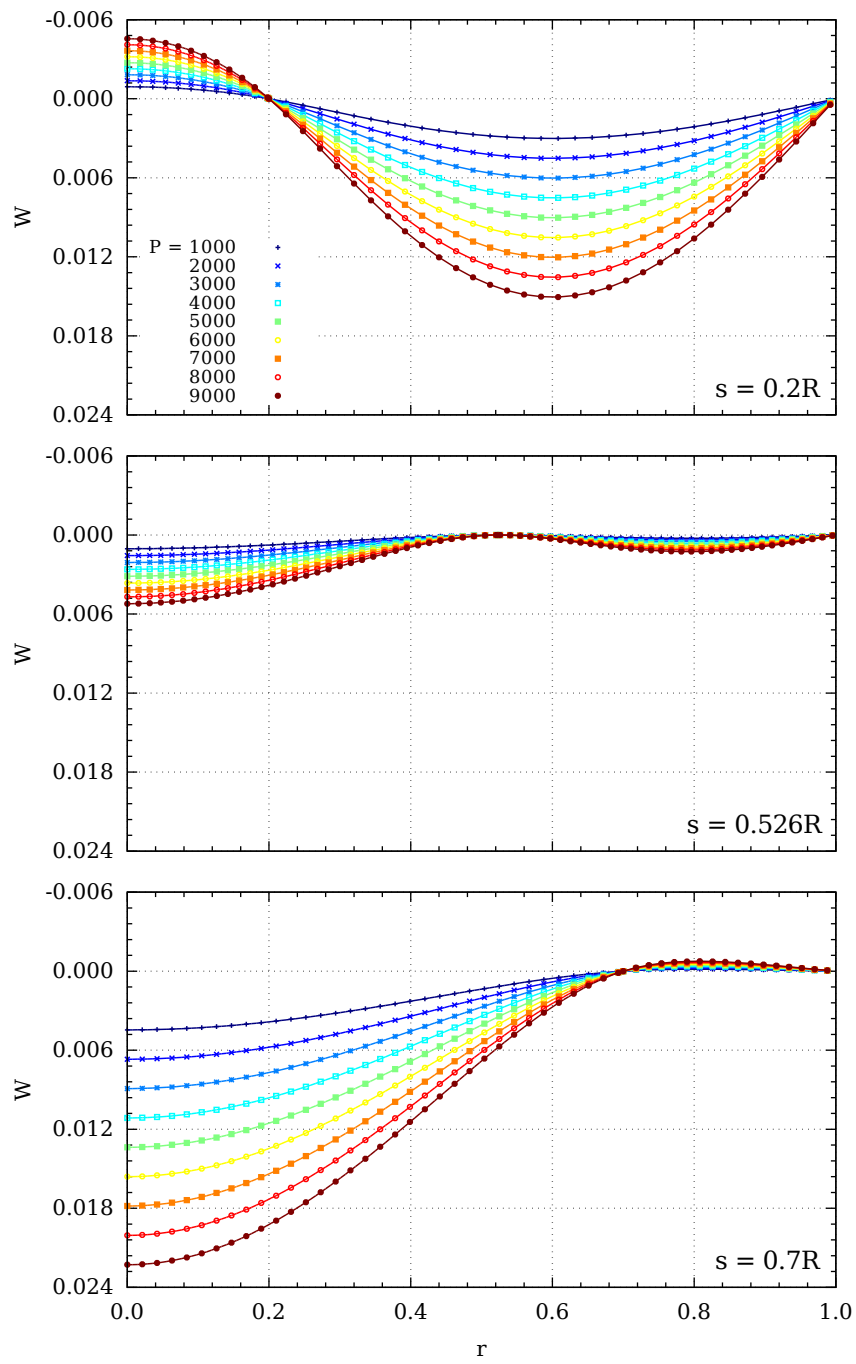


Figure 4.2: Deflections.

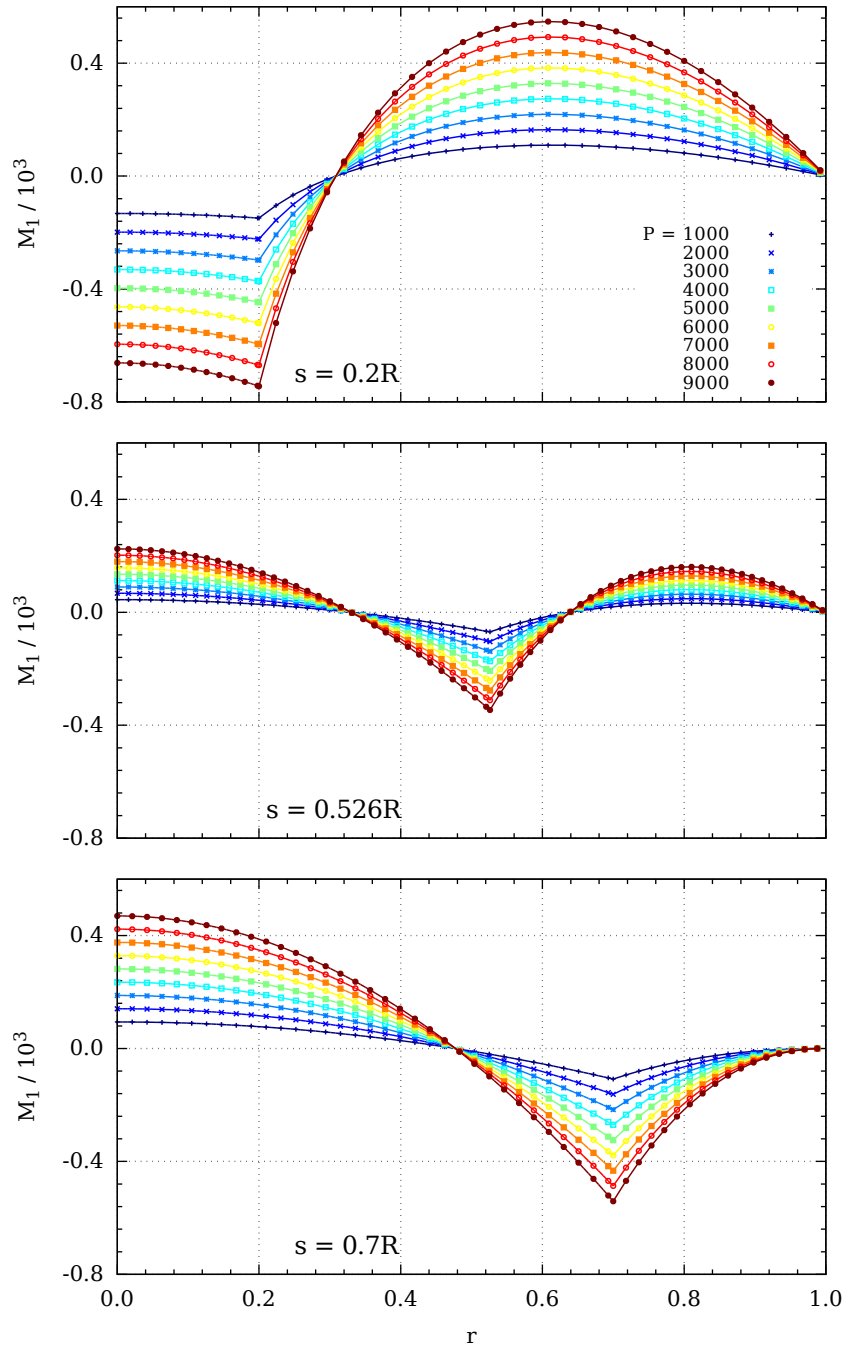


Figure 4.3: Radial bending moments.

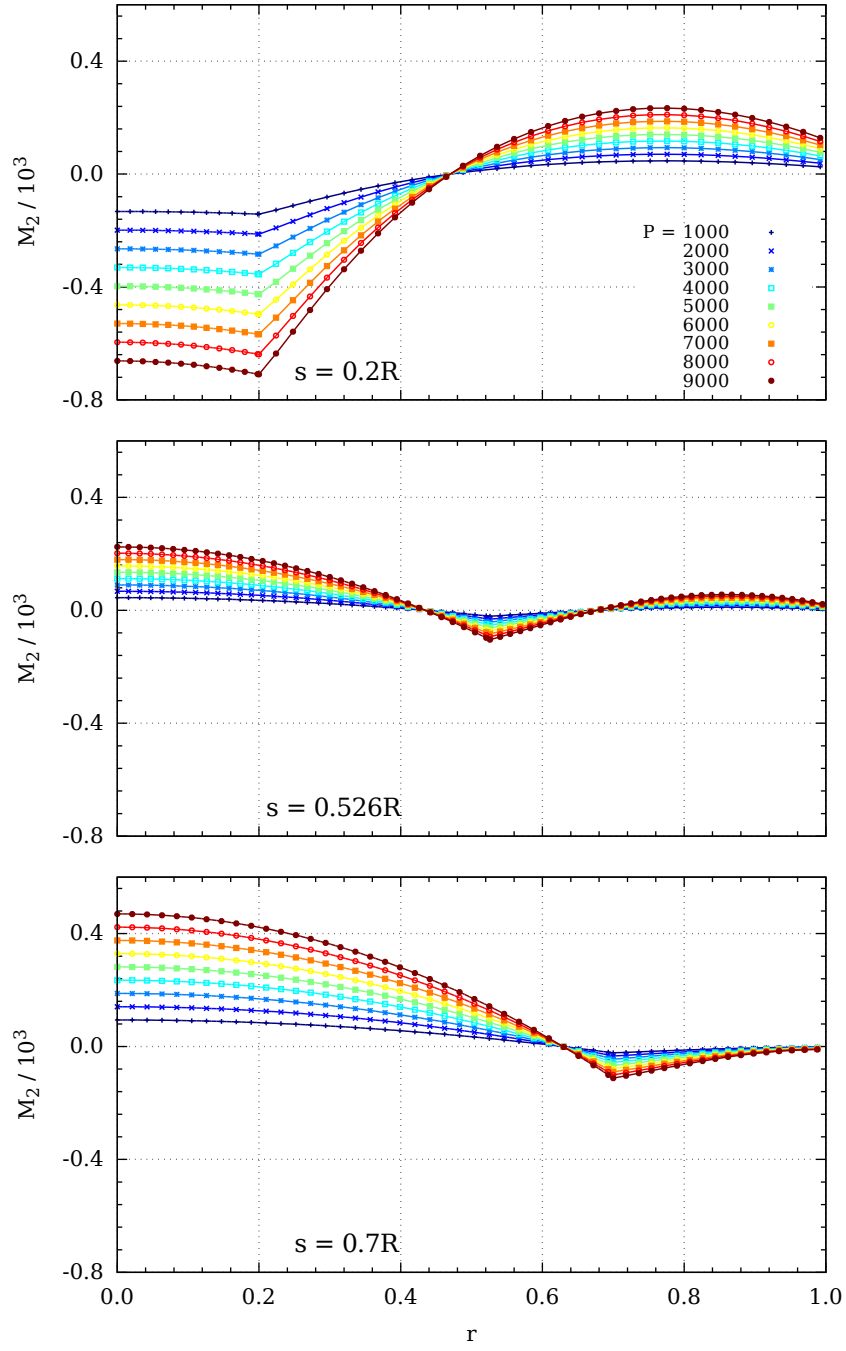


Figure 4.4: Circumferential moments.

Table 4.1: Efficiency of the design.

s/R	0.2	0.4	0.526	0.6	0.8
$10^{-4}J_0/R^6$	1.996	1.055	1.027	1.031	1.849
10^2e_1	1.562	0.826	0.803	0.807	1.447
10^2e_2	43.80	23.15	22.54	22.62	40.58

where J_0 stands for the value of the cost function (4.3) corresponding to the optimal position of the internal support. However,

$$J_1 = \int_0^R W r dr$$

in the case of the plate without additional supports and J_2 stands for the value of J in the case where internal support is located at the centre of the plate. Calculations carried out showed that the value of the cost function is very sensitive with respect to the location of the internal support (Table 4.1). It can be seen from Table 4.1 that in the case of the optimal location of the internal support the value of J is more than four times less than that corresponding to the plate with a support at its centre.

4.7 Concluding remarks

Variational methods of the theory of optimal control are used for solving the problem of optimal location of an additional rigid ring support in the case of a circular plate. The plate is made of an elastic material and subjected to a distributed transverse pressure. Necessary optimality conditions have been derived under the assumption that the cost of the additional support is proportional to its length. Numerical results have been presented for the plate simply supported at the edge and subjected to the uniformly distributed transverse pressure.

The results of calculations showed that the optimal position of the additional support allows diminishing essentially the cost function. It revealed by calculations that both the radial and circumferential bending moments are continuous over the entire plate.

CHAPTER 5

ANISOTROPIC PLATE

5.1 The optimization problem

Let us consider a circular plate of radius R made of a unidirectionally reinforced composite material. It is assumed that the fibers are embedded in the matrix material more or less uniformly so that the material can be modelled as a quasi-homogeneous anisotropic material. Two cases of unidirectional reinforcement will be considered in the present chapter. These are the radial and the circumferential reinforcements, respectively.

The plate under consideration is simply supported at the edge and it is subjected to the axisymmetric transverse pressure loading of intensity $P(r)$. Under these assumptions it is reasonable to presume that the stress strain state of the plate remains axisymmetric during the deformation.

The thickness h of the plate is assumed to be piecewise constant, e.g. $h = h_j$ for $r \in (a_j, a_{j+1})$ where $j = 0, \dots, n$.

The parameters h_j, a_j are treated as preliminarily unknown parameters to be determined so that the maximal deflection $W_0 = W(0)$ attains the minimum value under the given weight or material volume of the plate. The latter can be presented as

$$V = \pi \sum_{j=0}^n h_j (a_{j+1}^2 - a_j^2). \quad (5.1)$$

It is stipulated in (5.1) that $a_0 = 0, a_{n+1} = R$.

5.2 Equations of equilibrium and strain components

In the present chapter the governing equations (1.1) of the classical bending theory of thin plates will be used.

The generalized stresses are coupled with the principal stresses as

$$\begin{aligned} N_{1,2} &= \int_{-\frac{h}{2}}^{\frac{h}{2}} \sigma_{1,2} dz \\ M_{1,2} &= \int_{-\frac{h}{2}}^{\frac{h}{2}} \sigma_{1,2} z dz \end{aligned} \quad (5.2)$$

where σ_1, σ_2 stand for the normal stresses in the radial and circumferential directions, respectively. Here h and z are the thickness and the coordinate in the transversal direction, respectively.

The principle of virtual work states that

$$\delta E_i = \delta A_e. \quad (5.3)$$

Here δE_i stands for the variation of the internal energy induced by virtual displacements and δA_e is the variation of the work done by external forces. In the case of axisymmetric plates (see Jones [32], Ventsel and Krauthammer [101])

$$\delta E_i = \int_a^R (M_1 \delta \kappa_1 + M_2 \delta \kappa_2) r dr \quad (5.4)$$

whereas

$$\delta A_e = \int_a^R P(r) \delta W r dr. \quad (5.5)$$

In (5.5) κ_1 and κ_2 stand for the principal curvatures defined by (1.8).

Note that the principle of virtual work in the form (5.3) – (5.5) holds good in the case of axisymmetric deformations under the condition that shear deformations as well as the in-plane displacements can be disregarded. The in-plane displacements are taken into account in the non-linear plate theories.

5.3 Constitutive equations

It is known that in a unidirectional fiber-reinforced layer of material two perpendicular planes of symmetry exist at each point. The intersections of these planes with the middle plane of the lamina define two directions denoted by subscripts 1 and 2, respectively. These directions called the principal axis of orthotropy correspond to the direction of fibers and the transverse direction to the fibers.

In an orthotropic layer the assumptions of the plane stress hold good and thus the Hooke's law reads (see Daniel and Ishai [16], Jones [33])

$$\begin{Bmatrix} \sigma_1 \\ \sigma_2 \\ \tau_{12} \end{Bmatrix} = [Q] \cdot \begin{Bmatrix} \varepsilon_1 \\ \varepsilon_2 \\ \gamma_{12} \end{Bmatrix} \quad (5.6)$$

where $\sigma_1, \sigma_2, \tau_{12}$ are the stress components and $\varepsilon_1, \varepsilon_2, \gamma_{12}$ the corresponding strain components. The matrix $[Q]$ is defined as

$$[Q] = \begin{bmatrix} Q_{11} & Q_{12} & 0 \\ Q_{12} & Q_{22} & 0 \\ 0 & 0 & Q_{66} \end{bmatrix}. \quad (5.7)$$

The elements Q_{ij} in (5.7) are the so-called reduced stiffnesses related to the material constants. Let us denote by E_1, E_2 the Young's moduli in two principal directions and by ν_{12}, ν_{21} the corresponding Poisson's ratios.

For any combination of fibers and the matrix (see Jones [33])

$$\frac{\nu_{12}}{E_1} = \frac{\nu_{21}}{E_2} \quad (5.8)$$

and the reduced stiffnesses are

$$\begin{aligned} Q_{11} &= \frac{E_1}{1 - \nu_{12}\nu_{21}}, \\ Q_{22} &= \frac{E_2}{1 - \nu_{12}\nu_{21}}, \\ Q_{12} &= \frac{\nu_{21}E_1}{1 - \nu_{12}\nu_{21}}, \\ Q_{66} &= G_{12}. \end{aligned} \quad (5.9)$$

It can be seen from (5.8), (5.9) that the constitutive relations (5.6), (5.7) can be presented via four independent material constants.

In the following the main attention will be focused on the determination of bending moments assuming that the contribution of membrane forces and in-plane displacements to the stress strain state is relatively small in the range of small displacements. Thus, assuming that the fibers are embedded in the matrix material in the radial or circumferential direction only and that

$$\begin{aligned} \varepsilon_1 &= \varkappa_1, \\ \varepsilon_2 &= \varkappa_2 \end{aligned} \quad (5.10)$$

it follows from (5.6)

$$\begin{aligned} \sigma_1 &= z(Q_{11}\varkappa_1 + Q_{12}\varkappa_2), \\ \sigma_2 &= z(Q_{12}\varkappa_1 + Q_{22}\varkappa_2). \end{aligned} \quad (5.11)$$

Substituting (5.11) in (5.2) and taking (5.8), (5.9) into account one obtains

$$\begin{aligned} M_1 &= DE_1(\varkappa_1 + \nu_{21}\varkappa_2), \\ M_2 &= DE_2(\nu_{12}\varkappa_1 + \varkappa_2) \end{aligned} \quad (5.12)$$

where

$$D = \frac{h^3}{12(1 - \nu_{12}\nu_{21})}. \quad (5.13)$$

For the regions of constant thickness (a_j, a_{j+1}) where $h = h_j = \text{const}$ it is reasonable to denote

$$D_j = \frac{h_j^3}{12(1 - \nu_{12}\nu_{21})}. \quad (5.14)$$

Equations (5.12) with (5.13) present the constitutive equations for anisotropic (in the present case for orthotropic) layers and plates. Substituting the curvatures κ_1, κ_2 with the help of (1.8) in (5.12) one obtains

$$\begin{aligned} M_1 &= -E_1 D_j \left(\frac{d^2 W}{dr^2} + \frac{\nu_{21}}{r} \frac{dW}{dr} \right), \\ M_2 &= -E_2 D_j \left(\frac{\nu_{12} d^2 W}{dr^2} + \frac{1}{r} \frac{dW}{dr} \right) \end{aligned} \quad (5.15)$$

for $r \in (a_j, a_{j+1})$, where $j = 0, \dots, n$.

5.4 Solution of governing equations

Let us consider the case where the intensity of the transverse loading $P(r) = P = \text{const}$ in more detail. In this case the third equation in the system (1.1) can be easily integrated. In fact, the differentiation of the second equation in (1.1) and the substitution of the shear force results in

$$\frac{d}{dr} \left[\frac{d}{dr} (rM_1) - M_2 \right] = -Pr. \quad (5.16)$$

The integration of (5.16) gives

$$\frac{d}{dr} (rM_1) - M_2 = -\frac{Pr^2}{2} - B_{0j} \quad (5.17)$$

for $r \in (a_j, a_{j+1})$, $j = 0, \dots, n$. Here B_{0j} stands for an arbitrary constant.

Substituting the bending moments from (5.15) in (5.17) and accounting for the relation (5.8) results in

$$\frac{rd^3 W}{dr^3} + \frac{d^2 W}{dr^2} - \frac{E_2}{E_1} \cdot \frac{1}{r} \frac{dW}{dr} = \frac{Pr^2}{2E_1 D_j} + \frac{B_{0j}}{E_1 D_j} \quad (5.18)$$

for $r \in (a_j, a_{j+1})$. The shear force Q must be continuous at each $r \in [a, R]$. Thus $Q(a_j - 0) = Q(a_j + 0)$. Therefore, one can write

$$B_{0j} = B_0 \quad (5.19)$$

for each $j = 0, \dots, n$. Indeed, it immediately follows from (1.1), (5.17) that

$$Q(r) = \frac{1}{r} \left(-\frac{Pr^2}{2} - B_{0j} \right) \quad (5.20)$$

for $r \in (a_j, a_{j+1})$, $j = 0, \dots, n$. Thus at $r = a_j \pm 0$ one has

$$-\frac{Pa_j}{2} - \frac{B_{0j-1}}{a_j} = -\frac{Pa_j}{2} - \frac{B_{0j}}{a_j}. \quad (5.21)$$

From (5.21) one can see that $B_{0j-1} = B_{0j}$ for each $j = 1, \dots, n$ and therefore, (5.19) holds good.

Let us concentrate on the integration of the equation (5.18). It is reasonable to denote

$$E_2 = k^2 E_1. \quad (5.22)$$

Multiplying both sides of (5.18) by r and integrating the results in the second order differential equation (here C_{0j} is an arbitrary constant)

$$\frac{r^2 d^2 W}{dr^2} - \frac{rdW}{dr} + (1 - k^2)W = \frac{Pr^4}{8E_1 D_j} + \frac{B_0 r^2}{2E_1 D_j} + C_{0j}(1 - k^2) \quad (5.23)$$

for $r \in (a_j, a_{j+1})$. This is a linear non-homogeneous equation. The general solution of (5.23) consists of the sum of the general solution of the corresponding homogeneous equation

$$W_h = C_{1j} r^{1+k} + C_{2j} r^{1-k} \quad (5.24)$$

and of a particular solution of (5.23). The latter can be presented as

$$W_p = \frac{Pr^4}{8(9 - k^2)E_1 D_j} + \frac{B_0 r^2}{2(1 - k^2)E_1 D_j} + C_{0j}. \quad (5.25)$$

In (5.24), (5.25) C_{0j} , C_{1j} and C_{2j} are the arbitrary constants of integration.

Finally, the general solution of (5.23) for $(r \in a_j, a_{j+1})$, $j = 0, \dots, n$ can be presented as

$$W = C_{0j} + C_{1j} r^{1+k} + C_{2j} r^{1-k} + \frac{Pr^4}{8(9 - k^2)E_1 D_j} + \frac{B_0 r^2}{2(1 - k^2)E_1 D_j}. \quad (5.26)$$

From (5.26) one easily obtains

$$\begin{aligned}
\frac{dW}{dr} &= C_{1j}(1+k)r^k + C_{2j}(1-k)r^{-k} \\
&+ \frac{Pr^3}{2(9-k^2)E_1D_j} + \frac{B_0r}{(1-k^2)E_1D_j}, \\
\frac{d^2W}{dr^2} &= C_{1j}k(1+k)r^{k-1} + C_{2j}(1-k)(-k)r^{-k-1} \\
&+ \frac{3Pr^2}{2(9-k^2)E_1D_j} + \frac{B_0}{(1-k^2)E_1D_j}.
\end{aligned} \tag{5.27}$$

Substitution of (5.27) in equations (5.15) results in

$$\begin{aligned}
M_1 &= -E_1D_j \left[C_{1j}(1+k)(k+\nu_{21})r^{k-1} + C_{2j}(1-k)(\nu_{21}-k)r^{-k-1} \right. \\
&\quad \left. + \frac{Pr^2(3+\nu_{21})}{2E_1D_j(9-k^2)} + \frac{B_0(1+\nu_{21})}{E_1D_j(1-k^2)} \right], \\
M_2 &= -E_2D_j \left[C_{1j}(1+k)(k\nu_{12}+1)r^{k-1} \right. \\
&\quad \left. + C_{2j}(1-k)(1-k\nu_{12})r^{-k-1} + \frac{Pr^2(1+3\nu_{12})}{2E_1D_j(9-k^2)} + \frac{B_0(1+\nu_{12})}{E_1D_j(1-k^2)} \right]
\end{aligned} \tag{5.28}$$

which hold good for $r \in (a_j, a_{j+1})$, $j = 0, \dots, n$.

The governing equations (1.1) are accompanied with boundary conditions

$$\begin{aligned}
M_1(R) &= 0, \\
W(R) &= 0
\end{aligned} \tag{5.29}$$

and

$$\frac{dW(0)}{dr} = 0 \tag{5.30}$$

in the case of a simply supported plate. If membrane forces are taken into account extra requirements for in-plane quantities are needed.

5.5 Bending of a one-stepped plate

Let us focus our attention on the plate of piecewise constant thickness

$$h = \begin{cases} h_0; & r \in (0, a) \\ h_1; & r \in (a, R). \end{cases} \tag{5.31}$$

For the determination of the stress strain state of the plate one can use the relations (5.26) – (5.30) for $n = 1$ and the corresponding continuity requirements for the deflection W and the bending moment M_1 .

From physical considerations it is evident that the quantities W , $\frac{dW}{dr}$, M_1 and M_2 must be finite at the centre of the plate (for $r = 0$). This is possible only in the case where (here $k > 0$)

$$\begin{aligned} C_{10} &= 0, \\ C_{20} &= 0. \end{aligned} \quad (5.32)$$

Bearing (5.32) in mind, one can simplify the notation equalizing

$$\begin{aligned} C_{00} &= W_0, \\ C_{01} &= C, \\ C_{11} &= C_1, \\ C_{21} &= C_2. \end{aligned} \quad (5.33)$$

The continuity of the radial bending moment at $r = a$ leads to the relation

$$C_1(1+k)(k+\nu_{21})a^{k-1} + C_2(1-k)(\nu_{21}-k)a^{-k-1} = 0. \quad (5.34)$$

It is easy to deduce from (5.34)

$$C_2 = -\frac{C_1(1+k)(k+\nu_{21})a^{2k}}{(1-k)(\nu_{21}-k)}. \quad (5.35)$$

Employing the continuity condition for $\frac{dW}{dr}$ to (5.27), (5.30) one has

$$\begin{aligned} &C_1(1+k)a^k + C_2(1-k)a^{-k} + \frac{Pa^3}{2(9-k^2)E_1D_1} + \frac{B_0a}{(1-k^2)E_1D_1} \\ &= \frac{Pa^3}{2(9-k^2)E_1D_0} + \frac{B_0a}{(1-k^2)E_1D_0}. \end{aligned} \quad (5.36)$$

From (5.36) one can easily determine

$$B_0 = (1-k^2)E_1D_1 \left[\frac{2k(1+k)D_0a^{k-1}C_1}{(k-\nu_{21})(D_1-D_0)} - \frac{Pa^2}{2E_1D_1(9-k^2)} \right]. \quad (5.37)$$

The first requirement in (5.29) with (5.28), (5.35) and (5.37) allows defining

$$\begin{aligned} C_1 &= \frac{(k-\nu_{21})(\gamma-1)PR^2[\alpha^2(1+\nu_{21})-3-\nu_{21}]}{2(9-k^2)(1+k)E_1D_1R^{k-1}N}, \\ C_2 &= \frac{(k+\nu_{21})PR^2\alpha^{2k}(\gamma-1)[\alpha^2(1+\nu_{21})-3-\nu_{21}]}{2(9-k^2)E_1D_1R^{-k-1}N} \end{aligned} \quad (5.38)$$

where for the conciseness sake the notation

$$N = (k^2 - \nu_{21}^2)(1 - \alpha^{2k})(\gamma - 1) + 2k(1 + \nu_{21})\alpha^{k-1} \quad (5.39)$$

and

$$\begin{aligned} \gamma &= \frac{D_1}{D_0}, \\ \alpha &= \frac{a}{R} \end{aligned} \quad (5.40)$$

is introduced.

According to the second boundary condition in (5.29) and (5.26) one has

$$C + C_1 R^{k+1} + C_2 R^{1-k} + \frac{PR^4}{8(9-k^2)E_1 D_1} + \frac{B_0 R^2}{2(1-k^2)E_1 D_1} = 0. \quad (5.41)$$

The last equation with (5.35), (5.37), (5.40) permits defining

$$\begin{aligned} C &= R^{k+1} C_1 \left[\frac{(1+k)(k+\nu_{21})\alpha^{2k}}{(1-k)(\nu_{21}-k)} - \frac{k(1+k)}{(k-\nu_{21})(\gamma-1)} - 1 \right] \\ &+ \frac{PR^4(2\alpha^2-1)}{8(9-k^2)E_1 D_1}. \end{aligned} \quad (5.42)$$

Employing the continuity of the deflection W at $r = a$ one obtains

$$\begin{aligned} W_0 &+ \frac{Pa^4}{8(9-k^2)E_1 D_0} + \frac{B_0 a^2}{2(1-k^2)E_1 D_0} \\ &= \frac{Pa^4}{8(9-k^2)E_1 D_1} + \frac{B_0 a^2}{2(1-k^2)E_1 D_1} + C_1 a^{1+k} + C_2 a^{1-k}. \end{aligned} \quad (5.43)$$

Thus the maximal deflection can be calculated as

$$W_0 = \frac{1-\gamma}{E_1 D_1} \left[\frac{Pa^4}{8(9-k^2)} + \frac{B_0 a^2}{2(1-k^2)} \right] + C_1 a^{k+1} + C_2 a^{1-k} \quad (5.44)$$

where the constants B_0 , C_1 , C_2 , γ and α are defined by (5.37), (5.38), (5.40).

5.6 Optimal design of a stepped plate

The problem posed above consists of the minimization of the maximum deflection $W_0 = W(0)$ under the condition that the material volume V of the plate is constrained.

Evidently, the deflection $W(0)$ is a function of design parameters; $W_0 = W_0(a_1, \dots, a_n, h_0, \dots, h_n)$. The constrained minimum of W_0 can be defined employing the extended function

$$I_* = W_0(a_1, \dots, a_n, h_0, \dots, h_n) + \lambda(V - \bar{V}\pi R^2 h_0) \quad (5.45)$$

where λ is an unknown Lagrangian multiplier.

The necessary optimality conditions of (5.45) can be written as

$$\begin{aligned}\frac{\partial I_*}{\partial a_i} &= 0; & i &= 1, \dots, n \\ \frac{\partial I_*}{\partial h_j} &= 0; & j &= 0, \dots, n \\ \frac{\partial I_*}{\partial \lambda} &= 0.\end{aligned}\tag{5.46}$$

The system (5.46) consists of $2n + 2$ algebraic equations. These allows determining $2n + 2$ unknown parameters a_i ($i = 1, \dots, n$), h_j ($j = 0, \dots, n$) and λ for each given volume \bar{V} of the plate.

5.7 Numerical results and discussion

The non-linear system of equations (5.46) is solved numerically. Calculations are carried out with the aid of computer codes *Python* and *Mathematica*. Calculations are carried out for the plate with radius $R = 1$ m and $h_0 = 0.0025$ m.

Table 5.1: Optimal values of parameters.

$\frac{\bar{V}}{\pi}$	W_0	α	γ	W_*	e
0.45	0.0056	0.5701	0.1852	0.0262	0.2122
0.50	0.0044	0.5475	0.2860	0.0191	0.2306
0.55	0.0039	0.5466	0.3583	0.0143	0.2685
0.60	0.0035	0.5539	0.4230	0.0111	0.3146
0.65	0.0032	0.5670	0.4842	0.0087	0.3678
0.70	0.0030	0.5852	0.5437	0.0070	0.4278
0.75	0.0028	0.6088	0.6028	0.0057	0.4952
0.80	0.0027	0.6384	0.6624	0.0047	0.5709
0.85	0.0026	0.6755	0.7241	0.0039	0.6561
0.90	0.0025	0.7232	0.7904	0.0033	0.7530
0.95	0.0024	0.7887	0.8677	0.0028	0.8651
0.99	0.0024	0.8659	0.9600	0.0025	0.9705

The results of calculations are presented in Table 5.1 and Fig. 5.1 for the case $n = 1$. The results are obtained for the plate made of a Boron-Aluminium composite consisting of Aluminium matrix and Boron fibers. For this material $E_1 = 204$ GPa, $E_2 = 118$ GPa and $\nu_{12} = 0.27$.

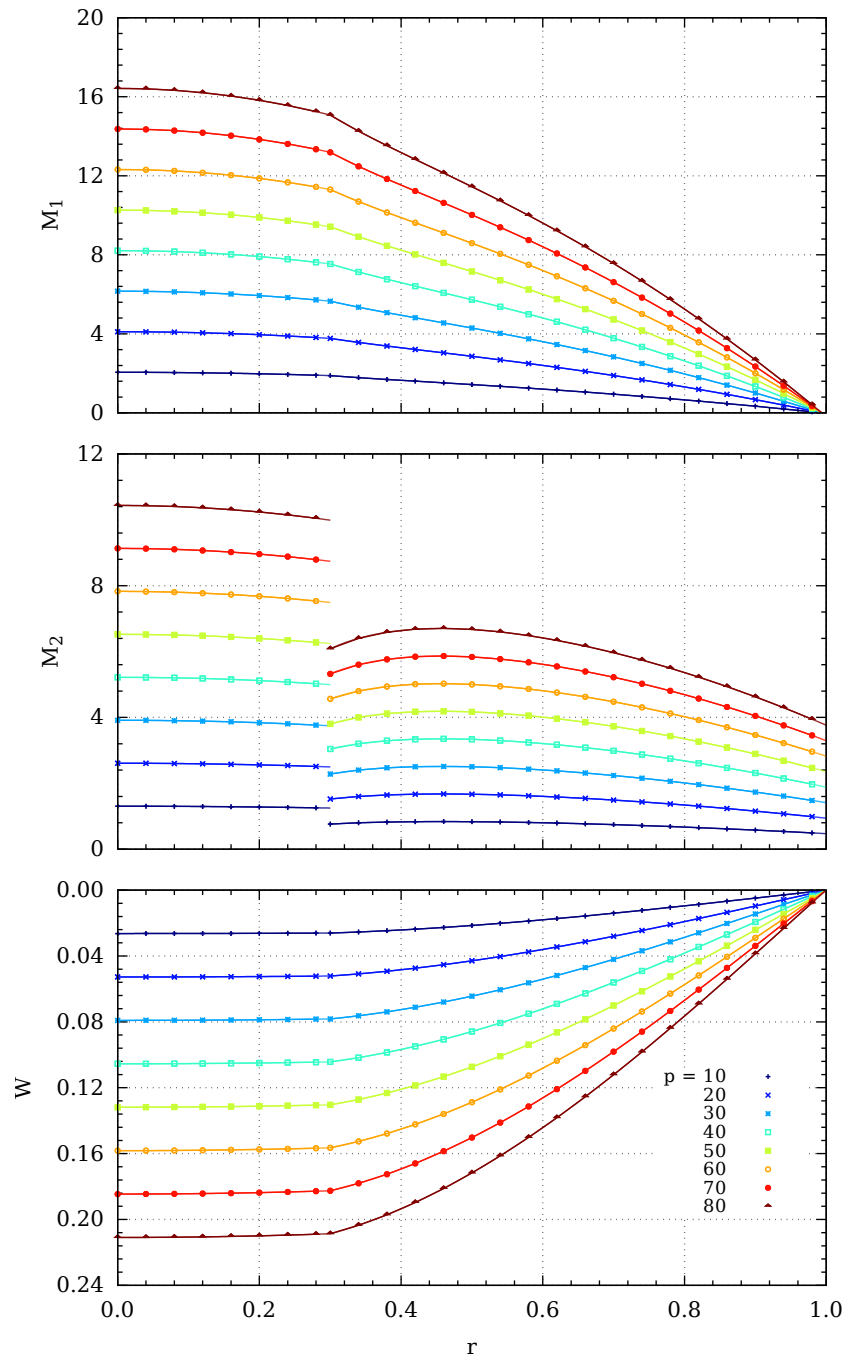


Figure 5.1: Bending moments and deflections.

It can be seen from the middle panel in Fig. 5.1 that the circumferential bending moment is discontinuous at $r = a$, as might be expected. Calculations carried out showed that the jump of M_2 at $r = a$ depends on the ratio of thicknesses in the adjacent sections of the plate.

The radial bending moment M_1 has a slope discontinuity at the step position (the top panel in Fig. 5.1) which is less remarkable in the cases of lower load intensities.

The displacements in the transverse direction are presented for different values of the intensity of the transverse pressure on the bottom panel in Fig. 5.1, for different load levels for the stepped plate with the step at $a = 0.3R$.

The efficiency of the design established above is assessed by the ratio

$$e = \frac{W_0}{W_*}, \quad (5.47)$$

W_* being the maximum deflection of the reference plate of constant thickness $h_* = \frac{V}{\pi R^2}$. The values of the coefficient e are accommodated in Table 5.1 together with optimal values α and γ . In the first column of Table 5.1 the values of the plate volume $\bar{V} = \frac{V}{\pi R^2 h_0}$ are presented. It reveals from Table 5.1 that for smaller values of \bar{V} the deflection of the reference plate of constant thickness W_* is larger, as might be expected. If \bar{V} increases then the optimal ratio of thicknesses $\gamma = \frac{h_1}{h_0}$ also increases and the step location $a = \alpha R$ moves towards the edge of the plate. However, the maximal deflection of the optimized plate decreases if the quantity \bar{V} increases.

Calculations carried out showed that the optimal values of α and γ are insensitive with respect to the changes of the load intensity. However, the optimal value of W_0 as well as the quantities W_* and e do depend on the value of the load intensity P .

5.8 Concluding remarks

A method for the analysis and optimization of fiber reinforced composite plates was developed. Considering the cases of unidirectional orientations of fibers, the composite was modelled as a quasi-homogeneous anisotropic material having different properties in different directions. Attention was focused on the cases of radial and circumferential orientation of fibers in the matrix material.

Invoking the methods of non-linear mathematical programming, the optimal design parameters of plates with piecewise constant thickness were determined. The optimization problems were solved with the aid of unknown Lagrangian multipliers. Numerical results were obtained with the aid of existing computer codes. It was shown that the optimal values of design parameters depend on the physical and geometrical parameters but these are insensitive with respect to the loading level.

CONCLUDING REMARKS

In this thesis, the circular and annular plates with the piecewise constant thickness and different support types are investigated using piecewise linear yield conditions.

The bending problem for the elastic plastic annular plate, simply supported at the outer edge, is solved by finding the deflections, the radial and circumferential bending moments for different loadings.

It appears that the stress strain state of the elastic plastic annular plate with the piecewise constant thickness, clamped at the inner edge and absolutely free at the outer edge, can be divided into three stages. The expressions of the deflections and the bending moments are found in the cases of elastic, elastic plastic and entirely plastic stress strain states, respectively.

The optimization problems regarding to the stepped circular plates made of homogeneous and anisotropic materials are solved numerically. For the fixed plate volume, the optimal values for the heights of the carrying layers and the location for the step are calculated while requiring minimal deflection at the centre of the plate. Also, the optimal locations for additional circular supports corresponding to the minimum of the mean are found in the case of the elastic simply supported plate.

As a result of the solution procedure, a succession of stress states which are in equilibrium with the external loading were constructed that led from the wholly elastic to the elastic plastic state and finally to the plastic collapse state.

The results of calculations showed that the optimal position of the additional support allows diminishing essentially the cost function. It revealed by calculations that both the radial and circumferential bending moments are continuous over the entire plate.

It was shown that the optimal values of design parameters depend on the physical and geometrical parameters but these are insensitive with respect to the loading level.

APPENDIX

A.1 Elastic stage of deformation of the annular plate

The transverse deflection can be presented as

$$W = \frac{P(r^4 - R^4)}{64D} + A_1(r^2 \ln r - R^2 \ln R) + A_2(r^2 - R^2) + A_3 \ln \frac{r}{R}, \quad (\text{A.1})$$

where

$$\begin{aligned} A_1 &= -\frac{Pa^2}{8D}, \\ A_2 &= \frac{P}{32D(1+\nu)(R^2 - a^2)} \cdot \left\{ (3+\nu)(a^4 - R^4) \right. \\ &\quad \left. + 2a^2[(R^2 - a^2)[2(1+\nu) \ln a + 3 + \nu] - 2R^2(1+\nu)(\ln a - \ln R)] \right\}, \\ A_3 &= -\frac{(y^2 + R^2)[-Py^3(1+3\nu) + 6Pa^2y\nu + 12M_0(a-2y) + 4Pa^3]}{48D(1+\nu)y}. \end{aligned} \quad (\text{A.2})$$

The bending moments have the form

$$\begin{aligned} M_1 &= -\frac{Pr^2(3+\nu)}{16} + \frac{Pa^2[2(1+\nu) \ln r + 3 + \nu]}{8} \\ &\quad - D \left[2A_2(1+\nu) + \frac{A_3(\nu-1)}{r^2} \right] \end{aligned} \quad (\text{A.3})$$

and

$$\begin{aligned} M_2 &= -\frac{Pr^2(1+3\nu)}{16} + \frac{Pa^2[2(1+\nu) \ln r + 1 + 3\nu]}{8} \\ &\quad - D \left[2A_2(1+\nu) + \frac{A_3(1-\nu)}{r^2} \right]. \end{aligned} \quad (\text{A.4})$$

A.2 Elastic plastic stage of deformation (Tresca criterion)

The transverse deflection can be calculated as

$$\begin{aligned}
 W = & \frac{r\{Pv(y^3 + 2a^3 - 3a^2y) + 6M_0[av - y(v - 1)]\}}{6D(v^2 - 1)} \\
 & + \frac{P[-3y^4 + 8a^2y^2 - R^4]}{64D} + \frac{PR^2a^2(\ln R - \ln y)}{8D} \\
 & - \frac{(y^2 + R^2)[-Py^3(1 + 3v) + 6Pa^2yv + 12M_0(a - 2y) + 4Pa^3]}{48D(1 + v)y} \\
 & + \frac{(\ln y - \ln R - 1)y[Py^3(1 + 3v) + 6Pa^2y(-1 - v) + 8a(3M_0 + Pa^2)]}{48D(v - 1)}
 \end{aligned} \tag{A.5}$$

for $r \in (a, y)$ and as

$$\begin{aligned}
 W = & \frac{(r^2 - R^2)[-Py^3(1 + 3v) + 6Pa^2yv + 12M_0(a - 2y) + 4Pa^3]}{48D(1 + v)y} \\
 & + \frac{Pa^2[r^2(\ln y - \ln r) + R^2(\ln R - \ln y)]}{8D} + \frac{P(r^4 - R^4)}{64D} \\
 & + \frac{y(\ln r - \ln R)[Py^3(1 + 3v) - 6Pa^2y(1 + v) + 8a(3M_0 + Pa^2)]}{48D(v - 1)}
 \end{aligned} \tag{A.6}$$

for $r \in (y, R)$. The radial bending moment has the form

$$M_1 = \frac{r - a}{r} \left[M_0 - \frac{P(r^2 + ar - 2a^2)}{6} \right] \tag{A.7}$$

for $r \in (a, y)$ and

$$\begin{aligned}
 M_1 = & \frac{-Pr^2(3 + v)}{16} - \frac{y[Py^3(1 + 3v) - 6Pa^2y(1 + v) + 8a(3M_0 + Pa^2)]}{48r^2} \\
 & + \frac{3Pa^2y(3 - v) + Py^3(1 + 3v) - 12M_0(a - 2y) - 4Pa^3 + 6Pa^2y(1 + v)(\ln r - \ln y)}{24y}
 \end{aligned} \tag{A.8}$$

for $r \in (y, R)$. The value for y depends on the load intensity P and can be obtained from the following equation

$$\begin{aligned}
 & \frac{PR^2(3 + v)}{16D} - \frac{Pa^2[2(1 + v)\ln R + 3 + v]}{8D} + \frac{1}{24Dy} \\
 & \cdot \{-Py^3(1 + 3v) + 6Pa^2y[(v + 1)\ln y + v] + 12M_0(a - 2y) + 4Pa^3\} \\
 & + \frac{y[Py^3(1 + 3v) - 6Pa^2y(1 + v) + 8a(3M_0 + Pa^2)]}{48DR^2} = 0.
 \end{aligned} \tag{A.9}$$

A.3 Elastic plastic stage of deformation (diamond yield condition)

In the plastic region the transverse deflection has the form

$$W = Ar^2 + B, \quad (\text{A.10})$$

where

$$A = \frac{Py^2(\nu + 1) - 4M_0(\nu - 1)}{16D_0(\nu^2 - 1)} \quad (\text{A.11})$$

and

$$B = \frac{Py^4[(\nu + 1) \ln y - \nu]}{16D_0(\nu - 1)} + \frac{1}{64D_0(\nu^2 - 1)} \left\{ 4R^2(\nu - 1) \cdot [Py^2(\nu + 1) + 4M_0] - 4(\nu + 1)^2 y^4 P \ln R + P(\nu^2 - 1)(y^4 - R^4) \right\}. \quad (\text{A.12})$$

However, in the elastic region, the transverse deflection is the following

$$W = \frac{Pr^4}{64D} + A_1 = r^2 \ln r + A_2 r^2 + A_3 \ln r + A_4 \quad (\text{A.13})$$

for $r \in (a_j, a_{j+1})$. In the case of a single-step plate

$$\begin{aligned} A_1 &= 0, \\ A_2 &= -\frac{Py^2(\nu+1)+4M_0}{16D_0(1+\nu)}, \\ A_3 &= \frac{Py^4(\nu+1)}{16D_0(\nu-1)}, \\ A_4 &= \frac{1}{64D_0(\nu^2-1)} \left\{ 4R^2(\nu-1)[Py^2(\nu+1) + 4M_0] \right. \\ &\quad \left. - 4(\nu+1)^2 y^4 P \ln R - PR^4(\nu^2-1) \right\}. \end{aligned} \quad (\text{A.14})$$

REFERENCES

- [1] B. Åkesson and N. Olhoff. Minimum stiffness of optimally located supports for maximum value of beam eigenfrequencies. *J. Sound Vibr.*, 120:457–463, 1988.
- [2] H. G. Allen. *Analysis and Design of Structural Sandwich Panels*. Pergamon Press, Oxford, 1969.
- [3] A. N. Andreev and Y. V. Nemirovskii. *Multilayered Anisotropic Shells and Plates: Bending, Buckling, Vibrations (in Russian)*. Nauka, Novosibirsk, 2001.
- [4] N. Banichuk. *Introduction to Optimization of Structures*. Springer, Berlin, 1990.
- [5] M. P. Bendsøe. *Optimization of Structural Topology, Shape, and Material*. Springer-Verlag, Berlin, 1995.
- [6] D. Bojczuk and Z. Mróz. On optimal design of supports in beam and frame structures. *Struct. Optim.*, 16,1:47–57, 1998.
- [7] D. Bojczuk and Z. Mróz. Determination of optimal actuator forces and positions in smart structures using adjoint method. *Struct. Multidisc. Optim.*, 30,4:308–319, 2005.
- [8] W. E. Boyce. A note on strain hardening circular plates. *J. Mech. Phys. Solids*, 7,2:114–125, 1959.
- [9] A. M. Brandt. *Foundations of the Optimum Design of Structural Elements (in Polish)*. PWN, Warsaw, 1978.
- [10] A. Bryson and H. Yu-Chi. *Applied Optimal Control*. Wiley, New York, 1975.
- [11] J. Chakrabarty. *Applied Plasticity*. Springer, Berlin, 2006.
- [12] K.-T. Cheng and N. Olhoff. An investigation concerning optimal design of solid elastic plastic plates. *Int. J. Solid Struct.*, 17,3:305–323, 1981.
- [13] A. V. Cherkaev. *Variational Methods for Structural Optimization*. Springer, New York, 2000.

- [14] F. S. Chou, C. M. Wang, and N. Cheng, G. D. Olhoff. Optimal design of internal ring supports for vibrating circular plates. *J. Sound Vibration*, 219,3:525–537, 1999.
- [15] M. Z. Cohn. *Analysis and Design of Inelastic Structures*. University of Waterloo Press, Waterloo, 1972.
- [16] I. M. Daniel and O. Ishai. *Engineering Mechanics of Composite Materials*. Oxford University Press, 1994.
- [17] D. C. Drucker and R. T. Shield. Bounds on minimum weight design. *Quart. Appl. Math.*, 15,3:269–281, 1957.
- [18] G. Eason. The elastic, plastic bending of a simply supported plate. *J. Appl. Mech.*, 28,3:395–401, 1961.
- [19] F. W. French. Elastic-plastic analysis of centrally clamped annular plates under uniform loads. *J. Franklin Inst.*, 277,6:575–592, 1964.
- [20] U. Gamer. Stress distribution in the rotating elastic-plastic disk. *ZAMM*, 65:T136–T137, 1985.
- [21] A. Garstecki and Z. Mróz. Optimal design of supports of elastic structures subjected to loads and initial distortions. *Mech. Struct. Mach.*, 15:47–68, 1987.
- [22] R. F. Gibson. *Principles of Composite Material Mechanics*. McGraw-Hill, Singapore, 1994.
- [23] M. Gorji and A. R. Akileh. Elastic-plastic bending of annular plates with large deflections. *Comp. Struct.*, 34,4:537–548, 1990.
- [24] U. Güven. Elastic-plastic stresses in a rotating annular disk of variable thickness and variable density. *Int. J. Mech. Sci.*, 34,2:133–138, 1992.
- [25] R. M. Haythornthwaite. The deflection of plates in the elastic-plastic range. *Proc. 2nd U.S. Natl. Congr. Appl. Mech.*, pages 521–526, 1955.
- [26] C. T. Herakovich. *Mechanics of Fibrous Composites*. Wiley and Sons, New York, 1998.
- [27] P. G. Hodge. Boundary value problems in plasticity. *Plasticity, Proc. 2nd Symposium Naval Struct. Mech.*, pages 297–337, 1960.
- [28] P. G. Hodge. *Limit Analysis of Rotationally Symmetric Plates and Shells*. Prentice Hall, New York, 1963.

- [29] P. G. Hodge. *Plastic Analysis of Structures*. Krieger, New York, 1981.
- [30] D. G. Hull. *Optimal Control Theory for Applications*. Springer, Berlin, 2003.
- [31] C. Hwang. Plastic bending of a work-hardening circular plate with clamped edge. *J. Aerospace Sci.*, 27,11:815–820, 1960.
- [32] N. Jones. *Structural Impact*. Cambridge University Press, Cambridge, 1997.
- [33] R. M. Jones. *Mechanics of Composite Materials*. Taylor & Francis, Philadelphia, 1999.
- [34] L. M. Kachanov. *Foundations of the Theory of Plasticity (in Russian)*. Nauka, Moscow, 1969.
- [35] S. Kaliszky. *Plasticity. Theory and Engineering Applications*. Elsevier, Amsterdam, 1989.
- [36] A. Khalili and J. Peddieson. Evaluation of elastic compensation using elastic/plastic rotating circular disk problems. *Mech. Res. Comm.*, 55:89–94, 2013.
- [37] J. Kirs. Optimal design of dynamically loaded annular plates, considering the hardening material. *Tras. Tartu Univ.*, 939:5–19, 1992.
- [38] U. Kirsch. *Structural Optimization: Fundamentals and Applications*. Springer-Verlag, Heidelberg, 1993.
- [39] L. M. Lackman. Circular plates loaded into the plastic region. *Proc. ASCE J. Eng. Mech. Div.*, 90,6:21–30, 1964.
- [40] J. Lellep. Optimal design of plates subjected to local loading (in Russian). *Trans. Tartu State Univ.*, 430:144–151, 1977.
- [41] J. Lellep. Parametrical optimization of plastic beams in the post-yield range. *Int. J. Eng. Sci.*, 20,1:67–75, 1982.
- [42] J. Lellep. Optimal location of additional supports for plastic cylindrical shells subjected to impulsive loading. *Int. J. Non-Linear Mech.*, 19,4:323–330, 1984.
- [43] J. Lellep. Optimum location of additional supports for a geometrically nonlinear plastic cylindrical shell. *Soviet Appl. Mech.*, 21,1:54–60, 1985.
- [44] J. Lellep. Parametrical optimization of plastic cylindrical shells in the post-yield range. *Int. J. Eng. Sci.*, 23,12:1289–1303, 1985.

- [45] J. Lellep. Optimal design of plastic reinforced cylindrical shells. *Control-Theory and Advanced Technology*, 5,2:119–135, 1989.
- [46] J. Lellep. *Optimization of Systems (in Estonian)*. University of Tartu Press, Tartu, 2013.
- [47] J. Lellep and Ü. Lepik. Analytical methods in plastic structural design. *Eng. Optim.*, 7,3:209–239, 1984.
- [48] J. Lellep and A. Paltsepp. Optimization of inelastic cylindrical shells with internal supports. *Struct. Multidisc. Optim.*, 41,6:841–852, 2010.
- [49] J. Lellep and J. Polikarpus. Optimization of elastic-plastic circular plates under axisymmetric loading. In L. Sakalauskas, G. W. Weber, and E. K. Zavadskas, editors, *Proc. 20th Int. Conf. "Continuous Optimization and Knowledge-Based Technology"*, pages 291–295, Vilnius, 2008. Technika.
- [50] J. Lellep and J. Polikarpus. Elastic plastic bending of stepped annular plates. In A. Zemliak and N. Mastorakis, editors, *American Conf. Appl. Math. "Applications of Mathematics & Computer Engineering"*, pages 140–145. WSEAS Press, 2011.
- [51] J. Lellep and J. Polikarpus. Optimization of elastic circular plates with additional supports. In N. Mastorakis and et al., editors, *Proc. 2nd Int. Conf. Theoretical Appl. Mech. "Recent Researches in Mechanics"*, pages 136–141. WSEAS Press, 2011.
- [52] J. Lellep and J. Polikarpus. Optimal design of circular plates with internal supports. *WSEAS Trans. Math.*, 11,3:222–232, 2012.
- [53] J. Lellep and J. Polikarpus. Elastic plastic bending of stepped circular plates. In J. Lellep and E. Puman, editors, *Proc. 2nd Int. Conf. "Optimization and Analysis of Structures"*, pages 81–87. University of Tartu Press, 2013.
- [54] J. Lellep and J. Polikarpus. Optimization of anisotropic circular plates. In M. V. Shitikova, L. Vladareanu, and C. Guarnaccia, editors, *Proc. 5th European Conf. Mech. Engin. "Recent Advances in Mechanical Engineering"*, pages 40–45. WSEAS Press, 2014.
- [55] J. Lellep and J. Polikarpus. Elastic plastic bending of annular plates. In J. Lellep and E. Puman, editors, *Proc. 3rd Int. Conf. "Optimization and Analysis of Structures"*, pages 73–79. University of Tartu Press, 2015.

- [56] J. Lellep and E. Puman. Optimization of elastic and inelastic conical shells of piece wise constant thickness. In N. Mastorakis and et al., editors, *Proc. 2nd Int. Conf. Theoretical Appl. Mech. "Recent Researches in Mechanics"*, pages 223–228. WSEAS Press, 2011.
- [57] J. Lellep, E. Puman, L. Roots, and E. Tungel. Optimization of rotationally symmetric shells. In C. A. Bulucea, V. Mladenov, E. Pop, M. Leba, and N. Mastorakis, editors, *Proc. 14th WSEAS Int. Conf. Appl. Math. "Recent Advances in Applied Mathematics"*, pages 233–238. WSEAS Press, 2009.
- [58] J. Lellep, E. Puman, L. Roots, and E. Tungel. Optimization of stepped shells. *WSEAS Trans. Math.*, 9,2:130–139, 2010.
- [59] J. Lellep and B. Vlassov. Optimization of stepped elastic plastic plates. In T. Wohlbier, J. Feng, and Y. Wu, editors, *Advanced Materials Research*, pages 209–214. Trans Tech Publications Ltd, 2013.
- [60] Ü. Lepik. Minimum weight design of circular plates with limited thickness. *Int. J. Non-Linear Mech.*, 7,4:353–360, 1972.
- [61] Ü. Lepik. Application of Pontryagin's maximum principle for minimum weight design of rigid-plastic circular plates. *Int. J. Solids and Struct.*, 9,5:615–624, 1973.
- [62] Ü. Lepik. Optimal design of beams with minimum compliance. *Int. J. Non-Linear Mech.*, 13,1:33–42, 1978.
- [63] Ü. Lepik and Z. Mróz. Optimal design of plastic structures under impulsive and dynamic pressure loading. *Int. J. Solids Struct.*, 13,7:657–674, 1977.
- [64] Ü. Lepik and Z. Mróz. Optimal design of impulsively loaded plastic beams for asymmetric mode motions. *Int. J. Solids Struct.*, 14,10:841–850, 1978.
- [65] K. Magnucki, P. Jasion, E. Magnucka-Blandzi, and P. Wasilewicz. Theoretical and experimental study of a sandwich circular plate under pure bending. *Thin-Walled Struct.*, 79:1–7, 2014.
- [66] E. S. Melerski. *Design Analysis of Beams, Circular Plates, Cylindrical Tanks on Elastic Foundations*. Taylor & Francis, London, 2006.
- [67] S. M. Mousavi and J. Paavola. Analysis of plate in second strain gradient elasticity. *Arch. Appl. Mech.*, 84,8:1135–1143, 2014.

- [68] S. M. Mousavi, J. Paavola, and J. N. Reddy. Variational approach to dynamic analysis of third-order shear deformable plates within gradient elasticity. *Mechanica*, 50,6:1537–1550, 2015.
- [69] Z. Mróz and T. Lekszycki. Optimal support reaction in elastic frame structures. *Comp. Struct.*, 14:179–185, 1981.
- [70] Z. Mróz and G. Rozvany. Optimal design of structures with variable support positions. *J. Optim. Theory Applic.*, 15:85–101, 1975.
- [71] Y. Nagai and K. Ito. An advanced analysis of axisymmetric plastic sheet bending including transverse shear deformation. *Int. J. Mech. Sci.*, 33,9:717–728, 1991.
- [72] P. M. Naghdi. Bending of elastoplastic circular plates with large deflection. *J. Appl. Mech.*, 19:293–300, 1952.
- [73] M. Oblak. Elasto-plastic bending analysis of a thick plate. *ZAMM*, 66:320–322, 1986.
- [74] Y. Ohashi and S. Murakami. Large deflection in elastoplastic bending of a simply supported circular plate under uniform load. *J. Appl. Mech.*, 33,4:866–870, 1966.
- [75] Y. Ohashi, S. Murakami, and A. Endo. Elasto-plastic bending of an annular plate at large deflection. *Ing.-Arch.*, 35,5:340–350, 1967.
- [76] N. Olhoff. *Optimal Design of Constructions (in Russian)*. Mir, Moscow, 1981.
- [77] N. Olhoff and B. Åkesson. Minimum stiffness of optimally located supports for minimum value of column buckling loads. *J. Struct. Optim.*, 3:163–175, 1991.
- [78] D. Pawlus. Solution to the static stability problem of three-layered annular plates with a soft core. *J. Theor. Appl. Mech.*, 44,2:299–322, 2006.
- [79] F. J. Plantema. *Sandwich Construction: the Bending and Buckling of Sandwich Beams, Plates and Shells*. Wiley and Sons, New York, 1966.
- [80] E. P. Popov, M. Khostjeh-Bakht, and S. Yaghmal. Analysis of elastic-plastic circular plates. *Proc. ASCE, J. Eng. Mech. Div.*, 93,EM 6:49–65, 1967.
- [81] W. Prager and G. Rozvany. Plastic design of beams: optimal locations of supports and steps in yield moment. *Int. J. Mech. Sci.*, 17,10:627–631, 1975.

- [82] J. N. Reddy. *Theory and Analysis of Elastic Plates and Shells*. CRC Press, Boca Raton, 2007.
- [83] J. N. Reddy and C. M. Wang. Relationships between classical and shear deformation theories of axisymmetric bending of circular plates. *AIAA J.*, 35,12:1862–1868, 1997.
- [84] R. M. Richard and B. J. Abbott. Versatile elastic-plastic stress-strain formula. *Proc. ASCE, J. Eng. Mech. Div.*, 101,4:511–515, 1975.
- [85] G. Rozvany. *Structural Design via Optimality Criteria*. Kluwer, Dordrecht, 1989.
- [86] M. A. Save, C. E. Massonnet, and G. de Saxcé. *Plastic Limit Analysis of Plates, Shells and Disks*. Elsevier, Amsterdam, 1997.
- [87] A. Sawczuk and M. Duszek. A note on the iteration of shear and bending in plastic plates. *Arch. Mechan. Stosow.*, 15,3:411–426, 1963.
- [88] A. Sawczuk and J. Sokół-Supel. *Limit Analysis of Plates*. Polish Scientific Publishers, Warsaw, 1993.
- [89] A. N. Sherbourne and N. K. Srivastava. Elastic-plastic bending of restrained pin-ended circular plates. *Int. J. Mech. Sci.*, 13,3:231–241, 1971.
- [90] V. V. Sokolovsky. Elastic-plastic bending of circular and annular plates (in Russian). *Prikl. Mat. Mech.*, 8,2:141–166, 1944.
- [91] D. Szelag and Z. Mróz. Optimal design of elastic beams with unspecified support positions. *ZAMM*, 58:501–510, 1978.
- [92] M. Tanaka. Large deflection analysis of elastic-plastic circular plates with combined isotropic and kinematic hardening. *Ing.-Arch.*, 41,5:342–356, 1972.
- [93] B. Tekinalp. Elastic, plastic bending of a simply supported circular plate under a uniformly distributed load. *Brown University, DAM Rep. C11-6*, 1955.
- [94] B. Tekinalp. Elastic-plastic bending of a built-in circular plate under a uniformly distributed load. *J. Mech. Phys. Solids*, 5,2:135–142, 1957.
- [95] G. J. Turvey. Large deflection of circular plates with affine imperfections. *Int. J. of Solids and Struct.*, 14,7:559–569, 1978.
- [96] G. J. Turvey. Axisymmetric elasto-plastic flexure of circular plates in the large deflection regime. *Proc. Inst. Civil Engin.*, 67:81–92, 1979.

- [97] G. J. Turvey and G. T. Lim. Axisymmetric full-range analysis of transverse pressure-loaded circular plates. *Int. J. Mech. Sci.*, 26,9-10:489–502, 1984.
- [98] G. J. Turvey and M. Salehi. Computer generated elasto-plastic design data for pressure loaded circular plates. *Comp. Struct.*, 41,6:1329–1340, 1991.
- [99] M. E. Tuttle. *Structural Analysis of Polymeric Composite Materials*. Marcel Dekker, New York, 2004.
- [100] M. Upadrasta, J. Peddieson, and G. R. Buchanan. Elastic compensation simulation of elastic/plastic axisymmetric circular plate bending using a deformation model. *Int. J. Non-Linear Mech.*, 41,3:377–387, 2006.
- [101] E. Ventsel and T. Krauthammer. *Thin Plates and Shells: Theory, Analysis and Applications*. Marcel Dekker, New York, 2001.
- [102] J. Vinson. *Plate and Panel Structures of Isotropic, Composite and Piezoelectric Materials, Including Sandwich Construction*. Springer, Dordrecht, 2005.
- [103] C. M. Wang, J. N. Reddy, and K. H. Lee. *Shear Deformable Beams and Plates: Relationships with Classical Solutions*. Elsevier, 2000.
- [104] C.-M. Wang, G. I. N. Rozvany, and N. Olhoff. Optimal plastic design of axisymmetric solid plates with a maximum thickness constraint. *Comp. Struct.*, 18,4:653–665, 1984.
- [105] C.-M. Wang, V. Thevendran, G. I. N. Rozvany, and N. Olhoff. Optimal plastic design of circular plates: Numerical solutions and built-in edges. *Comp. Struct.*, 22,4:519–528, 1986.
- [106] C. M. Wang, Y. Xiang, S. Kitipornchai, and K. M. Liew. Axisymmetric buckling of circular Mindlin plate with ring supports. *J. Struct. Eng.*, 119,3:782–793, 1993.
- [107] D. Wang. Optimization of support positions to minimize the maximal deflections of structures. *Int. J. Solids Struct.*, 41,26:7445–7458, 2004.
- [108] H. M. Wen. Deformation and tearing of clamped circular work-hardening plates under impulsive loading. *Int. J. of Pressure Vessels and Piping*, 75,1:67–73, 1998.
- [109] T. X. Yu and L. C. Zhang. *Plastic Bending. Theory and Applications*. World Scientific, Singapore, 1996.

KOKKUVÕTE

Elastsete-plastsete telgsümmeetriliste plaatide analüüs ja optimeerimine

Käesolevas töös uuritakse ümar- ja rõngasplaate, millele mõjub telgsümmeetriline ristkoormus. Ümarplaat on ringsilindriline keha, mille kõrgus on teiste mõõtmetega võrreldes väike.

Antud töös arvestatakse nii elastseid kui ka plastseid deformatsioone. Elastse deformatsiooni korral taastub keha esialgne kuju pärast koormuse eemaldamist, plastse deformatsiooni korral mitte.

Insenerimehaanikast on teada, et konstruktsioonielementide (talade, plaatide, koorikute) modelleerimisel on materjali kokkuhoiuks mõistlik arvestada lisaks elastsetele deformatsioonidele ka plastseid.

Käesolevas töös vaadeldakse nn *sandwich*-tüüpi ümar- ja rõngasplaate. *Sandwich*-tüüpi plaadiks nimetatakse ideaalset kahekihilist plaati, mille kandva kihi paksus h on kihtidevahelise kaugusega H võrreldes väike. Kuna *sandwich*-tüüpi plaadi korral võib pinged piki paksust lugeda konstantseteks, siis lihtsustab see oluliselt arvutusi. Võime eeldada, et kandva kihi teatud piirkond saab olla kas ainult elastses või täielikult plastses seisundis.

Kui plaadile rakendatakse väikseid koormusi, siis on kogu plaat elastne. Koormuse suurendamisel tekib plaadi sümmetriatelje ümber plastne piirkond. Plastses piirkonnas peab pingeseisundit iseloomustav punkt asuma voolavuspinna (voolavuskõvera) peal. Käesolevas töös uuritakse materjale, mis alluvad tükati lineaarsetele voolavuspindadele. Plastsusteooria põhiseoste kohaselt rahuldab pingeseisund peale voolavuspinna võrrandite ka nn assotseeritud voolavusseadust. Assotseeritud voolavusseaduse kohaselt on deformatsioonikiiruse vektor voolavuspinna igas punktis sellega risti ning suunatud pinnast väljapoole.

Lisaks elastsete-plastsete ümar- ja rõngasplaatide paindeülesannete uurimisele lahendatakse antud töös ka lisatugedega vabalt toetatud ümarplaadi optimeerimise probleem.

Käesolev doktoritöö koosneb viiest peatükist. Esimene peatükk on referatiivne. Selles esitatakse ümarplaadi jaoks tasakaaluvõrrandid, deformatsiooni kiiruse komponendid, plaadi läbipainde diferentsiaalvõrrandid ning selle üldlahend. Samuti tutvustatakse Tresca' voolavustingimust ning assotseeritud voolavusseadust.

Teises peatükis uuritakse konstantse paksusega elastset-plastset servast vabalt toetatud ümarplaati Tresca' ja rombi voolavustingimuse korral. Selgub, et mõlemal juhul saab plastse ja elastse piirkonna rajapunkti tuletada analüütiliselt, st välja arvutada biruutvõrrandist. Selles peatükis lahendatakse numbriliselt ka ühe astmega elastse ümarplaadi optimeerimisülesanne, kus etteantud plaadi ruumala korral arvutatakse optimaalsed kandvate kihtide paksused ning astme asukoht nii, et plaadi kesk-

punktis oleks läbipaine minimaalne. Samuti lahendatakse elastse-plastse konstantse paksusega servast vabalt toetatud rõngasplaadi paindeülesanne, st leitakse erinevate koormuste korral analüütiliselt ja numbriliselt plaadi läbipained ning radiaal- ja tangentsiaalsuunalised paindemomendid.

Kolmandas peatükis uuritakse tükati konstantse paksusega elastset-plastset seest jäigalt kinnitatud rõngasplaati. Selgub, et antud astmelise rõngasplaadi deformatsiooni protsessi saab jagada kolme erinevasse staadiumisse. Leitakse läbipaine ja paindemomentide avaldised vastavalt elastse, elastse-plastse ja täiesti plastse plaadi pingeseisundi korral.

Neljandas peatükis lahendatakse analüütiliselt ja numbriliselt lisatugedega servast vabalt toetatud elastse ümarplaadi optimeerimisülesanne. Leitakse ringtugede optimaalsed asukohad nii, et plaadi läbipaine oleks minimaalne.

Viiendas peatükis lahendatakse numbriliselt sarnaselt teise peatüki ülesandele ühe astmega servast vabalt toetatud anisotroopsest materjalist ümarplaadi optimeerimisülesanne. Selle ülesande lahendamiseks tuletatakse analüütiliselt plaadi tasakaaluvõrrandid, läbipaine ja paindemomentide avaldised anisotroopse materjali korral.

Antud doktoritöö tulemused on publitseeritud seitsmes artiklis [49, 50, 51, 52, 53, 54, 55].

ACKNOWLEDGEMENTS

May I first express my deepest gratitude to my supervisor, Professor Jaan Lellep. I have been privileged to learn from Professor Lellep, he has not only taught me how to do research or teach, but he has been a good model of kindness and humanity. Professor Lellep, I especially admire your patience and excellency in explaining complicated things in an easy and understandable manner. I admire your readiness to learn new things.

I am genuinely grateful to my parents, sisters and grandparents for being with me and supporting me throughout the process of writing the thesis. I thank you for looking after the children and, above all, I am truly thankful that you are part of my life.

I thank all my friends from the school, from the sorority Patriae and from the Tartu Calvary Baptist Church for being beside me. Tiina Kr, you have been a fantastic friend and colleague. Tiina T, I truly appreciate the supportive speech you gave at a pretty criterial moment.

I also thank all my former and current colleagues from the former Tartu Forselius Gymnasium, Hugo Treffner Gymnasium, the former Tartu Kivilinna Gymnasium and from the University of Tartu. You have always given me valuable support.

I take this opportunity to express my appreciation towards my teachers and lecturers for being good models in my life. I also thank the people with whom I have been in contact over the last 10 years, both in Estonia and abroad, for their help.

I would like to sincerely thank my family for your love and support.

Finally, I offer my humble thanks to God for this journey.

The thesis was financially supported by the Estonian Science Foundation Grant 9110 “Optimization of structural elements”, the institutional research project IUT20-57 “Structural Problems in Analysis, Algebra, and Geometry, with Applications to Numerical Analysis” of the Estonian Ministry of Education and Research, Estonian Doctoral School of Mathematics and Statistics, European Social Fund’s Doctoral Studies and Internationalisation Programme DoRa, sorority Filiae Patriae California chapter.

CURRICULUM VITAE

Personal data

Name	Julia Polikarpus
Date and place of birth	5 May 1981, Tartu, Estonia
Citizenship	Estonian
Address	University of Tartu, Institute of Mathematics J. Liivi 2, Tartu, Estonia
Phone	(+372) 737 6428
E-mail	julia.polikarpus@ut.ee

Education

2005 – 2013	University of Tartu, doctoral studies in mathematics
2005	University of Tartu, Teacher of Mathematics in Upper Secondary School
2003 – 2005	University of Tartu, master's studies in mathematics
1999 – 2003	University of Tartu, bachelor's studies in mathematics
1993 – 1999	Hugo Treffner Gymnasium

Employment

2013 – ...	University of Tartu, Office of Academic Affairs, senior specialist for curriculum development
2011 – ...	University of Tartu, Institute of Mathematics, researcher of theoretical mechanics
2007 – 2011	Tartu Kivilinna Gymnasium, teacher of mathematics
2008 – 2011	University of Tartu, Institute of Mathematics, assistant of theoretical mechanics
2004 – 2008	University of Tartu, Institute of Mathematics, extraordinary assistant of theoretical mechanics
2004 – 2005	Hugo Treffner Gymnasium, teacher of mathematics
2003 – 2005	Tartu Forseliuse Gymnasium, teacher of mathematics

Professional training

02.06 – 11.06.2007	Summer school “Continuum Physics and Engineering Applications” Ráckeve, Hungary
01.10 – 06.10.2007	Autumn school “Structures of the mechanics of complex bodies” Centro di Ricerca Matematica Ennio De Giorgi, Pisa, Italy

- | | |
|--------------------|--|
| 06.11 – 13.11.2011 | Autumn school “Mathematical Principles for and Advances in Continuum Mechanics” Centro di Ricerca Matematica Ennio De Giorgi, Pisa, Italy |
| 25.11 – 29.11.2013 | Autumn school “Multi-scale and Multi-field Representations of Condensed Matter Behavior” Centro di Ricerca Matematica Ennio De Giorgi, Pisa, Italy |

Language skills

Estonian (mother tongue), English, Russian, French

Scientific work

The main fields of interest are elastic, elastic plastic circular and annular plates, optimization of plates. Results have been presented at the following 9 scientific conferences: “Finnish Mathematical Days 2006 and 2. Finnish-Estonian Mathematical Colloquium” in Tampere, Finland (2006), “Continuum Physics and Engineering Applications” in Ráckeve, Hungary (2007), “The 20th EURO Mini Conference Continuous optimization and Knowledge-Based Technologies” in Neringa, Lithuania (2008), “FinEst Math 2009, 3rd Finnish-Estonian Mathematical Colloquium” in Tartu, Estonia (2009), “American Conference on Applied Mathematics *Applications of Mathematics & Computer Engineering*” in Puerto Morelos, Mexico (2011), “International Conference on Optimization and Analysis of Structures” in Tartu, Estonia (2011), “The 3rd International Conference on Engineering Optimization”, in Rio de Janeiro, Brazil (2012), “The 2nd International Conference on Optimization and Analysis of Structures” in Tartu, Estonia (2013), “The 3rd International Conference on Optimization and Analysis of Structures” in Tartu, Estonia (2015).

ELULOOKIRJELDUS

Isikuandmed

Nimi	Julia Polikarpus
Sünniaeg ja -koht	5. mai 1981, Tartu, Eesti
Kodakondsus	Eesti
Aadress	Tartu Ülikool, matemaatika instituut J. Liivi 2, Tartu, Eesti
Telefon	(+372) 737 6428
E-post	julia.polikarpus@ut.ee

Haridustee

2005 – 2013	Tartu Ülikool, matemaatika doktoriõpe
2005	Tartu Ülikool, gümnaasiumi matemaatikaõpetaja
2003 – 2005	Tartu Ülikool, matemaatika magistriõpe
1999 – 2003	Tartu Ülikool, matemaatika bakalaureuseõpe
1993 – 1999	Hugo Treffneri Gümnaasium

Teenistuskäik

2013 – ...	Tartu Ülikool, õppeosakond, õppekvaliteedi peaspetsialist
2011 – ...	Tartu Ülikool, matemaatika instituut, teoreetilise mehaanika teadur
2007 – 2011	Tartu Kivilinna Gümnaasium, matemaatikaõpetaja
2008 – 2011	Tartu Ülikool, matemaatika instituut, teoreetilise mehaanika assistent
2004 – 2008	Tartu Ülikool, rakendusmatemaatika instituut, teoreetilise mehaanika erakorraline assistent
2004 – 2005	Hugo Treffneri Gümnaasium, matemaatikaõpetaja
2003 – 2005	Tartu Forseliuse Gümnaasium, matemaatikaõpetaja

Erialane enesetäiendus

02.06 – 11.06.2007	Suvekool „Continuum Physics and Engineering Applications“ Ráckeve, Ungari
01.10 – 06.10.2007	Sügiskool „Structures of the mechanics of complex bodies“ Centro di Ricerca Matematica Ennio De Giorgi, Pisa, Itaalia
06.11 – 13.11.2011	Sügiskool „Mathematical Principles for and Advances in Continuum Mechanics“ Centro di Ricerca Matematica Ennio De Giorgi, Pisa, Itaalia

25.11 – 29.11.2013 Sügiskool „Multi-scale and Multi-field Representations of Condensed Matter Behavior“ Centro di Ricerca Matematica Ennio De Giorgi, Pisa, Itaalia

Keelteoskus

eesti keel (emakeel), inglise keel, vene keel, prantsuse keel

Teaduslik tegevus

Peamised uurimisvaldkonnad on elastsed ning elastsed-plastsed ümar- ja rõngasplaadid, nende optimeerimine. Tulemusi on esitatud 9 teaduskonverentsil:

„Finnish Mathematical Days 2006 and 2. Finnish-Estonian Mathematical Colloquium“ Tampere Soomes (2006),

„Continuum Physics and Engineering Applications“ Ráckeves Ungaris (2007),

„The 20th EURO Mini Conference Continuous optimization and Knowledge-Based Technologies“ Neringal Leedus (2008),

„FinEst Math 2009, 3rd Finnish-Estonian Mathematical Colloquium“ Tartus Eestis (2009),

„American Conference on Applied Mathematics *Applications of Mathematics & Computer Engineering*“ Puerto Morelos Mehhikos (2011),

„International Conference on Optimization and Analysis of Structures“ Tartus Eestis (2011),

„The 3rd International Conference on Engineering Optimization“, Rio de Janeiro Brasiilias (2012),

„The 2nd International Conference on Optimization and Analysis of Structures“ Tartus Eestis (2013),

„The 3rd International Conference on Optimization and Analysis of Structures“ Tartus Eestis (2015).

LIST OF PUBLICATIONS

1. J. Lellep and J. Polikarpus. Optimization of elastic-plastic circular plates under axisymmetric loading. In L. Sakalauskas, G. W. Weber, and E. K. Zavadskas, editors, *Proceedings of the 20th International Conference "Continuous Optimization and Knowledge-Based Technology"*, pages 291–295, Vilnius, 2008. Technika.
2. J. Lellep and J. Polikarpus. Elastic plastic bending of stepped annular plates. In A. Zemliak and N. Mastorakis, editors, *American Conference on Applied Mathematics "Applications of Mathematics & Computer Engineering"*, pages 140–145. WSEAS Press, 2011.
3. J. Lellep and J. Polikarpus. Optimization of elastic circular plates with additional supports. In N. Mastorakis and et al., editors, *Proceedings of the 2nd International Conference on the Theoretical and Applied Mechanics 2011 "Recent Researches in Mechanics"*, pages 136–141. WSEAS Press, 2011.
4. J. Lellep and J. Polikarpus. Optimal design of circular plates with internal supports. *WSEAS Transactions on Mathematics*, 11,3:222–232, 2012.
5. J. Lellep and J. Polikarpus. Elastic plastic bending of stepped circular plates. In J. Lellep and E. Puman, editors, *Proceedings of the 2nd International Conference "Optimization and Analysis of Structures"*, pages 81–87. University of Tartu Press, 2013.
6. J. Lellep and J. Polikarpus. Optimization of anisotropic circular plates. In M. V. Shitikova, L. Vladareanu, and C. Guarnaccia, editors, *Proceedings of the 5th European Conference of Mechanical Engineering "Recent Advances in Mechanical Engineering"*, pages 40–45. WSEAS Press, 2014.
7. J. Lellep and J. Polikarpus. Elastic plastic bending of annular plates. In J. Lellep and E. Puman, editors, *Proceedings of the 3rd International Conference "Optimization and Analysis of Structures"*, pages 73–79. University of Tartu Press, 2015.